A STUDY OF

THE EMISSION OF NEGATIVE IONS FROM

HOT METALLIC SURFACES

by

A.L. FARRAGHER Grad.R.I.C. A.C.T.(Birm)

"Q,_____, is the letter of
perpetual question."

Robert Graves
"The White Goddess"

SUMMARY

The interaction of gas molecules with a hot metal surface may result in the abstraction of an electron from the metal and the formation of a negative ion. The transition state theory of Glasstone, Laidler and Eyring is applied to the problem of the calculation of the emission currents with considerable success. The treatment used is simply applicable to the emission of both ions and electrons and is used in the latter case to interpret changes in the electron currents and thermionic electron work functions of metal surfaces exposed to low pressures of gases which can be strongly adsorbed.

The formation of negative ions in sparse surface layers is investigated and comparison of theory and experiment is made for ion formation by substituted benzoquinones and cyanocarbon derivatives. The strong adsorption of tetracyanoethylene is investigated in some detail and the ions are shown to be formed in a secondary adsorbed layer located above the primary adsorbed material.

The experimental data is used to derive the electron affinities of the capturing molecules. This quantity is

shown to be directly proportional to the number and nature of the substituents in the molecule. Charge-dipole interactions are assumed to be of importance in charge transfer spectra and a simple electrostatic calculation of the interaction energy of the excited state of the complex allows the energy of the charge transfer absorption band to be calculated.

PREFACE

This dissertation, which is being submitted for the degree of Doctor of Philosophy in the University of Aston in Birmingham, is an account of the work done under the supervision of Professor F.M. Page B.A., Ph.D, Sc.D. in the Department of Chemistry of the College of Advanced Technology, Birmingham from October 1962 to December 1965. Except where references are given in the text, the work described herein is original and has not been nor is being submitted for a degree at any other University.

I wish to express my gratitude to Prof. F.M. Page for his patience, guidance and encouragement during the past three years.

A.L. Farragher

February 1966.

CONTENTS

PART I

INTRODUCTION

1 INTRODUCTION

It has been frequently stated that Chemistry consists of a study of the properties of the outermost electrons of atoms and molecules. Chemical bonds are formed by the sharing of these electrons and ions are produced when their number in a given system is increased or decreased.

A knowledge of their binding energies is therefore of fundamental importance in any chemical investigation, and the use of such data is to be found in most chemistry text books.[1] Methods of measuring the binding energy of the outermost electron in neutral atoms or molecules are equally well described[2] and compilations of such data are available for many substances.[3,4] The reverse is true for the corresponding electron in negative ions and this lack of general reference accurately reflects the paucity of the quantitative experimental data.

The stability of a negative ion is usually given in terms of the electron affinity of the parent molecule. This is defined as the work done in bringing an electron up to the molecule from infinity and adding it to the

lowest lying vacant orbital of the isolated gas molecule. Experimentally there are three possible approaches to the measurement of this quantity, which are,

1. Determination of the energy threshold for the destruction of the ion.
2. Determination of the energy threshold for formation of the ion.
3. Studies of the equilibria between electrons, molecules and ions.

Typical of the first group are the photodetachment studies of Branscombe [5] where the determination of the limiting frequency, at which the incident light falling upon a beam of ions is sufficiently energetic to cause detachment of an electron, allows the activation energy of the detachment process to be evaluated. This method, being spectroscopic, is capable of extreme accuracy, but the experimental technique is difficult and few ions have been studied. Such results as are available provide useful standards with which the figures obtained by other methods may be compared.

The second group, of which mass spectrometric electron capture studies are typical,[6] is to some extent the converse of the first since the quantity measured is the activation energy for formation of the ion. In order to obtain electron affinities by this means it is necessary that the activation energy be finite, thereby restricting the measurements to dissociative and charge-transfer reactions. Unfortunately the products of such reactions are often formed with excess kinetic energy and the usefulness of the method has been limited by the difficulty of estimating this.

Typical of the third group are studies of the equilibria in flames and at heated metal surfaces. The energy changes involved are computed either from the temperature dependence of the equilibrium constant (second law methods) or by the methods of statistical mechanics (third law methods).

Measurements in flames, as pioneered by Rolla and Piccardi,[7] are dependent upon a measurement of the attenuation of the electron level in a flame consequent upon the addition of an electron acceptor. This method

is subject to considerable experimental difficulty and requires an extensive knowledge of the reactions occurring in the flame. Perhaps the most severe limitation, however, is the requirement that the electron level be sufficiently attenuated for the measurements to be practicable. This limits the method to a study of strong thermally stable electron acceptors.[8-10]

Of the procedures available for studying the equilibria at hot metal surfaces the space-charge method of Glockler and Calvin[11] is the most simple. This requires only the determination of the current-voltage characteristics of a space-charge limited diode both with and without the presence of an electronegative gas. From this the contribution made to the total current by negative ions may be evaluated. Unfortunately this method again has the limitation that the ions must constitute an appreciable fraction of the total current.

In the method of Dukelskii and Ionov[12] a collimated beam of alkali halide molecules is allowed to impinge upon a heated tungsten filament and the ratio of positive to negative ions produced is measured by separating the species with a magnetic field. Use of

the Saha-Langmuir equation then allows the electron affinity of the halides to be computed. This method gives results which are in good agreement with the latest spectroscopic measurements.

The final method in this group is the 'Magnetron method' of Sutton and Mayer [13] in which the negative ion current formed at a heated filament is compared with the thermionic electron current derived from the same source. The electrons and ions are separated by the use of a cylindrical triode filament-grid-anode assembly mounted in a solenoid with the axis parallel to the filament. In the presence of the magnetic field the electrons are constrained into helical paths and are captured by the grid whereas the heavy negative ions are virtually unaffected and pass through to the anode. The main disadvantage of this method lies in the fact that the identification of the ions is only indirect and therefore complex reactions, which give rise to similar numbers of ions of differing mass, may be misinterpreted in terms of a simple reaction.

The magnetron method showed the most promise for development into a general method for the determination of electron affinities and was chosen by Page for an extensive study of the stabilities of negative ions.[14-25] Most of the reactions studied in this work proved to be of the dissociative-capture type because the simple direct-capture reactions tend only to occur at the lowest temperatures where the experimental measurements are the most difficult.

The present work represents an extension of these measurements and is an attempt to study these direct-capture reactions in the magnetron in order to try to establish the theory of the method with more certainty and to provide reference data which may be used to relate the experimental gas phase electron affinities to the solution measurements of charge transfer spectra and polarography, which are thought to furnish relative electron affinity values.

2. PRELIMINARY THEORETICAL CONSIDERATIONS

2.1. Statistical Theory

The early measurements of Mayer [13, 26-29] were an attempt to measure directly the electron affinities of atoms derived from the dissociation of molecules at a hot filament surface. He assumed that atoms, electrons and ions were in equilibrium at this surface and that it was therefore possible to compute the equilibrium constant and hence the energy change for the reaction;

$$A(g) + e(g) = A^-(g)$$

If the gas surrounding the filament comprises molecules of A_2, the number, $Z(A_2)$, striking unit area of surface per second is given by kinetic theory as;

$$Z(A_2) = \frac{P_{A_2}}{(2\pi MkT_g)^{1/2}} \qquad ----- \quad 2.1$$

where $p(A_2)$ is the pressure of A_2 in the apparatus, M is the molecular weight of the gas, T_g its temperature and k is Boltzman's constant. If every molecule which strikes the surface is excited to the filament

temperature (T), and T is sufficiently high for all of these molecules to become dissociated, the number of atoms leaving the surface may be equated to twice the number striking it. These atoms may be considered as being derived from a hypothetical gas of atoms at the filament temperature, and pressure p(A), whence;

$$Z(A) = \frac{p_A}{(2.\overline{\Pi}.m_A.k.T)}1/2 \qquad ------ 2.2$$

Therefore utilising the relationship $Z(A) = 2.Z(A_2)$ and noting $M = 2.m_A$;

$$p_A = p_{A_2}\left[. \; 2.T/T_g\right]^{1/2} \qquad ------ 2.3$$

Also since $Z_A-/Z_e- = i_i/i_e$, where i_e is the non space charge limited electron current deriving from the surface and i_i is the corresponding ion current,

$$K = \exp(-\Delta G^{\circ}/RT) = p_i/(p_e.p_A)$$

$$= \frac{i_i}{p_{A_2}.i_e}\left[\frac{m_A.T_g}{2.m_e.T}\right]^{1/2} \qquad - - - -2.4$$

The standard free energy change, ΔG° , is related to the electron affinity, $-\Delta E^{\circ}$, by the equation,

$$-\Delta E^{\circ} = -\Delta G^{\circ}(T) + G^{\circ}_A-(T) - G^{\circ}_e-(T) - G^{\circ}_A(T) \; - - \; 2.5$$

Since none of the species involved possesses rotational freedom their standard free energies are given by;

$$G^{o}(T) = RT.\log\left[\left\{\frac{h^2}{2.\pi.m.k.T}\right\}^{3/2}.\ \frac{1}{k.T.Q}\right] - - 2.6$$

Q represents the internal partition function, taken as being 2 for the electron. Combining equations 2.4 ; 2.5 , and 2.6 ;

$$-\Delta E^{o} = RT.\log\left[\frac{2\sqrt{2}.\pi^{3/2}k^{5/2}.m_e.m_{A_2}^{1/2}.T^2.T_g^{1/2}.i_i.\frac{Q_A}{i_e}\frac{}{Q_A-}}{h^3.p_{A_2}}\right] \quad 2.7$$

The value of Q_A can be evaluated from spectroscopic measurements and provided that the degeneracy of the ground state of the ion is known Q_A- can be evaluated, since excited states of atomic negative ions are improbable due to the nuclear shielding being almost complete when the electron is in a quantum state higher than the ground state.

By the use of equation 2.7 Sutton and Mayer [13] estimated the electron affinity of the iodine atom as 72.4 $\pm$ 1.5 kcals/mole. Doty and Mayer [26] measured the electron affinity of the bromine atom and obtained a value of 80.49 $\pm$ 0.4 kcals/mole, in good agreement with

the previous estimate of 80.04 kcals/mole obtained by Weisblatt using the same technique. Attempts by Mitchell and Mayer [29] to study chlorine in a tantalum apparatus were hampered by the formation of tantalum pentachloride which appeared to pyrolise upon the heated filament. By cooling the vessel in solid CO_2 they were able to reduce this effect and estimated the electron affinity of the chlorine atom as 92.7 kcals/mole. This work was subsequently repeated by McCallum and Mayer [27] using a silver apparatus thinly coated with silver chloride. They obtained a figure of 85.84 $\pm$ 1.0 kcals/mole, using both Cl_2 and $SnCl_4$ as substrates. Bernstein and Metlay[32] used fluorine as the substrate and estimated the electron affinity of the fluorine atom as 82.2 $\pm$ 4 kcals/mole.

These figures are in good agreement with the latest spectrographic measurements [33] of 83.2 kcals/mole for chlorine, 77.5 kcals/mole for bromine, 70.6 kcals/mole for iodine and 79.4 kcals/mole for fluorine.

Attempts to use the magnetron method for the measurement of the electron affinity of the oxygen atom [28,34] appear, in the light of modern estimates,[35,36] to have been uniformly unsuccessful. This may have been due to

the reaction of the gas with the filament or a failure to accurately calculate the degree of dissociation of the gas at the hot surface. The former of these effects is known to markedly affect the thermionic work function of a tungsten surface[37] and the latter involves a knowledge of the manner in which the gas molecules interact with the filament. This failure to find suitable substrates caused the method to be abandoned until Page [14] made a further study of the halogens using hydrogen halides as the source of halogen atoms.

2.2 Kinetic theory

In the arguments advanced by Mayer the ions are assumed to be formed by the capture of electrons which have been emitted by the filament. If this were so the total current density should always be the same as that deriving from the filament at the same temperature in vacuo. Page, however, noticed that the total current was inversely proportional to the gas pressure and interpreted this in terms of an adsorption process which resulted in a raising of the work function of the surface. The arguments developed lead to essentially the same results as Mayer's for the case of fission of a homonuclear

diatomic molecule of low bond energy, but a very different interpretation with other substrates.

The electron current from an area A cm^2 of filament surface covered by a film of adsorbed gas of area $A\Theta$ cm^2, which raises the work function, will be given by Richardson's equation [38] as;

$$i_e = B.A.T^2.(1-\Theta).\exp[-\chi/RT] \quad - - - - - \quad 2.8$$

where χ is the work function of the surface, T its absolute temperature and B is a constant equal to 120 amps cm^{-2} $degree^{-2}$. In the present case this is a reasonable assumption since the negative ions are presumed to be formed upon the covered surface and this must necessarily lead to the formation of an electrical double layer with the negative portion directed away from the filament.[39]

A similar expression to equation 2.8 would be expected to hold for the ion current, whence;

$$i_i = C.A.T^m.\Theta.\exp\left[(E-q_A-\chi')/RT\right] \quad - - - \quad 2.9$$

Here C and m are constants, E is the electron affinity of the acceptor, q_A is its activation energy for desorption and χ' is the electron work function appropriate to the emission of ions. If the measurements are limited

to conditions where θ is small χ and χ' are identical.

The Langmuir relation,[40]

$$\theta = k_1.p/(k_2 + k_1.p) \qquad ----- 2.10$$

may be substituted for θ, since at these low surface coverages interaction effects will be negligible and therefore the heat of adsorption of the gas (W) may be reasonably expected to be constant. Hence, combining equations 2.8 ; 2.9, and 2.10;

$$\frac{i_e}{i_i} = \frac{B.T^{(2-m)}.k_2}{C.k_1.p}.\exp\left[(q_A - E)/RT\right] \qquad --- 2.11$$

k_2 may be written in exponential form as $k_2 = k.\exp -W/RT$ and W may be resolved[41,42] into $W = q_A + q_r - D$, where D is the energy of the bond broken in producing A and the fragment, r, which have heats of adsorption q_A and q_r respectively. Substituting this into equation 2.11, taking logs and differentiating with respect to 1/T gives the 'apparent' electron affinity E'(T);

$$E'(T) = E + q_r - D + (2-m)RT \qquad ----- 2.12$$

Since the experimental electron affinity is derived from plotting $\log(i_e/i_i)$ against 1/T, this corresponds to the apparent electron affinity at a temperature $\bar{T}$, where $\bar{T}$

is defined by the mean value of 1/T of the measurements.

In order to calculate the electron affinity of the acceptor the apparent electron affinity must be corrected to $0^{o}K$;

$$E'_o = E + q_r - D = E'(\bar{T}) - (2-m)R\bar{T} \quad ----- 2.13$$

In the interpretation of his results Page assumed that the ratio $i_e.p/i_i$ defined the equilibrium constant K_p for the reaction $A^-(g) + B = AB(g) + e^-(g)$ where g refers to the gas phase. The apparent electron affinity is then defined by;

$$E'(\bar{T}) = -R(d.\log\left[i_e.p/i_i\right])/d.(1/T) = RT^2.d.\log.K_p/dT$$
$$= \Delta H(\bar{T}).$$

$\Delta H(\bar{T})$ is the enthalpy change for the reaction at the mean temperature $\bar{T}$.

The relationship between the heat of reaction at a temperature T and that at $0^{o}K$ is given by, $\Delta H(T) = \Delta H_o + \int_o^{\bar{T}} C_p.dT$, where C_p is the difference in the heat capacities at constant pressure of reactants and products. Therefore,

$$E'_o = E'(\bar{T}) - \int_o^{\bar{T}} C_p.dT. \quad ------ 2.14$$

If both reactants and products are assumed to have attained filament temperature the changes in heat capacity due to changes in the number of degrees of translational or rotational freedom may be treated classically as R/2 kcals/mole for each degree of freedom. Changes in the number of vibrational degrees of freedom may be corrected for utilising the relationship given by Fowler and Guggenheim,[43]

$$\frac{C}{K} = \frac{(\phi/2.T)^2}{\sinh^2(\phi/2T)}$$

where $\phi = h\nu/k$, ν being the vibration frequency and C the associated heat capacity. Integrating with respect to T and rearranging,

$$\Delta H/RT = x.\coth.x - x \qquad ----- 2.15$$

where $x = 0.72\nu/T$. Since the vibration frequencies associated with the bonds in any radicals formed in the reaction are not, in general, known it is necessary to assume that bonds which are not broken in the course of the reaction are unaffected by fragmentation. It is then only necessary to identify the vibration frequencies in the parent molecule which are associated with the bond broken.

Using this approach Page and his collaborators[14-25] investigated the ion formation by a wide range of substrates and confirmed the essential validity of the method. The results obtained are summarised in the following table.

TABLE 1

Ref.	Ion.	Substrate	E_o (kcals/mole)	Other data obtained
14	I	I_2	74.5	
	Cl	HCl	84	
	Br	HBr	82	
16	O	N_2O	33.4	
	O	O_2	33.6	
	O	H_2O	34	
25	O	NO_2	33.4 $\pm$ 2	
17	NH_2	N_2H_4	27.6 $\pm$ 2	
		NH_3	assumed	D_{N-H} = 104.7 $\pm$ 2.3
18	CH_3	$Hg(CH_3)_2$	26	
		$Pb(CH_3)_2$	26	
		$Pb(C_2H_5)_4$	26.8	
	C_2H_5	$Hg(C_2H_5)_2$	22	
		$Pb(C_2H_5)_4$	22.4	
	$n\text{-}C_3H_7$	$Hg(C_3H_7)_2$	16.3	
	$n\text{-}C_4H_9$	$Hg(C_4H_9)_2$	15.3	

TABLE 1 (cont'd)

Ref.	Ion.	Substrate	E_o(kcals/mole)	Other data obtained
19	SH	H_2S_2	52.7 ± 0.7	
	S	H_2S	48.2 ± 1.5	
21	CN	C_2N_2	59.1 ± 1.2	
		HCN	assumed	D_{H-CN} = 110.3 ± 2.4
	SCN	$(SCN)_2$	50.2 ± 0.5	
		HCNS	assumed	D_{H-CNS} = 114.0 ± 1.8
22	C_6H_5	$(C_6H_5CO)_2$	50.9 ± 1.1	
		C_6H_6	57.4 ± 2.4	
	$C_6H_5CH_2$	$(C_6H_5CH_2)_2$	20.8 ± 1.9	
		$C_6H_5CH_3$	assumed	D_{CH_2-H} = 77.1 ± 2.9
24	SF_5	S_2F_{10}	84.2 ± 1	
		SF_6	assumed	D_{S-F} = 82.6 ± 2.2
	SF_6	SF_6	34.3 ± 5	
25	NO	NO	20.6 ± 2.5	
	NO_2	NO_2	92.0 ± 3.7	

Where these results differ from those given in the references they are taken from the review of Kay and Page.[44]

These figures show the kinetic approach to be far more flexible than the statistical one and represent a considerable advance in the interpretation of the mode of ion formation in the magnetron. There are however several points at which the theory may be criticised. The first of these is the assumption that the ratio $i_e.p/i_i$ defines the pressure equilibrium constant for the reaction postulated. From the derivation given this is by no means certain. This therefore throws some doubt upon the identification of the apparent electron affinity as the enthalpy change for this reaction. Also, in the correction of the experimental results to $0^{o}K$ it is assumed that the gas molecules which ultimately dissociate to form ions are energetically at the filament temperature. Unless the residence time of these molecules upon the surface is considerably longer than one vibration this is unlikely to be true. Increasing the residence time will increase the fraction of surface covered by the gas and may invalidate one of the fundamental assumptions of the theory. The final criticism is one of the interpretation of the results. Since there is no direct means of identifying the reaction occurring in the

magnetron, the measurements can only be interpreted on the basis of the reasonableness or otherwise of the energy changes associated with the process postulated.

The broad measure of agreement between the results obtained and other estimates, quoted in the original papers, suggests that these criticisms are not serious. However, in order to obtain accurate and reliable electron affinities it is important to know just what errors these effects contribute and part of the present work is directed towards deriving this information.

PART II

THEORY AND EXPERIMENT

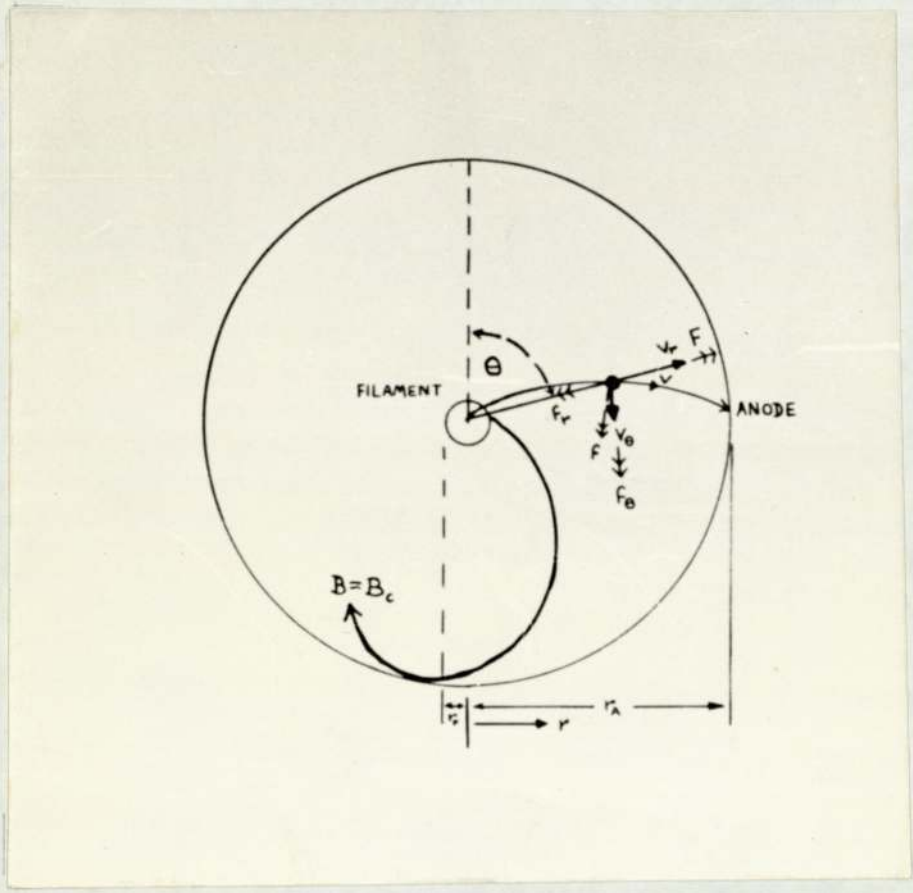

The forces acting upon an electron.

FIGURE 1.

3. THE APPARATUS

3.1 The principle of the method

The original paper on the operation of the magnetron diode was published by Hull.[45] The discussion given here[46] illustrates the essential features of the instrument.

Figure 1 shows the forces acting upon an electron emitted from the hot central filament of a diode placed in a uniform magnetic field, of flux density B, running parallel to the length of the filament. The electrostatic and electromagnetic forces acting upon the electron are respectively;

$$F = \epsilon.E = \epsilon.(dV/dr)$$

and, $f = B.\epsilon.v.$, where ϵ is the electronic charge, V is the potential at a distance r from the filament and v is the velocity of the electron at this point. If v is resolved into components v_r and v_Θ, along and perpendicular to the radius vector, then the components of f will be; $f_r = B.\epsilon.v_\Theta$, and $f_\Theta = B.\epsilon.v_r$.

If Θ is the angle between the radius vector, r, and an arbitrary line in the azimuthal plane, the angular

velocity of the electron is, $\omega = (d\theta/dt) = v/r$.

The equation of radial motion therefore becomes,

$$\frac{d}{dt}\left[m.\frac{dr}{dt}\right] = F - f_r = \epsilon.\frac{dV}{dr} - B.\epsilon.r.\frac{d\theta}{dt} \quad - 3.1$$

where m is the electron mass.

The equation of azimuthal motion is found by equating the moment of the impressed force to the rate of change of the angular momentum, thus;

$$r.f_\theta = r.B.\epsilon.\frac{dr}{dt} = \frac{d}{dt}\left[m.r^2.\omega.\right]$$

Integrating each side with respect to time and noting that $\omega = 0$ as the electron leaves the filament gives,

$$\omega = \frac{B.\epsilon.}{2.m}\left[1 - (r_f^2/r^2)\right] \quad ----- 3.2$$

If the small thermal velocity with which the electron leaves the filament is ignored, its velocity at a point at which its potential is V will be given by,

$$v = \sqrt{\frac{2.\epsilon.}{m}V} = \left[\left(\frac{dr}{dt}\right)^2 + r^2\left(\frac{d\theta}{dt}\right)^2 + \left(\frac{dz}{dt}\right)^2\right]^{1/2}$$

At a certain value of the magnetic field strength, $B = B_c$, the electron will just fail to reach the anode.

At this point, $V = V_a$; $dr/dt = dz/dt = 0$; $r = r_a$, and $d\theta/dt = v$, whence,

$$\omega = \frac{v_\theta}{r_a} = \frac{1}{r_a}\sqrt{\frac{2.\epsilon.}{m}V_a} \qquad \text{- - - - - 3.3}$$

Therefore, equating 3.2 and 3.3,

$$B_c = \sqrt{8.V_a} \Big/ r_a\left[1 - (r_f^2/r_a^2)\right]\sqrt{\epsilon/m} \qquad \text{- 3.4}$$

whence, if $r_a \gg r_f$,

$$B_c = \sqrt{\frac{8.m.V_a}{\epsilon.r_a^2}} \qquad \text{- - - - - 3.5}$$

Equation 3.4 shows the value of B_c to be independent of the potential distribution between the anode and cathode so that the presence of other electrodes or space charge effects should not alter the cut - off conditions. In practice the cut-off is not so sharp with grids present, probably because of the distortion of the magnetic and electric fields by these structures.

In the magnetron triode the electrons are captured by the grid and so prevented from creating a large space charge near the filament which would affect the emission of the negative ions. The magnetic field strength is usually made greater than B_c so that the apogee occurs

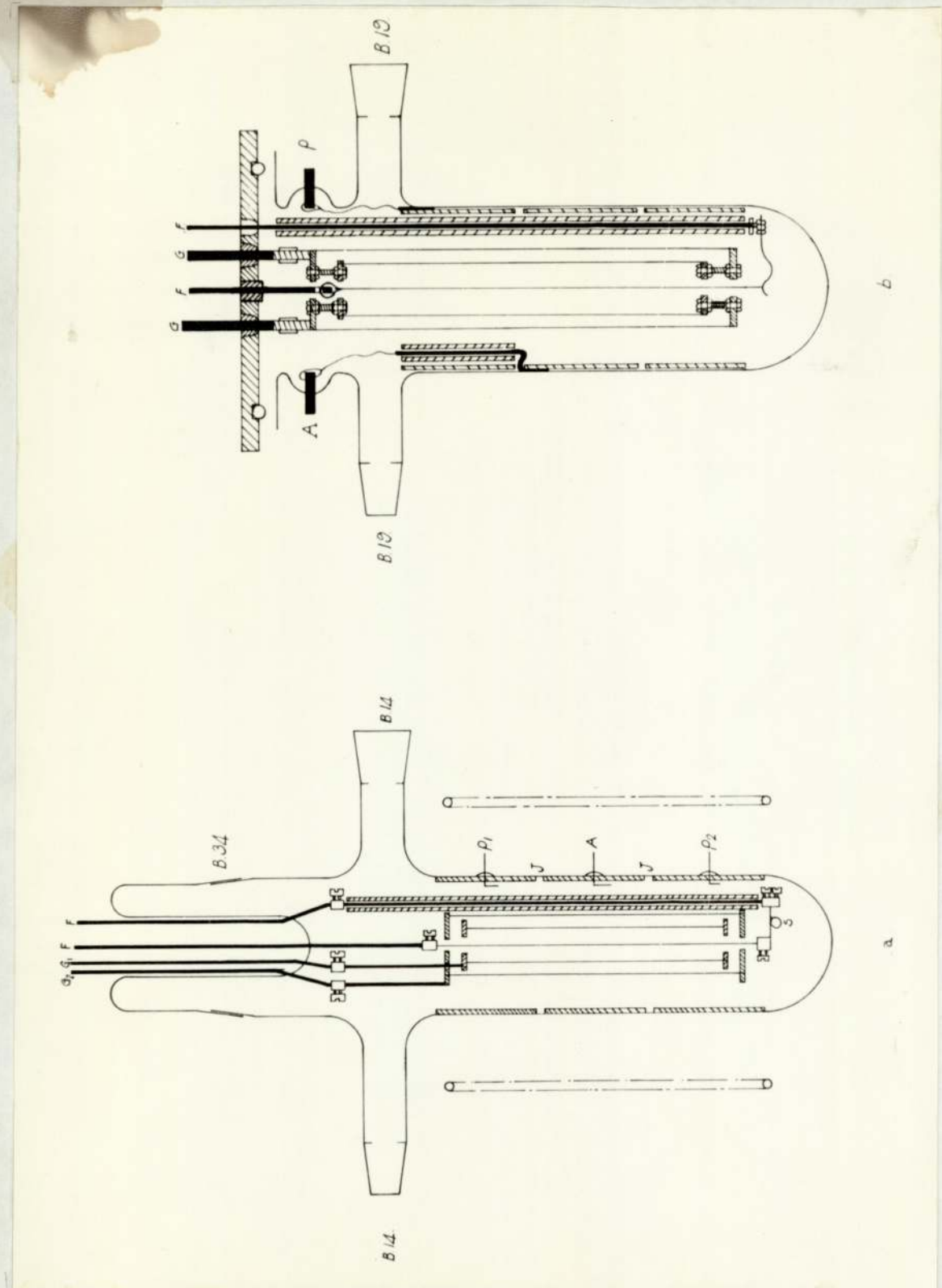

The magnetron assembly.

FIGURE 2.

near the grid. This causes the electrons to approach it tangentially and results in a greater efficiency of electron removal. The presence of a second grid was shown by Page[14] to lead to a further increase in efficiency, presumably because of its action in trapping electrons which had passed through the first grid because of potential and geometrical asymmetry within the apparatus.

3.2 The General design

Figure 2.a shows the apparatus as used by Page and 2.b the modified design used for the measurements described in this dissertation. The apparatus consists essentially of a central filament (F) surrounded by two coaxial grids (G_1, G_2) and an anode (A) which is flanked by guard plates (P_i, P_2). These latter ensure an even temperature over the length of filament from which the measured thermionic currents derive. In the early design the anode and guard plates were formed from a layer of vacuum deposited silver, the plates being separated by marking (J) with a steel scribe. When using this system, considerable difficulty was encountered in ensuring that the silver formed a good electrical contact with the

tungsten seals set in the wall of the bottle. The main disadvantage of the system, however, seemed to result from the adsorption of chemicals upon the scribed marks, rapidly leading to electrical short circuiting between the anode and the plates. It proved to be impossible to adequately clean the apparatus after this had occurred without dissolving off the silver and replating. This resulted in the bottle becoming badly marked in the region J. The ground glass joint between the top cap and the main body of the bottle also tended to seat very firmly and since the grid assembly was rather delicate, it was easily broken while being dismantled. A further disadvantage of this arrangement was a lack of rigidity in the filament and grid supports making the apparatus very sensitive to vibration.

In the final design, the rigidity was improved by mounting the grids upon 6 B.A brass studding which was insulated by inserting it into glass tubing which also served to add some support. The plated anodes were replaced by 4 cm long x 1 mm thick molybdenum sheet which was sprung into position. The connections to this were made by inserting copper wire between the sheet and

the wall of the bottle. The connection to the tungsten seals P and A were made by means of miniature 'crocodile' clips. This arrangement made it a simple matter to remove the anode and plates and clean them and the bottle without disturbing the filament assembly.

In the early apparatus the filament was secured at one end by a grub screw and at the other by means of a tensioning spring (S) made of spring steel. This arrangement worked well for tungsten filaments, but was incapable of retaining sufficient tension in more ductile filaments without stretching them and causing them to sag into the grids when hot. This was overcome by making the spring out of 0.01" dia. tungsten wire. This proved to be ideal for the purpose and enabled a much wider range of metals to be used as filament materials. The filament assembly was mounted directly on A.E.I S5 metal to glass seals which were brazed into a 1/4" thick brass baseplate (B). This was sealed on a ground glass flange by means of a rubber 'O' ring which was lightly coated with Apiezon L or N high vacuum grease. The bottle was made by Mr. W. Sabin of the Department of Chemistry and was

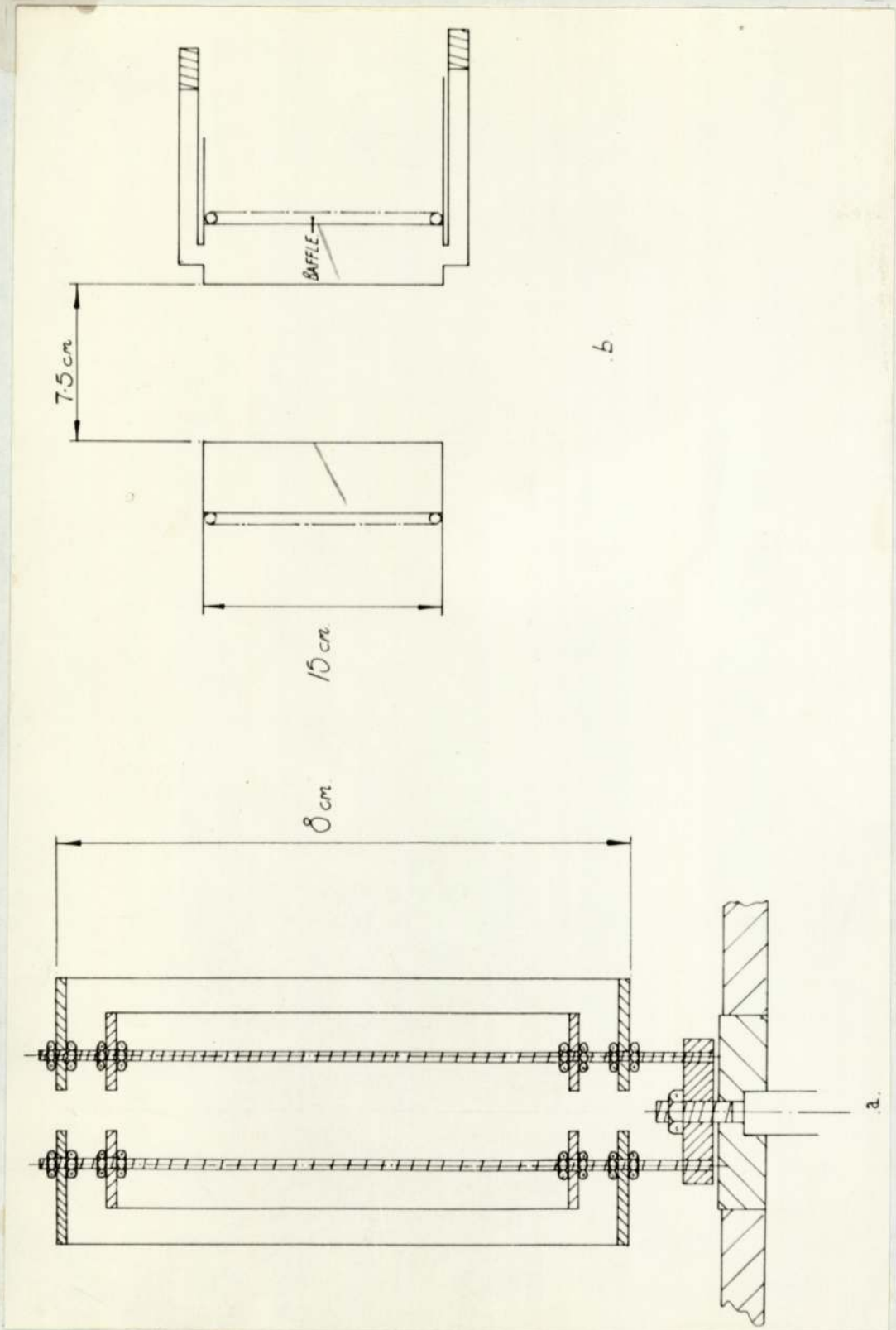

Grid & magnet assemblies.

FIGURE 3.

typically 2.5" internal diameter and 9" in length.

Figure 3a shows details of the grid assembly which was wound with 40 swg nickel wire, mounted on an A.E.I S13 metal to glass seal and secured by means of a 2 B.A nut. This arrangement enabled it to be removed from the base-plate for ease of rewinding. Normally the two grids G_1 and G_2 were connected directly together since the measurements described in section 3.5 showed that there was no improvement in the performance of the apparatus if they were maintained at different voltages. This arrangement has more rigidity than separate mountings.

Figure 3b shows the magnet design. The early models were cooled by means of a coil of 1/4" dia copper tube which was brazed to the copper magnet former. This was very inefficient and caused the magnet to become appreciably warm during use. This led to a change in the resistance of the wire and hence the magnet current falling with use. The model shown here completely obviated this trouble. The solenoid itself was wire wound, different models having between 10 and 15 layers (900 - 1500 turns) of 20 s.w.g. enamelled copper wire which were not

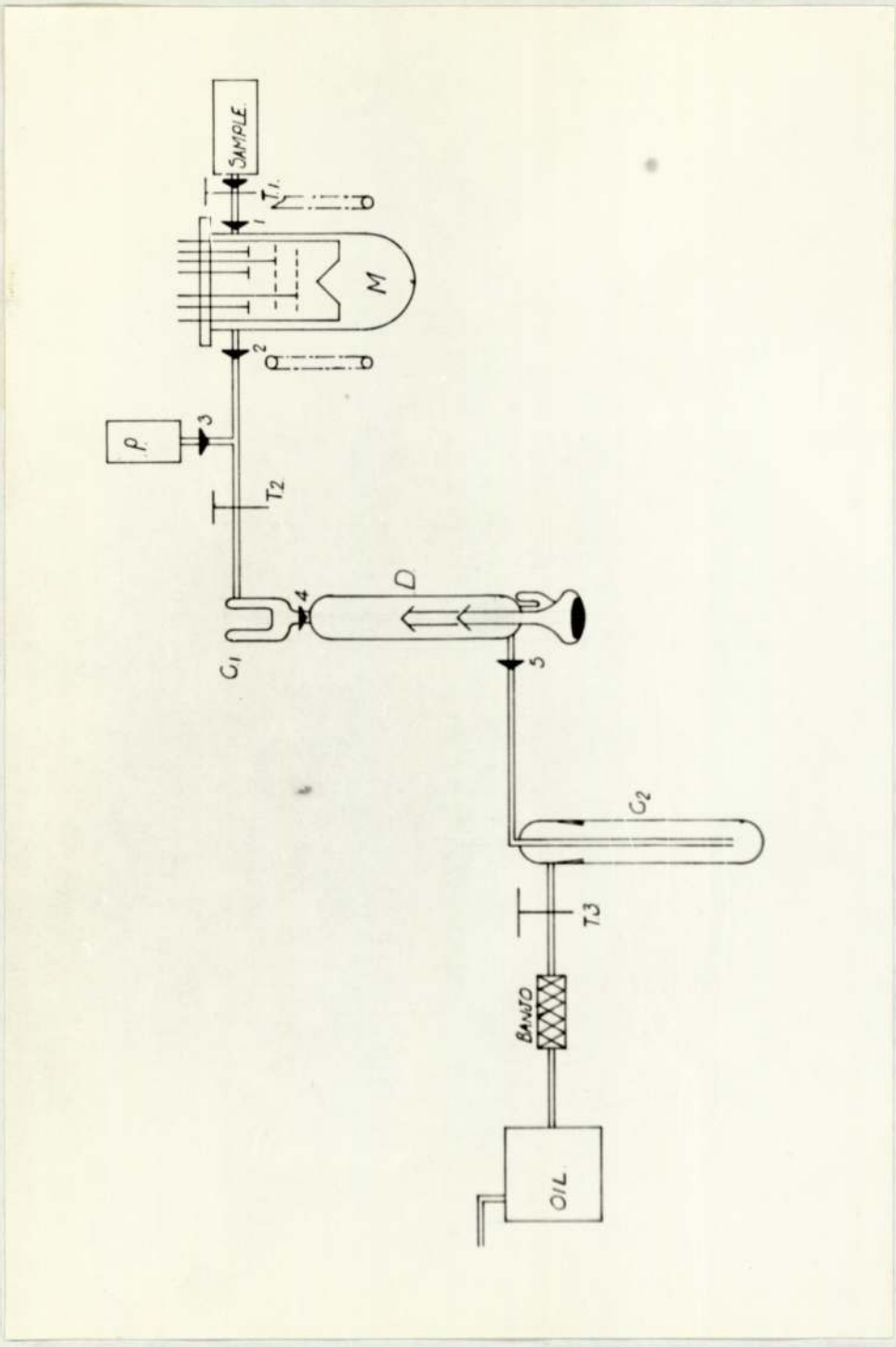

Block diagram of the apparatus.

FIGURE 4.

separated by any insulating layers in order to improve the heat transfer properties. The operating current usually lay between 4 and 6 amps where the heating effect was not troublesome.

Several of these magnetron assemblies were constructed, during the course of this work, which differed only in minor details of dimension and structure. The description given in this section is quite typical since these differences in no way affected the operation of the apparatus.

3.3 The Ancillary Equipment

Figure 4a shows a diagram of the apparatus. The sample is contained in a side arm of the magnetron vessel and is admitted through the 10 mm bore high vacuum tap, T_1. The other taps and all the connecting tubing are of the same internal diameter as T_1, and are constructed of pyrex. The joints 1, 2, 4 and 5 are standard B 19 and the pirani-head (Edwards G5B-2), B 14. The liquid nitrogen trap, C_1, is 1.5" dia and 4" deep and C_2, 0.75" dia and 9" deep. The two, or three, stage mercury diffusion pump, D, was backed by a rotary oil pump and

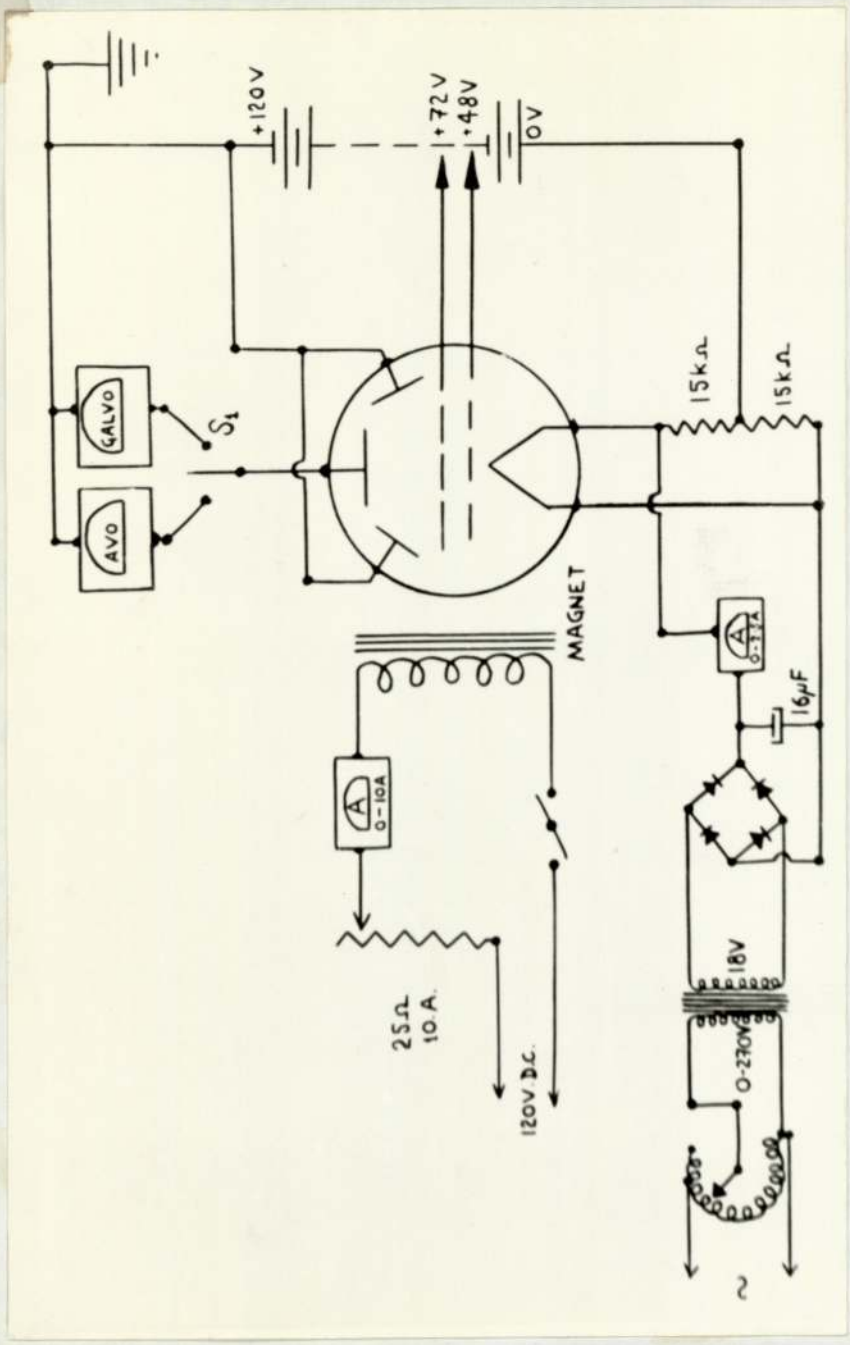

Circuit diagram.

FIGURE 5.

the system was capable of maintaining a pressure of less than 10^{-5} torr.

The electrical circuitry is shown in figure 5. The anode currents were measured on an Avo, DC 1388B amplifier in the range 10^{-14}-10^{-6} amps and by a Pye, 7906/S 'scalamp' or equivalent instrument in the range 10^{-6}-10^{-3} amps. All currents are expected to be accurate to better than $\pm$ 5%. The plate and grid voltages were supplied by an Exide, H1006 battery and the magnet current was supplied from a 120V stack of lead acid accumulators.

Figure 6 shows the components of the sample introduction system. Gases were introduced to the needle valve, 6a, from the gas container, 6b, which was filled in an auxiliary vacuum system, in which the gases were also purified. Volatile solids and liquids were contained in the simple bent side arm, 6c. Non volatile solids were introduced from the heated sample holder, 6d, which enabled them to be sublimed directly on to the filament. With some compounds the magnetron bottle was heated with an 'Isomantle' heating tape or hot air blower in order

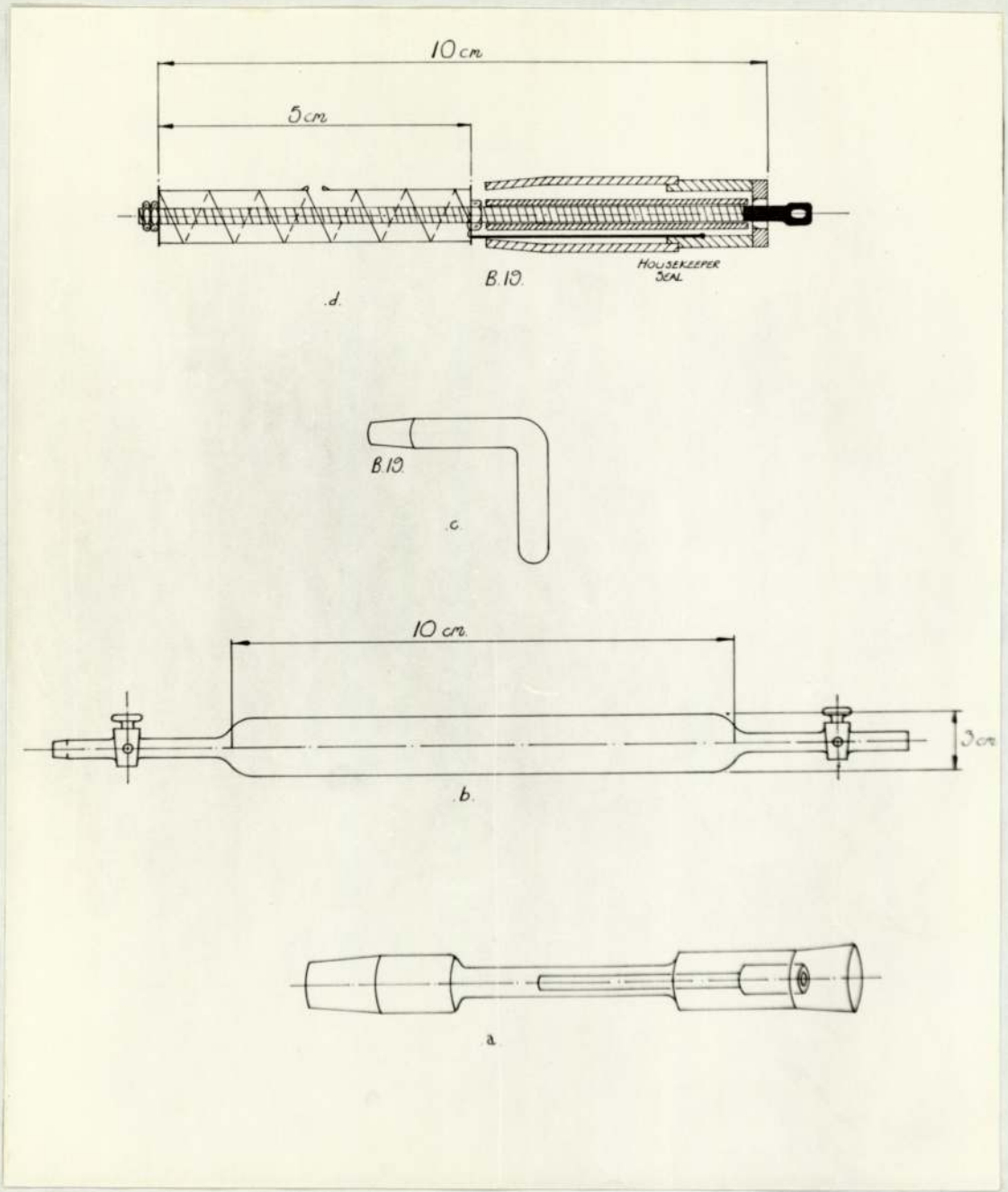

Sample introduction system.

FIGURE 6.

to prevent condensation of the material upon the walls of the apparatus.

3.4 The measurement of temperature

Because of the deposition of material upon the walls of the vessel, it was not always possible to measure the temperature of the filament after each measurement of an electron or ion current. In order to avoid this necessity the filament temperature was measured at fixed values of the filament heating current when the apparatus was clean and this calibration was checked periodically during use. The calibration was always performed with the sample gas flowing over the filament in order to allow for any changes in the properties of the metal due to cooling by the gas or adsorption. These temperatures were then used, in conjunction with the measured electron currents, to evaluate the work function of the material using Richardson's equation (2.8). This was used as a check upon the reliability of the figures[14] in both its second and third law forms.

The temperatures were measured with a Leeds and

Northrup disappearing filament pyrometer through one thickness of glass. In the temperature range 1000 - 2000°K the mean correction for absorption by the glass is about +24°K[47], the measured temperatures, in °C, were therefore added to 300 to give the temperatures in °K. This procedure should be sufficiently accurate for the kinetic approach and the measured work functions seem to confirm this. The highest temperatures measured always occurred at the extreme lower end of the highest scale of the pyrometer where considerable difficulty was experienced in obtaining reproducible measurements. In order to assist the calibration of the temperature - heating current characteristics of the filament, the latter function was plotted against the square of the absolute temperature.

If the filament is long and the emission current is only measured from the central portion, any heat losses due to conduction from the ends may be neglected and, therefore at equilibrium, the rate of heat loss by radiation is equal to the rate of supply. Hence $\sigma.T^4=I^2.R.$, where σ is Stefan's constant, T the absolute temperature of the filament (assumed to be a perfect black body

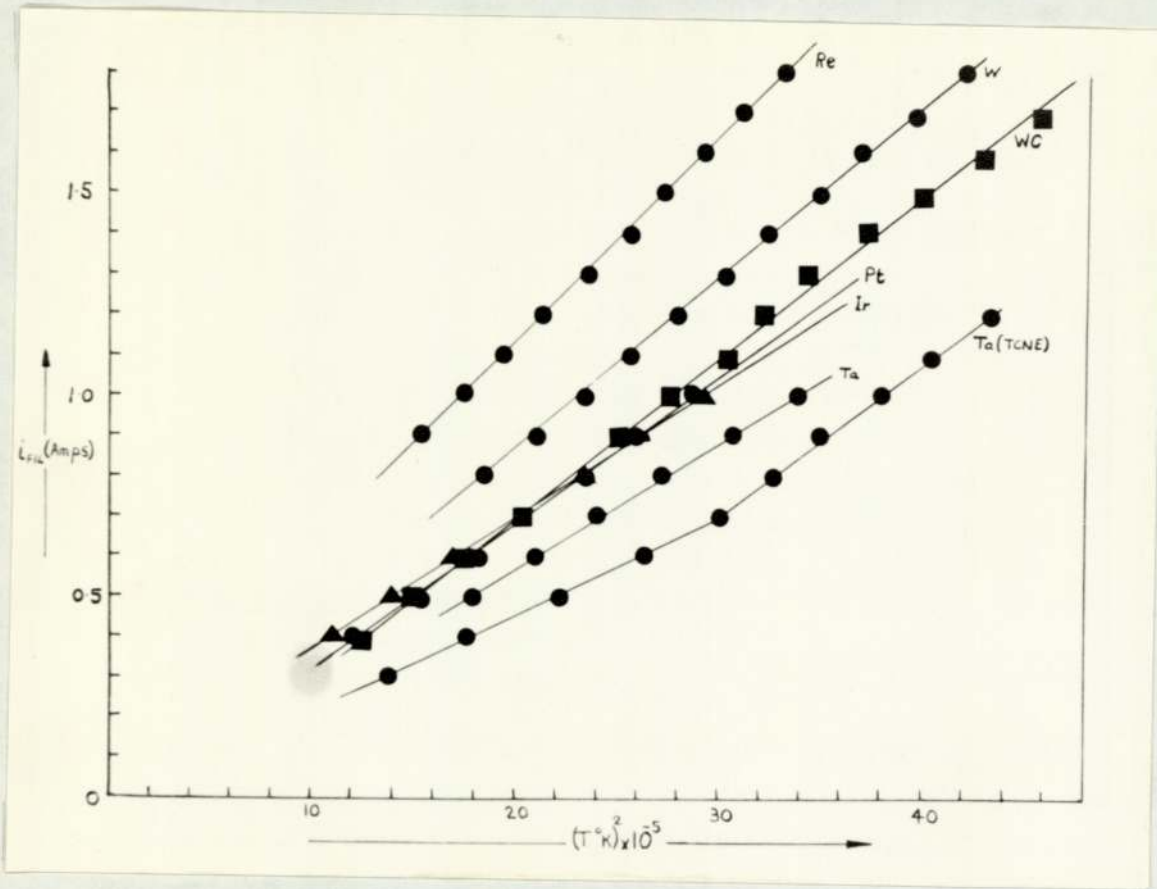

Filament temperature calibration.

FIGURE 7.

radiator), I the filament heating current and R the resistance of the filament (assumed constant over the temperature range studied). Plotting I against T^2 will give a straight line over a range of temperatures for which these assumptions are true. This is illustrated in figure 7. When the measured temperatures did not fall upon a straight line, a smooth curve was drawn through the points. The only exceptions to this procedure were tungsten in the presence of tetracyanoethylene vapour, where adsorption was found to cause an almost discontinuous change in the emissivity of the surface and molybdenum carbide in the presence of the same gas, which was found to exhibit a phase-change. (Figure 41)

With the original design of apparatus the measurement of temperatures was very difficult. In order to circumvent this difficulty Gaines and Page[22] used the electron currents to define the temperature of the filament. The basic equation for the determination of electron affinities may be written as;

$$i_i/i_e p = (K/T^2).\exp(E'/RT) \quad ---- \quad 3.6$$

where i_i is the ion current, i_e the electron current

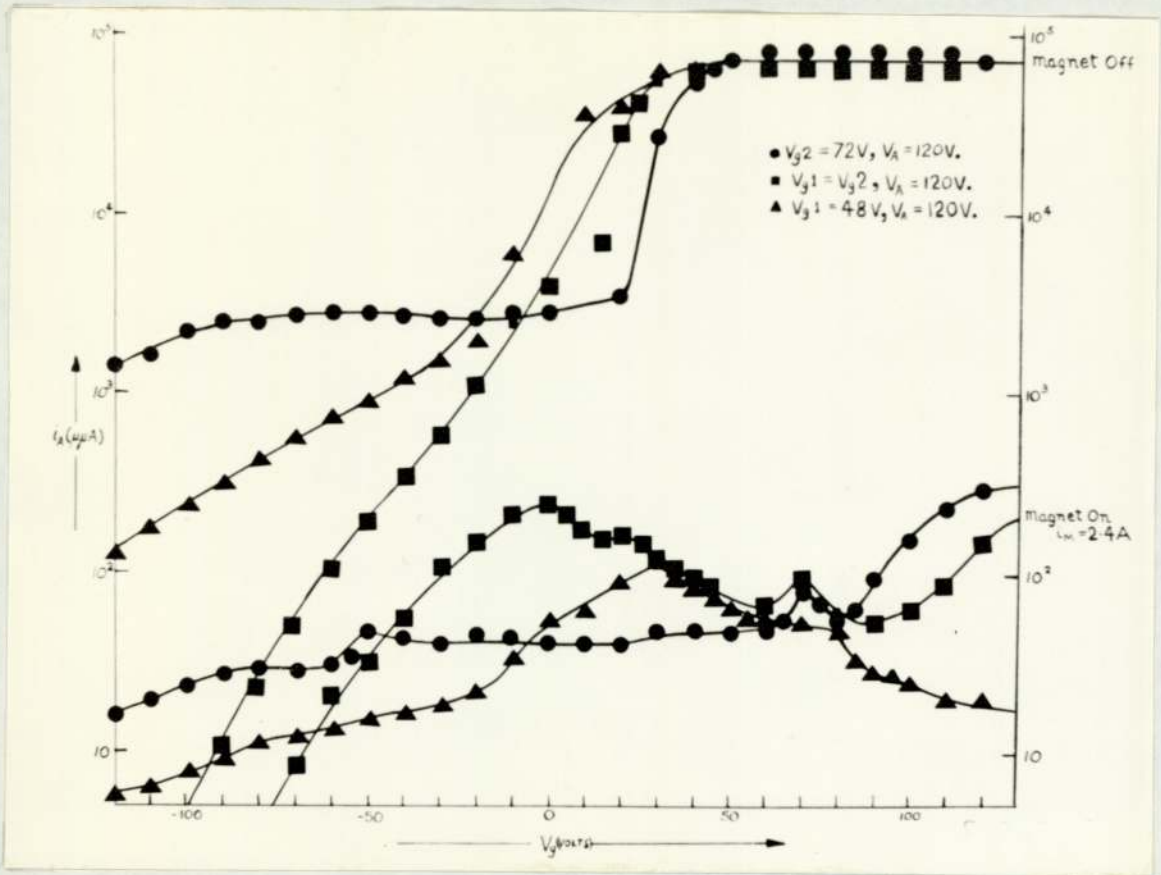

The effect of grid voltage upon anode current.

FIGURE 8.

and K is a constant. i_e is given by Richardson's equation (2.8), which upon substitution into equation 3.6 gives,

$$\log.i_i = \frac{(\chi-E')}{\chi}.\log.i_e + \log.p - 2\frac{(\chi-E')}{\chi}.\log.T + \log.K + \frac{E'}{\chi}.\log.(B.A) \quad ----- 3.7$$

Variations in log.T may be neglected compared to variations in $\log.i_e$ and so, if the pressure is held constant throughout the measurements, a plot of $\log.i_i$ against $\log.i_e$ should yield a straight line of slope $(\chi-E')/\chi$, from which E' may be evaluated if χ is known.

This procedure has been used several times in the course of this work, but in all cases χ and E' have also been measured by the normal Arrhenius procedure in order to ensure that both methods yield the same results.

3.5 The operation of the apparatus

Figure 8 shows the effect upon the anode current of changes in the grid voltages, both with and without the magnetic field. The anode current was found to saturate at +50V plate voltage but in order to ensure that there

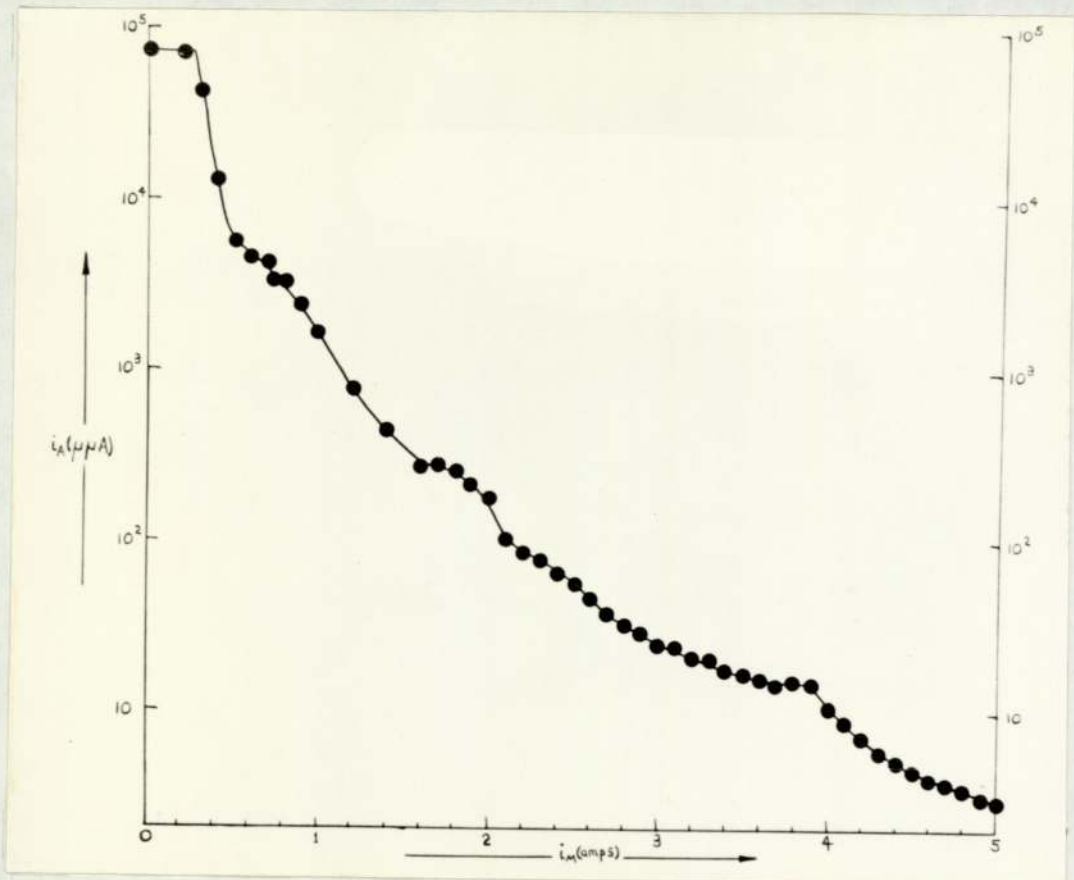

The effect of magnet current upon anode current.

FIGURE 9.

was no possibility of space charge effects it was normally set at +120V. The most favourable grid voltages were expected to be those which maintained a uniform field between the filament and the anode. With 120V on the anode (r = 2.25cm) the expected voltages were V(G2) = 93V, (r = 1.75cm) and V(G1) = 59V (r = 1.10cm). Figure 8 shows that there is evidence for this effect although the voltages do not appear to be very critical and equally good performance could be obtained with any of the following arrangements;

V(A) = 120V; V(G2) = 72V; V(G1) = 80V;

V(A) = 120V; V(G2) = 72V; V(G1) = 50V;

V(A) = 120V; V(G2) = 80V; V(G1) = 48V;

V(A) = 120V; V(G2) = 48V; V(G1) = 48V.

In the particular instrument upon which these measurements were made, V(G1) and V(G2) were normally maintained at 48V and 72V respectively. In all other models both grids were maintained at 48V.

Figure 9 shows the effect of the magnet current upon the anode current. The sharp drop in the latter at 0.26 amps magnet current is assumed to be due to the

critical cut-off condition at the anode defined by equation 3.5. Substituting for B_c the expression,

$$B_c = 2.\pi.n.i/a \qquad - - - - - 3.8$$

and utilising the data i = 0.26 amps, n = 142 turns/cm, a (the magnet radius) = 6.35cm, r_a = 2.25cm and V_a = 120V gives $\epsilon/m = 1.42 \times 10^7$ abs.e.m.u.gm^{-1}. This is in satisfactory agreement with the modern value of 1.76×10^7 abs.e.m.u.gm^{-1}. The inflexions in figure 9 presumably correspond to the positions where the electrons are captured by the grids, but the magnet currents necessary to produce these effects are much higher than expected, possibly because of shielding of the magnetic field by the nickel wires used in the construction of the grids. This effect could also explain the rather low value for ϵ/m calculated above.

In operation the magnet current was set at 4.0 amps with the magnet cold. This fell rapidly to 3.8 amps with the magnet in use and a further fall to about 3.5 amps with prolonged usage. Since there is a plateau on the magnet current - anode current curve in this region these changes should be unimportant.

In use the heated filament caused some outgassing of the glass and metal parts of the magnetron bottle and it was necessary to ensure that this process was carried out to completion before any measurements were made. The usual procedure adopted was to maintain the filament at as high a temperature as practicable, this being determined by the melting point of the metal and its rate of attack by oxygen at the outgassing temperature, until the background pressure fell to below 10^{-5} mm.Hg at the maximum operating temperature. After this treatment the sample material was allowed to flow over the hot filament until measurements showed the system to have become stabilised. The filament temperatures were then calibrated in the presence of the gas. This procedure was greatly facilitated by maintaining the apparatus under vacuum, with frequent pumping, even when not in use.

In making the measurements of the electron and ion currents, there are two possible approaches, either a series of ion currents can be measured at fixed temperatures or else the electron and then the ion currents may be measured at each temperature. Both of these methods

have advantages and disadvantages. The main advantage of the former system is the rapidity with which a series of measurements may be made. In the case of gaseous substrates this can be very important as the pressure can change appreciably in the course of a run and these effects are minimised by making a series of rapid measurements of the ion currents. The disadvantages of this procedure are that the electron currents are not measured at exactly the same temperature nor under exactly the same conditions as the ion currents. In general, however, the electron currents are exactly the same with and without the gas present in the apparatus and any errors introduced from the failure to reset the filament temperature to exactly the same value as that at which the associated ion current was measured are usually small compared to errors due to changes in the pressure of the substrate. The main disadvantage of the latter system, as already noted, is the tendency for the pressure to change during the course of a run. This can be particularly troublesome with unstable substrates such as NO_2 which may decompose to an extent which is a function of the filament temperature. Any electron affinity

measured under such circumstances will be in error by an amount which will depend upon the extent of the decomposition at each temperature of measurement. This source of error is minimised by working in a flow system and making the measurements as rapidly as possible. This same effect can be caused by the apparatus being warmed by the radiation from the filament during the course of the measurements. This may either lead to increased decomposition of the substrate or desorption of gases from the walls of the vessel. In the extreme case this may result in the measurement of seemingly different apparent electron affinities when the measurements are made from high to low or low to high temperatures.

Because of these effects the ion currents deriving from gases and non volatile solids were measured separately from the electron currents, and those deriving from liquids, and volatile solids, were measured together at each temperature. Whenever the latter procedure was used, measurements were made from low to high and high to low temperatures in order to ensure that both methods gave the same result.

4. ELECTRON CAPTURE BY THE OXIDES OF NITROGEN UPON PLATINUM FILAMENTS *

4.1 Experimental

The NO was supplied by the Matheson Co Inc and was used unpurified. The NO_2 was prepared either by heating lead nitrate in a stream of oxygen, following the directions of Dodd and Robinson,[48] or by oxidation of NO and was purified by fractional distillation before use. Attempts to measure the electron affinity of NO_3, produced by pyrolysis of the volatile anhydrous copper nitrate,[49] were abandoned due to the absence of essential bond energy data and the general similarity of the results to the NO_2 data. This compound was kindly supplied by Professor C.C. Addison.

The filament materials used were platinum and platinum - 13% rhodium, there being no significant difference in the results from either source.

---

* The contents of this section formed the basis of a paper submitted[25] to the Discussions of the Faraday Society.37.1964.

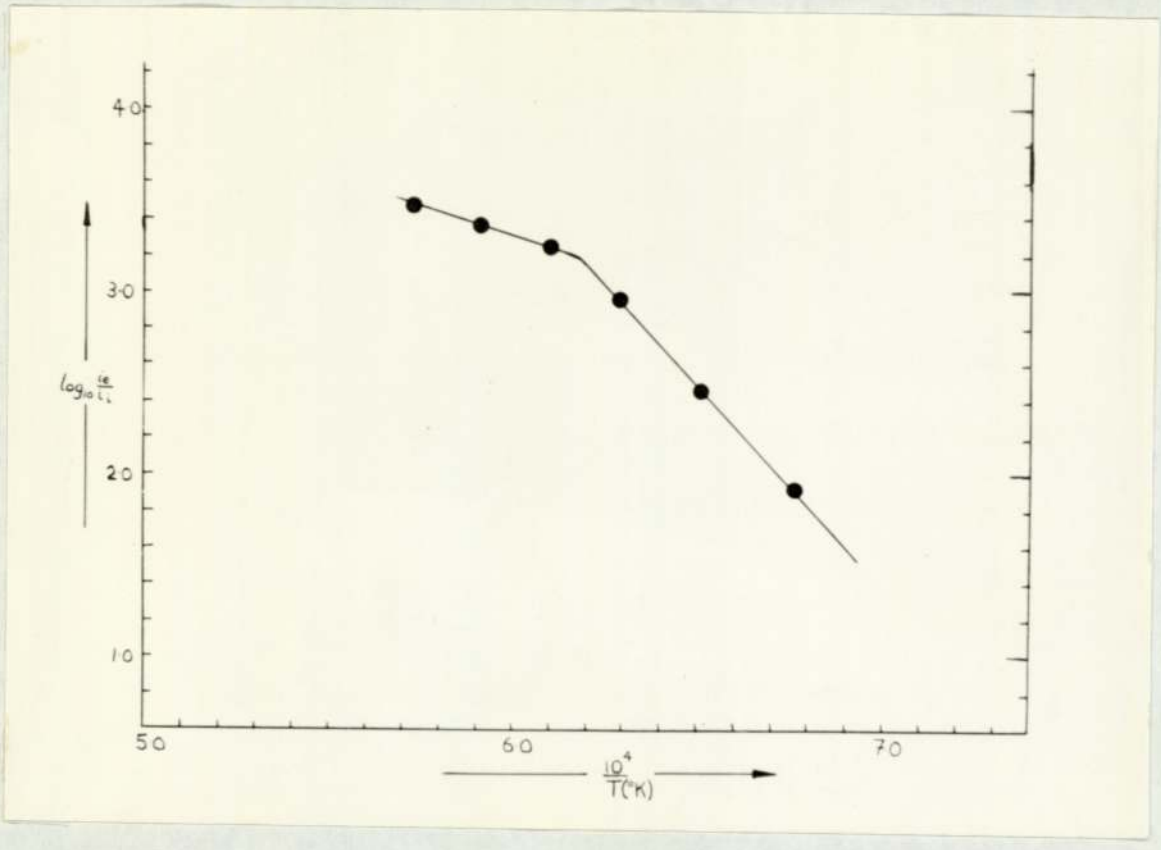

Electron capture by nitrogen dioxide.

FIGURE 10.

4.1.1. Nitrogen dioxide

The graphs obtained from plotting log (i_e/i_i) against $10^4/T^oK$ characteristically consisted of three parts: (i) a low temperature portion having a slope corresponding to an apparent electron affinity $E'(\bar{T})$ of 96 kcals/mole at the mean temperature $\bar{T}$; (ii) an intermediate region with $E'(\bar{T})$ = 5 kcals/mole; (iii) a high temperature portion with $E'(\bar{T})$ = -32 kcals/mole. Although all of the graphs were of the same form, the individual portions were not shown well together.

Low-temperature region

The 20 runs which showed this portion well enough for a reasonable line to be drawn gave a mean value of 94 $\pm$ 10 kcals/mole. The most reliable experimental lines from this set had slopes corresponding to 92.8, 99.7, 97.0, 94.3, 90.5, 102 and 97.0 kcals/mole. Hence E'_{1537^oK} = 96.2 $\pm$ 3.7 kcals/mole. A typical result is shown in figure 10.

It is unreasonable to suppose that this magnitude of energy change can correspond to any process other than the direct capture of an electron by NO_2, since, if any

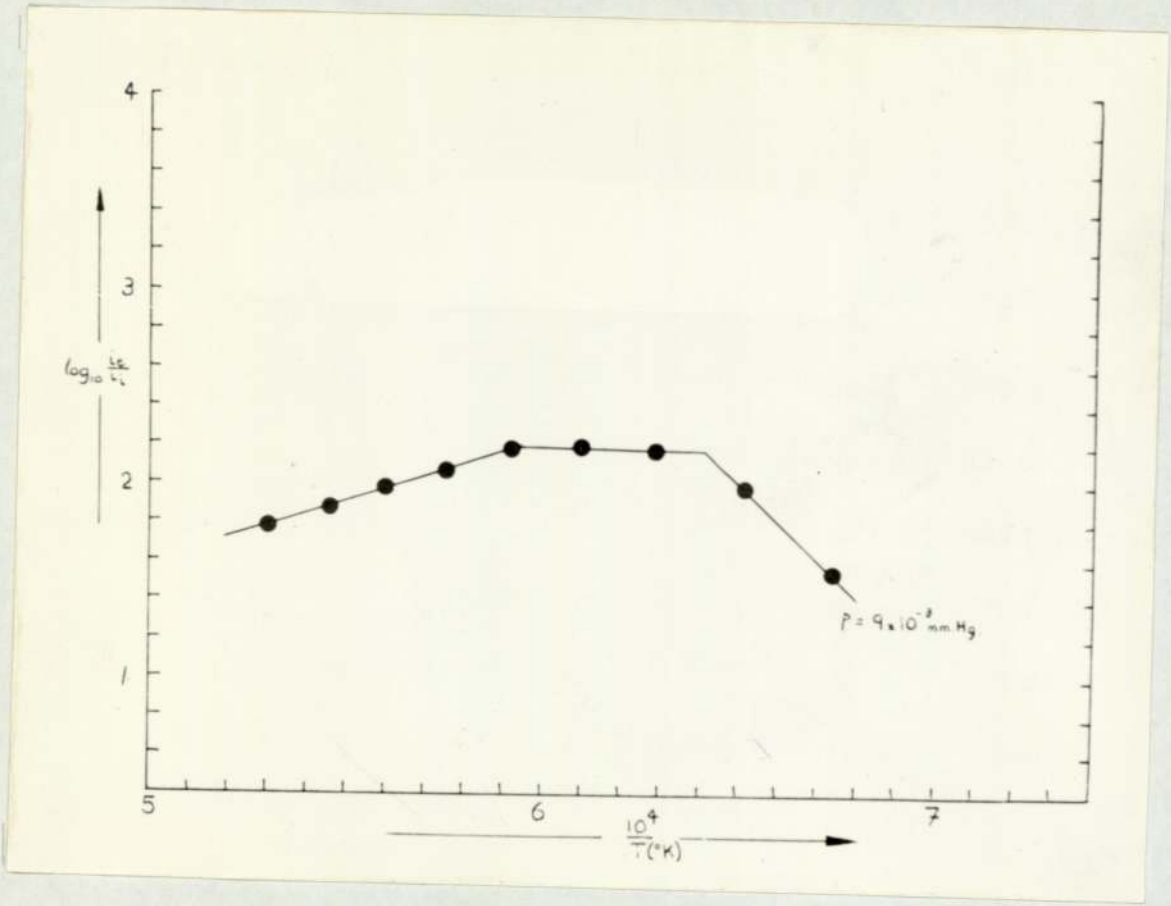

Electron capture by nitrogen dioxide.

FIGURE 11.

bonds are broken the final electron affinity of the fragment must exceed 96 kcals/mole. This result must, therefore, be attributed to the process $NO_2 + e \longrightarrow NO_2^-$. The specific heat correction is that due to the loss of the three translational degrees of freedom of the electron and is therefore $-(3/2).R\bar{T}$. Hence,

$E_o(NO_2) = 92 \pm 3.7$ kcals/mole.

The scatter in these results is understandably large since the measured values will be influenced by the decomposition of the substrate which must be occurring upon the hot filament and also because the measured ion currents were very small ($10^{-12} - 10^{-13}$A), close to the limit of detection of the apparatus (10^{-14}A) and comparable with the current induced by the vibration of the apparatus in the field of the solenoid. The experimental slope was also strongly affected by small errors in the measured temperatures.

High temperature region

The most reliable lines had slopes corresponding to $-E'(\bar{T})$ being 31, 31, 34, 33, 33, 34 and 29 kcals/mole (fig. 11). Hence, $E'_{1830^oK} = -32.1 \pm 1.7$ kcals/mole.

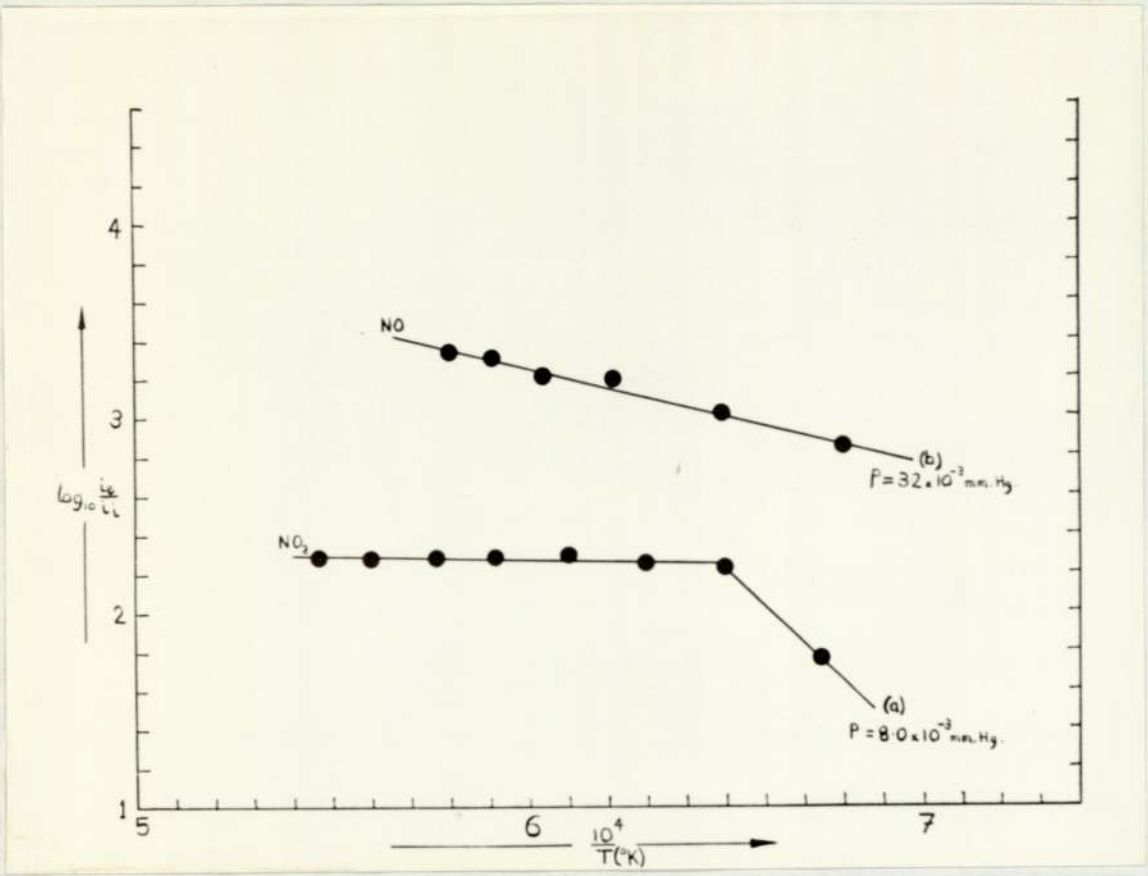

Electron capture by nitrogen dioxide & nitric oxide.

FIGURE 12.

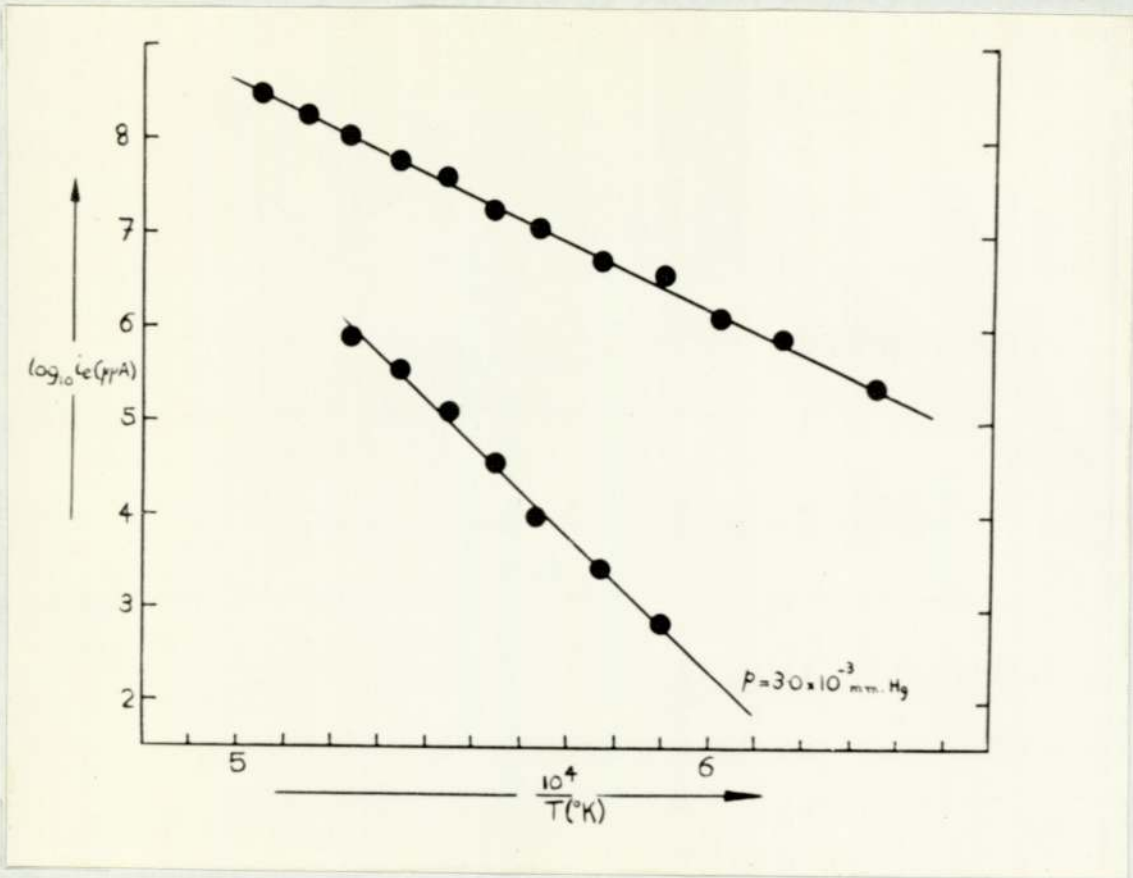

Electron work functions, W & NO_2/W.

FIGURE 13.

This is attributed to the process $NO_2 + e \longrightarrow NO + O^-$. The specific heat correction is estimated as $-(5/2).R\bar{T}$, so that $E'_o = -40.8 \pm 1.7$ kcals/mole. The O-NO bond energy is 72 kcals/mole[50] and since $E'_o = E_o - D$, $E_o(O) = 31.2 \pm 1.7$ kcals/mole. This is in satisfactory agreement with the value of 34 kcals/mole deduced from measurements upon N_2O, H_2O and O_2.[16]

Intermediate region

The results in this region predicted a mean apparent electron affinity of 5.0 ± 5 kcals/mole (20 runs), the best straight lines having slopes of 3.2, 6.4, 6.9, 1.8, 1.8, 5.0, 4.6, 7.7 and 7.7 kcals/mole. Hence $E'_{1670^oK} = 5.0 \pm 2.2$ kcals/mole (fig 12a).

There are several possible explanations of this result. The most obvious is that, since this region corresponds to a maximum, the apparent slope has no real meaning. This is unlikely to be true since the only results which were considered had flat portions which extended over too great a temperature range to be mere experimental error. They had moreover, no sign of a maximum and so the reasonable assumption is that they

represent a real process.

The reactions occurring on either side of this region can both be attributed to the interaction of NO_2 with the filament and so it appears probable that this process also involves NO_2. There is, however, the possibility that the result is due to electron capture by NO, formed by the gas phase decomposition of NO_2. In order to eliminate this, the electron affinity of NO was measured. The data obtained showed that, with NO at the same pressure as the NO_2, the ion currents were 10 times lower than those found in this region and the apparent electron affinity was 26 kcals/mole. These figures are plotted in figure 3b, for comparison. It therefore seems very unlikely that this result is due to NO.

This leaves a reaction involving NO_2 and yielding a positive apparent electron affinity. Fission of the molecule is impossible since the only reasonable products, NO^- or O^-, would both give rise to negative values of E'. The only possible reaction would therefore seem to be $NO_2 + e \longrightarrow \left[NO_2^-\right]^*$. The specific heat correction will be $-(3/2).R\bar{T}$ and so $E'_o(NO_2)^* = 0 \pm 2.2$ kcals/mole.

4.1.2. Nitric oxide

As previously mentioned, the ion currents from NO were very much lower than those from NO_2. The results obtained were 27.4, 26.1, 21.1, 28.4 and 25.0. Whence $E'_{1630^\circ K} = 25.6 \pm 2.5$ kcals/mole. The specific heat correction will again be $-(3/2)R\bar{T}$, so that

$E_o(NO) = 20.6 \pm 2.5$ kcals/mole,

4.2 Discussion of results

Previous estimates of the electron affinity of NO_2 vary greatly. X-ray diffraction has established[51] the structure of the ion as angular with an O-N-O angle of 125° and an N-O bond length of 1.13Å. The axial ratio is therefore about 2:1 and the assumption of spherical ions will not lead to a large error. From the known densities of sodium, potassium and silver nitrites the crystal radius of the ion may be estimated as 2.05, 1.98, and 1.96Å, giving a mean radius of 2.0Å. This is greater than the "thermochemical" radius of 1.55Å proposed by Yatskimirskii[52] and used by him in conjunction with the lattice energy formula of Kapustinsky[53] to derive the lattice energies of the alkali metal nitrites.

Based on this work Pritchard[54] proposed an electron affinity of 37.5 kcals/mole for NO_2. If the radius of 2.0Å is substituted into Kapustinsky's formula the electron affinity becomes some 20 kcals higher. The uncertainty in these estimates is, however, considerable.

Smith and Seman[55] claim to have observed photodetachment of the electron at photon energies of 3.0 e.V thus placing an upper limit of 69 kcals/mole on the electron affinity. Conversely Curran[56] has observed charge transfer between the ions O^-, SF_6^-, SF_5^-, Cl^- and NO_2. This places a lower limit of 87 kcals/mole on the electron affinity. Such a high value would be in agreement with the ease of forming NO_2^- by electrical discharges in air, but is to be contrasted to the difficulty of forming it by direct electron capture or discharges in NO_2.[57] The electron capture cross-section of NO_2 has been estimated by Fox[58] as $10^{-20} cm^2$, approximately one hundredth that of oxygen.

There have been few previous estimates of the electron affinity of NO, due largely to the impossibility of performing lattice energy calculations. Pritchard[54] has suggested a small positive value and the figure

given here is in accord with this.

From the observations cited above it seems that the formation of NO_2^- is favoured by the possibility of bimolecular collision processes, but direct electron capture is inefficient. This may be explained if the thermoneutral process observed here leads to the formation of an excited ion. The promotion energy of the excited state corresponds closely to the weak absorption band occurring at 3100Å in the nitrite ion, alkaline nitrite solutions, nitromethane, nitrosyl chloride, nitric acid and the nitrates. This has been attributed to an $n_o, \overline{\pi}^*$ transition.[59] The occurrence of this transition at a wavelength corresponding so closely to the electron affinity of NO_2 adds some support to the identification of the thermoneutral process.

Of the processes leading to the formation of the ground-state nitrite ion, those which involve direct electron capture or simple bond formation, e.g.,

$$NO_2 + e \longrightarrow NO_2^- \qquad \text{- - - - - 4.1}$$

$$NO + O^- \longrightarrow NO_2^- \qquad \text{- - - - - 4.2}$$

are exothermic by at least 92 kcals/mole, and the resultant ions will break down so that the process will be very inefficient. The intervention of a chaperon molecule will increase the efficiency but the corresponding processes leading to the formation of the excited ion will always be favoured. Since the transition to the ground state and electron detachment are in almost exact resonance, the excited ions will also break down very rapidly. The overall process will therefore always be one of very low efficiency.

Any process involving formation of the ground state of the ion by a bimolecular mechanism would be expected to be much more efficient and two possible examples are

$$NO_2 + X^- \longrightarrow NO_2^- + X \qquad ------ 4.3$$

$$NO + O_2^- \longrightarrow NO_2^- + O \qquad ------ 4.4$$

In both cases ΔH will be less than the excitation energy of the ion and there is also the possibility of kinetic energy transfer to the eliminated fragment. Reaction 4.3 corresponds to the charge transfer observed by Curran, and the value of 92 kcals/mole proposed here for the electron affinity of NO_2 supports Curran's

lower limit of 87. Reaction 4.4 is of interest since Branscombe[57] has noted that the NO_2^- formed in discharges through air seems to be formed at the expense of O_2^- ions.

In the light of these facts it seems probable that the observation by rocket-borne mass spectrometers[60] that the majority of the negative ions in the E layer of the upper atmosphere are NO_2^-, must be explained on the basis of reactions 4.3 and 4.4. Since 96.5% of the negative ions are NO_2^-, the overall equilibrium given by reaction 4.1 may be assumed and the Saha equation used to compute the electron affinity from the known upper atmosphere concentrations.

$$\log_{10} K_p = - \frac{5040\ V}{T} + \frac{5}{2}\log_{10} T - 5.9 \quad - - - \quad 4.5$$

If $T = 280^{\circ}K$, $K_p = [NO_2][e] / [NO_2^-]$, $[NO_2^-]/[e] \simeq 10^{-14}$ (61) and taking $[NO_2]$ as $10^7 cm^{-3}$ (62) gives $V = 0.48$ eV.

It is clear therefore that the NO_2 and NO_2^- are not in thermodynamic equilibrium with the electrons. Alternatively, assuming processes 4.3 or 4.4, since the entropy of the reaction will be negligible,

$$\log K_p \simeq \exp(-H/RT). \qquad ---- \quad 4.6$$

Substitution again leads to the conclusion that the NO_2^- is not in thermodynamic equilibrium with the oxygen ions.

The NO_2^- ion is probably present at a steady state concentration determined by the rate of photodetachment of the electrons, but in the absence of any data on the rate of the radiative attachment process it is not possible to estimate the position of equilibrium. It is probable, however, that the rate of photodetachment from the excited state will be prohibitively large and the NO_2^- in the upper atmosphere is in the ground state condition. This conclusion is borne out by the observation[63] that the local polar radio dawn occurs at a time which suggests that visible light from the sun is not effective in causing photodetachment of the electron from some unidentified negative ion. It appeared that the ion must have an electron affinity such that radiation shorter than 2900Å was needed for detachment to occur. This strongly suggests the ion to be NO_2^- .

Since this work was completed a further estimate of the electron affinity of NO_2 has been made from a mass

spectrometric study of the alkyl nitrites.[6] The result obtained is in almost exact agreement with the figure proposed here.

The results of this study can be seen to give a good account of the known chemistry of the nitrite ion in the gas phase. In view of the extreme difficulty experienced in making the measurements upon this system, the agreement between the present results and other studies is extremely encouraging since few other compounds have given so much trouble in measurement.

The general theory of the formation of negative ions upon metal surfaces, developed later predicts slightly different specific heat corrections than those used here. The effect upon the results of this section is however only marginal and does not alter the arguments in any way.

5. ELECTRON CAPTURE BY THE OXIDES OF NITROGEN UPON TUNGSTEN FILAMENTS AND RELATED STUDIES

5.1 Experimental

The NO_2 was prepared in the same manner as described in section 4.1. NO, CO and N_2O were supplied by the Matheson Co Inc and O_2 by the British Oxygen Co. Ltd. All were used unpurified.

5.1.1. Nitrogen dioxide upon tungsten

The measurements made upon this system were made difficult by the erosion of the filament by the NO_2. This necessitated the measurement of the temperature of the filament for each point in a run. In order to avoid this the results were analysed by the procedure due to Gaines and Page described in section 3.4. This procedure requires a knowledge of the thermionic work function of the filament. This was measured and values of 9.61, 9.74, 9.54 and 9.51 eV were obtained, giving a mean value of 9.60 eV. This result was not in agreement with the 'third law' value calculated from a single electron current, assuming Richardson's equation,

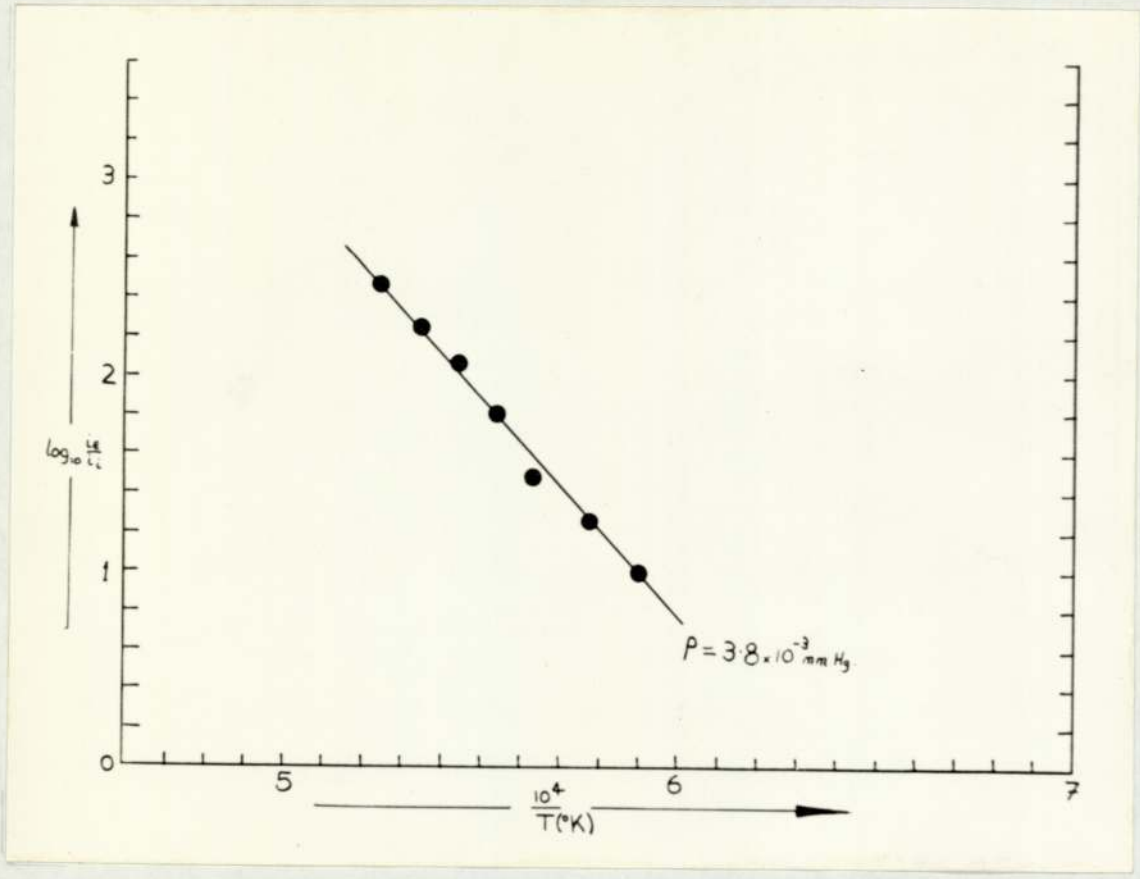

Ion - electron current ratio NO_2/W.

FIGURE 14.

which suggested a figure of approximately 5.5 eV. It was clear however that the electron affinities derived from Arrhenius and log - log plots were only in agreement when the work function of 9.60 eV was used in the analysis of the latter.

The following electron affinities were obtained:

(i) Arrhenius analysis, E'_{1792^oK} = 107, 105, 103 kcals/mole.

(ii) Log - log analysis, E'_{1792^oK} = 108, 107, 93.6, 90.0, 87.5, 88.4, 92.5 kcals/mole. (= 9.60 eV.)

Figure 13 shows a work function plot together with a measurement made upon the same filament in the absence of NO_2 vapour. This latter corresponds to a 'clean surface' work function of 4.79 eV. An Arrhenius plot of the current ratio is shown in figure 14.

5.1.2. Nitrogen dioxide upon rhenium

These results were very similar to the W ones in that the thermionic work function was raised from 4.0 eV to 7.5 eV. The measured values of the apparent electron affinity were E'_{1550^oK} = 83, 81.5 and 94 kcals/mole. Measurements with this system were made difficult by the deposition of a brown substance on the interior surfaces

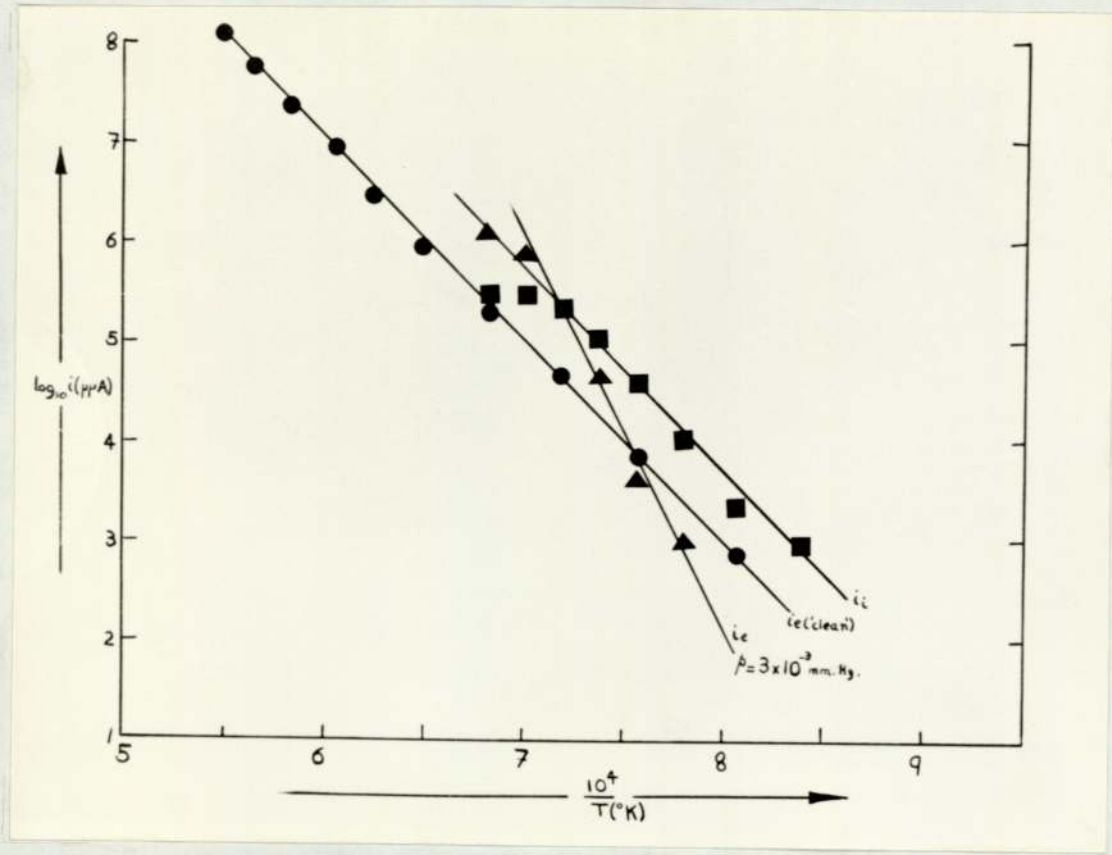

Thermionic currents, Re & NO_2/Re.

FIGURE 15.

of the apparatus. This was presumed to be an oxide of rhenium and its rate of deposition suggested that reactions with the filament were occurring at an appreciable rate. The most unusual feature of the results was that the ion currents were generally larger than the electron currents. This is shown in figure 15 where these figures are combined with a 'clean surface' work function measurement.

5.1.3. Nitric oxide upon tungsten

This system again showed an anomalous thermionic work function. The measured values were, $\chi'_{1788^{o}K}$ = 160, 161, 161, 160, 159 and 158 kcals, all at a pressure of 1.8×10^{-3} mm Hg. The results were more complex than the NO_2/W figures in that there was evidence for a sudden rise in the thermionic work function at low temperatures. Although this effect was well authenticated it was not possible to draw a reliable line through the limited number of points available in this temperature range. The evidence however suggests a rise in the thermionic work function to approximately 230 kcals in this region. These effects are shown,

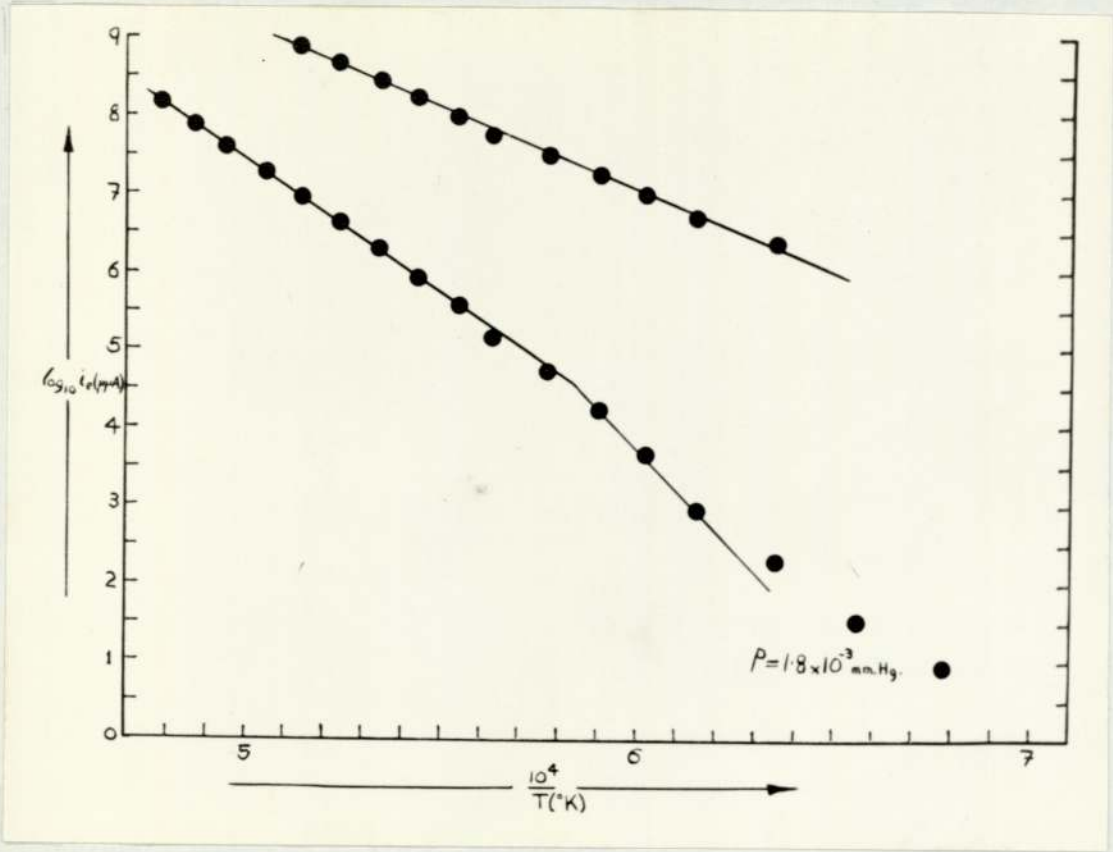

Electron work function, W & NO /W.

FIGURE 16.

together with a 'clean surface' work function measurement, in figure 16.

Arrhenius plots of the electron/ion current ratio were linear over the temperature range in which the work function showed changes and were non-linear in the range in which the work function plots were linear. These effects are shown in figure 17. The measured apparent electron affinities were, $E'_{1740^{o}K}$ = 74.1, 73.1, 74.5, 79.1 and 81.5 kcals/mole.

5.1.4. Carbon monoxide upon tungsten

The complexity of the NO_2 and NO measurements upon W and Re suggested that comparison data would be valuable, especially if the anomalous work functions could be reproduced in the presence of gases which were simpler than NO_2 and did not have the possibility of forming such stable ions. Work function and adsorption data are available for CO and O_2 upon W and so these were chosen for study.

The CO results were very similar to the NO in form, but it proved impossible to distinguish the ion currents from the background current. The measured thermionic

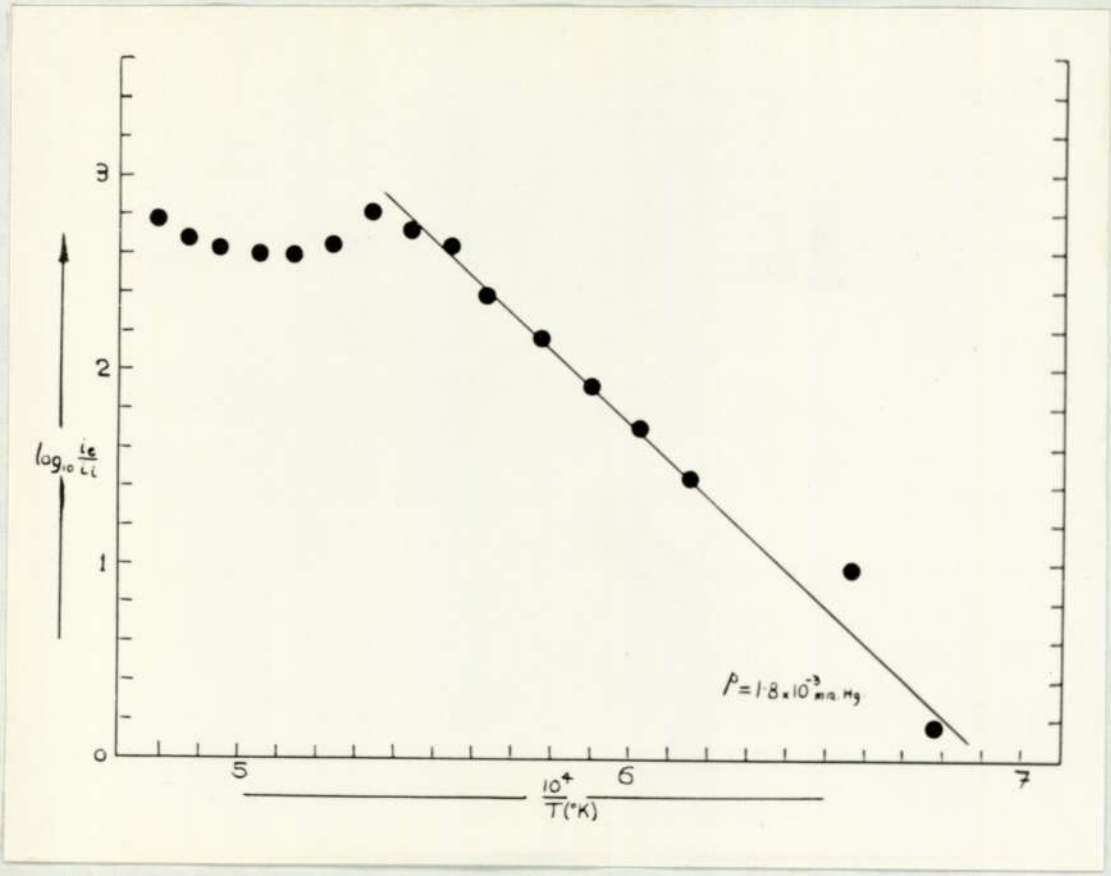

Thermionic ion current NO/W.

FIGURE 17.

work functions at a pressure of 8×10^{-3} mm Hg were,

$$\chi'_{1750^\circ K} = 162,\ 164,\ 165 \text{ kcals.}$$

$$\chi'_{1610^\circ K} = 231,\ 229,\ 228 \text{ kcals.}$$

Figure 18 shows the effect of CO and O_2 upon the thermionic electron current deriving from a 'clean' W surface.

5.1.5. Oxygen upon tungsten

Two distinct series of measurements were made upon this system in different types of apparatus. The high pressure series were made in the conventional magnetron described in section 3.2. The low pressure measurements were made in a linear form of the apparatus described in ref 20. The results of both series are summarised below. As in the previous system, the ion currents were indistinguishable from the background.

χ'_o = 184, 214, 205, 207, 205, 200, 196, 205, 198, 206, 197.

p = 1.0, 1.3, 2.6, 3.3, 3.9, 4.6, 5.2, 6.5, 7.5, 400, 110.

$\chi'_o = \chi'_T - 2RT$ and p is in units of 10^{-5} mm Hg.

At the lower temperatures the line of the work function plot has a pronouced curvature, presumably due to the

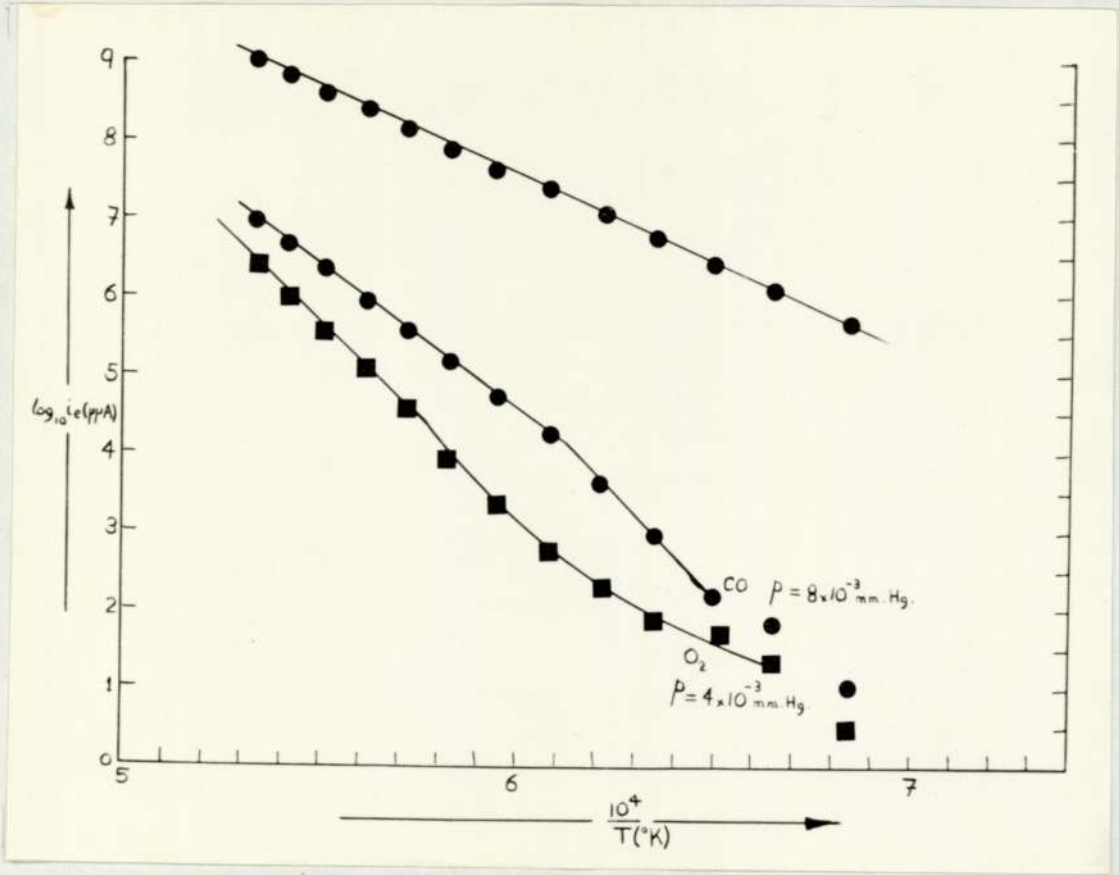

Electron work functions; W, CO/W & O_2/W.

FIGURE 18.

reaction of the gas with the filament and desorption of WO_3.

5.1.6. Oxygen upon iridium

Attempts to measure the electron affinity of the oxygen molecule upon this filament material were hampered by the adsorption of the gas giving rise to an anomalous thermionic work function and very small ion currents. The work function data are summarised below and the data for p = 1.2×10^{-3} mm Hg are shown in figure 19 together with a measurement of the 'clean surface' work function.

$\chi'_{1590^\circ K}$ = 160, 166, 162, 157, 158, 156. kcals.

p (mm Hg x 10^3) = 12, 10, 9, 8.5, 7.5, 7.0.

$\chi'_{1570^\circ K}$ ('clean') = 87.0 kcals.

5.1.7. Nitrous oxide upon iridium

This system also gave rise to very small ion currents and an increased thermionic work function. At the highest pressures the measurements indicated a single work function of 147 kcals. As the pressure was reduced this became resolved into two regions of constant thermionic work function. Figure 19 shows the effect

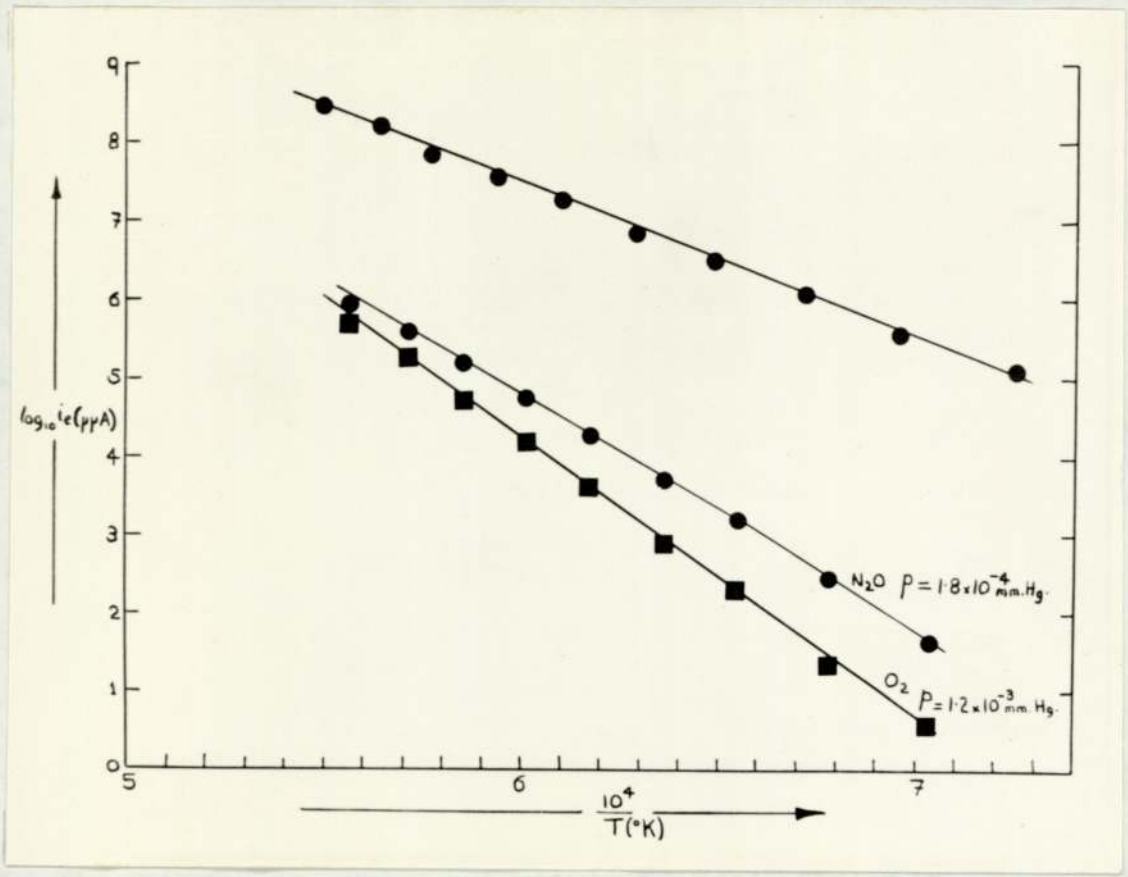

Electron work functions; Ir, O_2/Ir & N_2O/Ir.

FIGURE 19.

at $p = 1.8 \times 10^{-4}$ mm Hg. The work functions obtained were,

$\chi'_{1678^\circ K}$ = 147, 140, 135, 126, 123, 128, 122 (kcals.)

p = 13, 9, 3.5, 2.5, 1.8, 1.0, 0.8 (mm Hg $\times 10^3$)

$\chi'_{1522^\circ K}$ = - , - , 160, 169, 151, - , 143 (kcals.)

The 'clean surface' work function of 87.0 kcals compares favourably with figures of 87.8, 89.2, 87.8, 88.3, 88.3, and 89.2 kcals measured with other filaments from the same sample of iridium. With these measurements and the O_2/Ir ones, it was impossible to distinguish the ion currents from the background (approximately $10^{-5} i_e$).

5.2 Discussion of results

5.2.1. Work functions

The most obvious feature of the results quoted in the previous section is the anomalous thermionic work function of metal surfaces exposed to low pressures of oxygen containing gases. This is possibly due to the adsorption of the gas upon the surface and it is therefore necessary to consider the probable consequences of this process upon such measurements.

A polycrystalline surface of total area A cm^2 may be considered to be composed of i patches, where the ith patch occupies an area $\Theta_i A$ cm^2 and has a characteristic work function χ_i. If Richardson's equation [38] (2.8) describes the emission current from each patch, then

$$i_t = \sum_i . i_i = \bar{d}_m BAT^2 \sum_i \Theta_i . \exp(-\chi_i/RT) \quad ----- 5.1$$

where i_t is the total current from A cm^2 of surface and $\bar{d}_m$ is the mean transmission coefficient. The 'apparent thermionic work function' may be defined by,

$$\chi'(T) = -R.d\log.i_t/d(1/T) \quad ----- 5.2$$

whence, by differentiation of equation 5.1,

$$\chi'(T) = 2RT + \sum_i \phi_i \chi_i + RT^2 \sum_i \phi_i . d\log.\Theta_i/dT - T \sum_i \phi_i d\chi_i/dT \quad ----- 5.3$$

where $\phi_i = i_i/i_t$.

For clean surfaces χ_i and Θ_i may be considered to be temperature independent so that

$$\chi'(T) = 2RT + \sum_i \phi_i \chi_i \quad ----- 5.4$$

Equation 5.4 may be used to define the mean apparent thermionic work function of the surface,

$$\chi'_m(T) = \sum_i \phi_i \chi_i \qquad \text{- - - - - 5.5}$$

The mean apparent thermionic work function is not the same as the mean work function as measured from contact potential differences, which is defined[64] as,

$$\overline{\chi}(T) = \sum_i \Theta_i \chi_i \qquad \text{- - - - - 5.6}$$

Since the weighting factors of the two summations differ exact agreement between contact potential and thermionic work functions is not to be expected for anything other than uniform surfaces.

If Richardson's equation is written in the form,

$$i_t = \bar{a}_m BAT^2 \exp(-\chi_m(T)/RT) \qquad \text{- - - - - 5.7}$$

then, by differentiation,

$$\chi'_m(T) = \chi_m(T) - T.d\chi_m(T)/dT \qquad \text{- - - 5.8}$$

For emission from clean surfaces, the last term in equation 5.7 approximates to zero and $\chi'_m(T)$ and $\chi_m(T)$ may be assumed to be identical. For this to be generally true, differentiation of equation 5.5 gives,

$$\sum_i \chi_i d\phi_i/dT = 0 \qquad \text{- - - - - 5.9}$$

This will only be rigorously true when $\phi_i = 1$ and $\chi_i = \chi'_m(T)$. Its validity in other cases is associated with the form assumed for equation 5.1.

Although a polycrystalline surface may be considered as consisting of discrete regions of differing work function, it is not possible to continue the summation of equation 5.1 over such areas as the patches become smaller. Under the conditions of small anode fields present in the magnetron, the Schottky barrier, which defines the point which the emitted electrons must pass before being free from all significant interaction with the metal, is located at about 10^{-4}cm from the surface. Up to this distance the electrons must be considered as being in equilibrium with those inside the metal. Patches on an atomic scale are not discernable to electrons at such a distance and so it is only meaningful in such circumstances to consider the surface as being composed of areas with a mean work function which is dependent upon the size and distribution of the crystallites.

The thin wires used for filaments in the magnetron will have a surface structure which will normally be essentially random due to the high curvature of the surface. This will result in all patches having much the same work function and equation 5.8 being true. The converse however would be expected with ribbon filaments where the flat surface would favour the growth of particular crystal faces. This would result in a curvature of the normal plot of Richardson's equation. Such behaviour has been observed with zirconium ribbon filaments but it is by no means certain that this was the cause of the effect.

For the data given in section 5.1, the values of $\chi'_m(T)$ and $\chi_m(T)$ are identical for the 'clean' surface work function measurements but not for the 'covered' surface measurements. In all of the systems studied (excepting the NO_2/Re) the general effects are the same, a reduction in the absolute magnitude of the electron current relative to that deriving from the 'clean' surface and an abnormally large apparent thermionic work function.

The change in the mean thermionic work function $\chi_m(T)$, relative to the same surface in the absence of gas, may be calculated by comparing the 'clean' and 'covered' electron currents;

$$i_o/i_t = \exp(\chi_m(T) - \chi_o)/RT = \exp. \Delta\chi_m(T)/RT. \quad 5.10$$

where $\chi_m(T)$ is the mean thermionic work function of the surface in the presence of the gas and χ_o the corresponding figure in the absence of the gas. The data of figures 13, 16, 18 and 19 yields the following values of $\Delta\chi_m(T)$ (in kcals).

System	NO_2/W	NO/W	CO/W	O_2/W	N_2O/Ir	O_2/Ir
p(mm x 10^4)	30	18	80	40	1.8	12
χ_o	103	91	105	105	81	81
T^oK						
1887	18.6	18.3				
1852	20.3	19.1	18.2	23.3		
1818	22.0	19.9	19.0	25.1		
1786	23.6	20.8	19.7	26.6	18.6	21.0
1754	25.1	21.4	20.6	28.4	19.0	21.9
1724	26.5	22.2	21.4	30.5	19.5	22.8
1695	28.0	23.6	22.0	32.6	20.0	23.8
1667		25.1	22.7	33.5	20.4	24.6
1639		26.6	23.6	34.5	20.8	25.4
1613			25.1	34.8	21.1	26.1
1587			26.6	35.4	21.5	26.8
1563			28.2	34.8	21.8	27.6
1539			29.7	32.9	22.1	28.6
1515			29.6	32.4	22.6	29.0

TABLE 5.1.

System	NO_2/W	NO/W	CO/W	O_2/W	N_2O/Ir	O_2/Ir
T^oK						
1493			29.6	32.5	23.2	29.7
1471			30.8	33.5	23.9	30.4
1449					24.4	31.0
1429					25.0	31.6

TABLE 5.1. (cont)

It is apparent from this table that $\Delta\chi_m(T)$ varies inversely with T, as would be expected if the adsorbed gas which causes the increased mean work function was being desorbed as the temperature was raised. Figures 13, 16, 18 and 19 show that $\chi'(T)$ is sensibly constant over considerable ranges of temperature and the data given in section 5.1 shows $\chi'(T)$ to be, to a first approximation, independent of the pressure of the gas.

The CO and O_2/W data in table 5.1 may be compared with other measurements of the change in mean work function ($\sum_i \theta_i \chi_i$) consequent upon the adsorption of these gases. The agreement in the case of the CO/W data is not very satisfactory. Eisinger[65] measured

the potential difference between clean 113 faces and those covered by CO by a photo-electric method and found a maximum change of 0.86V (19.8 kcals) at $\theta = 1$. These measurements however were made at much lower temperatures and on a surface of low packing density (3.7×10^{14} atoms cm^{-2} compared to the present surface with approximately 10^{15} atoms cm^{-2}). Increasing this latter would increase $\Delta\chi_m$ by rather less than the simple ratio of the packing densities because of the mutual polarisation of the surface dipoles. The present results differ from those of Eisinger by approximately the expected amount.

Measurements of the corresponding function for O_2/W are summarised in table 3 of reference 64, giving a mean value of 1.77V (40.8 kcal). This compares favourably with the present estimate of about 35 kcal. The data are also in agreement with the work of Kingdon[37] who measured the apparent thermionic work function of tungsten filaments exposed to low pressures of oxygen and obtained a figure of 212 kcal for χ_o'. Measurements at different pressures showed this to be

independent of the gas pressure and Kingdon therefore concluded that the surface was fully covered by oxygen ($\theta = 1$). This assumption was later criticised by Reiman[66] who used equation 5.7 and estimates of A and χ_o to obtain a figure of 1.75 eV (40.3 kcals) for $\Delta\chi_m$ (1500°K) from Kingdon's data. Repeating this calculation but using estimates of 0.6 for $\bar{d}_m$, a surface roughness factor of 1.3 [66] and the present measured value of χ_o = 105 kcals, gives the data in table 5.2.

$T^{\circ}K$	1667	1639	1613	1587	1563	1539	1515	1493
$\Delta\chi_m(T)$	27.7	29.1	30.3	31.7	32.8	34.1	35.2	36.3

TABLE 5.2.

Considering the uncertainties in the calculation, the agreement with the present data is very satisfactory.

All of the work function changes calculated from the thermionic data are lower than the modern estimates of the maximum contact potential difference between clean and oxygenated tungsten surfaces. This adds more weight to Reiman's original criticism of the estimate of $\Theta = 1$. Reference to the field emission work of George

and Stier[67] suggests that in the present system Θ changes from 0.8 at low temperatures to 0.4 at the highest. These would appear to be reasonable estimates.

The difference between the values of $\chi'_m(T)$, evaluated graphically, and $\chi_m(T)$, calculated from equation 5.7, in the case of metals exposed to oxygen containing gases indicates that either ϕ_i or χ_i is temperature dependent. The absence of any such dependence for the former function in the case of emission from the 'clean' surfaces would suggest that any variation must be associated with χ_i. If the decrease in $\Delta\chi_m(T)$ with increasing temperature is due to desorption of the gas, equation 5.8 may be used to obtain a more explicit form for $\chi'_m(T)$.

Substituting $d\chi_m(T)/dT = [d\chi_m(T)/d\Theta][d\Theta/dT]$, and evaluating $d\Theta/dT$ by differentiation of the general isotherm

$$(1-\Theta) = \Theta.k_o.T^n.\exp[-q(T)/RT] \quad - - - - \quad 5.11$$

gives, if $\Theta(1-\Theta)dq(T)/d\Theta$ is large compared to RT,

$$\chi'_m(T) = \chi_m(T) - q(T).d\chi_m(T)/dq(T) - nRT.d\chi_m(T)/dq(T)$$

$$- - - - \quad 5.12$$

The relationship between changes in the work function and heat of adsorption has been studied by Mignolet.[68] He considered the change in work function to be due to the transfer (partial or complete) of an electron from the conduction band of the metal into a vacant adsorbate orbital and showed that, if the reduction in the heat of adsorption may be entirely attributed to the reduction in the energy of the highest occupied level of the adsorbate, then $-\Delta\chi = \Delta q$. $\Delta\chi$ and Δq being the changes in the work function and the differential heat of adsorption respectively. Therefore, if

$$\chi_m(T) = \chi_o + \Delta\chi_m(T) \quad \text{and} \quad q(T) = q_o - \Delta\chi_m(T),$$

substitution into equation 5.12 gives,

$$\chi'_m(T) = \chi_o + q_o + nRT. \quad ----- \quad 5.13$$

Heats of adsorption calculated from equation 5.13 are given in table 5.3.

These assumptions also enable equation 5.7 to be expanded into a more useful form. Substitution of equation 5.11 into equation 5.7 gives,

$$i_t = \bar{d}_m BAk \frac{T^{(2+n)}}{p^x} \cdot \frac{\theta}{(1-\theta)} \cdot \exp\left[-(\chi_o + q_o)/RT\right]$$

$$----- \quad 5.14$$

where $k_o = k'/p^x$. The assumption of approximate constancy of Θ over the range of measurements (or alternatively $\Theta(1-\Theta)dq(T)/d\Theta$ being large compared to RT) leads to equation 5.13 by direct differentiation of 5.14. The value of k' will be characteristic of the adsorption desorption process occurring and is in principle calculable by the methods of statistical mechanics. A considerable simplification of equation 5.14 may be effected by comparing the electron currents deriving from the same surface in the presence and absence of the gas. Combining 5.7 and 5.14,

$$\frac{i_t}{i_o} = \frac{k'T^n \cdot \Theta}{p^x (1-\Theta)} \cdot \exp(-q_o/RT). \qquad ----- 5.15$$

Equating the $\Theta/(1-\Theta)$ to unity, assuming the values of x given in the table and making the approximation $\chi'_m(T) - \chi_o = q_o$ enables the values of $k'T^n$ given in table 5.3 to be calculated.

System	NO_2/W	NO/W		CO/W		O_2/W	O_2/Ir	N_2O/Ir	
q_o+nRT (kcals)	111	62	132	53	118	98	73	42	67
$\bar{T}^oK$	1792	1788	1640	1750	1610	1800	1590	1678	1522
$\log_{10}k'T^n$	10.0	5.3	14.4	4.6	13.6	9.2	6.4	2.6	6.0
x	0.5	0.5	1.0	0.5	1.0	0.5	0.5	0.5	0.5
$\log_{10}i_o/i_t$	2.84	2.54	3.56	2.56	3.44	3.13	3.71	2.63	3.35
$\log_{10}p$ (mm)	$\bar{3}.48$	$\bar{3}.26$	$\bar{3}.26$	$\bar{3}.90$	$\bar{3}.90$	$\bar{3}.60$	$\bar{3}.08$	$\bar{4}.26$	$\bar{4}.26$

TABLE 5.3

For non-dissociative reactions, transition state theory[69] gives the value of $k'T^n$ as; $kT.n_s.\frac{Q(g).Q^*(d)}{Q(A).Q^*(a)}$, where T is the surface temperature, n_s the number of adsorption sites per cm^2, k is Boltzman's constant, Q(g) the gas phase partition function per unit volume, Q(A) the adsorbed state partition function per unit area and Q* represents the partition function for the transition state for adsorption (a) or desorption (d). This equation is derived in section 6.2. $k'T^n$ will have a numerical value of 10^{11} - 10^{15} depending upon whether the adsorbed layer is mobile or immobile and the

associated value of x will be 1.

Assuming this value of x clearly gives a reasonable value of $k'T^n$ for the low temperature NO and CO figures. Unfortunately there is no comparison data available for the heat of adsorption of NO upon tungsten but there have been several studies of the CO/W system. Rigby[70] estimated the activation energy for desorption of the β_3 state of carbon monoxide on tungsten from the temperature of its maximum rate of desorption (about 1600°K), by assuming first order kinetics and a rate constant of 10^{13} sec^{-1}, as 90 kcals/mole. This is in agreement with the results of Ehrlich[71] (100 kcals/mole) and Redhead[72] (75 kcals/mole) who used the same method. The present estimate of 118 kcals/mole represents an upper limit for q_o. q(T) will be given by $q_o - \Delta\chi_m(T)$ and will be approximately 93 kcals/mole. Redhead found the heat of adsorption in the β_3 state to be approximately independent of the total surface coverage. Although an exact comparison of the data is not possible it is noteworthy that in these measurements $\Delta\chi_m(T)$ and hence q(T) changes by only 6 kcals/mole over the temperature range where this species is desorbing (1540 - 1640°K).

Since $\Delta\chi_m(T)$ reflects a change in the average energy of the highest occupied level of the adsorbate, $\Delta q(T)$ represents the change in the average heat of adsorption per adsorbed species. For the process AB(g) = A(s) + B(s), where g and s refer to the gas phase and adsorbed phase respectively, $q_o = Q_o/2$ where Q_o is the molecular heat of adsorption at zero surface coverage. Equations 5.14 and 5.15 therefore remain valid for dissociative adsorption-associative desorption processes. This treatment has ignored any variations in the $\Theta/(1-\Theta)$ term which will result from changes in the mobility of the adsorbed layer. This neglect is only justified so long as this term does not contribute to the apparent thermionic work function. This is only true to a first approximation, but its assumption greatly simplifies the interpretation of the results.

For the dissociative adsorption of diatomic molecules transition state theory gives

$k'T^n = \sqrt{kT.n_s^2.Q(g).Q^*(d)/Q(A).Q(B).Q^*(a)}$. If $Q^*(a) \backsim Q^*(d)$ this should lie between 10^3 and 10^7 depending upon the mobility of the adsorbed species. In

this case the associated value of x will be 0.5 and the molecular heat of adsorption will be approximately $2(q_o + nRT)$.

The NO/W and CO/W high temperature results fall within the expected range of $k'T^n$ but suggest an immobile adsorbed layer, which is unlikely at these high temperatures. An alternative interpretation would be that the transition state for desorption is more mobile than that for adsorption. This conclusion is also apparently necessary in order to interpret the ion current measurements of sections 8.1 and 8.2. It is also possible that the neglect of the $\Theta/(1-\Theta)$ term could introduce an error of a factor of 10. The assumption that the desorption process leads only to AB and not A,B,A_2 or B_2 is also probably an oversimplification. The broad measure of agreement between the observed and calculated values of $k'T^n$ however tends to confirm the assumption that the measurements correspond to dissociative adsorption reactions.

Again no comparison data are available for the NO/W figures but the dissociative heat of adsorption of NO

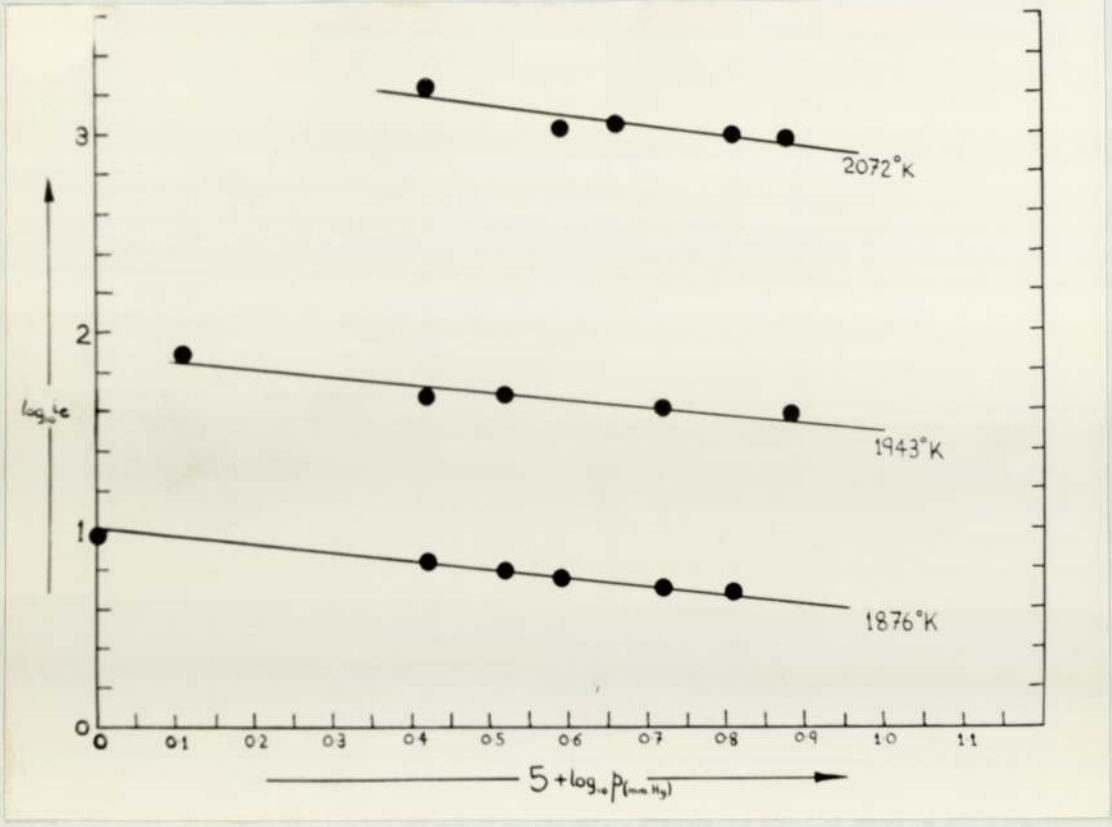

Pressure dependence of the electron current, O_2/W.

FIGURE 20.

may be estimated from the known heats of adsorption of N_2 and O_2 on W.[73] $Q(NO) = Q(O_2) + Q(N_2) - D(N-N) - D(O-O) + D(N-O) = 194 + 95 - 225 - 118 + 162 = 108$ kcals/mole, which compares favourably with the present estimate of 124 kcals/mole. The O_2/W results are also thought to be of this type and in this case there is sufficient data for the pressure dependence of the electron current to be determined. This is illustrated in figure 20 where the slopes of the lines approximate to 0.5. The large value of $k'T^n$ suggests that the transition state for adsorption and also the adsorbed atoms are considerably less mobile than the transition state for desorption. The heat of adsorption of 196 kcals/mole agrees well with the calorimetric figure of 194 kcals/mole.[73]

The molecular heat of adsorption of oxygen upon iridium, 146 kcals/mole, measured here, is more similar to that upon rhodium, 118 kcals/mole,[73] than to that upon platinum, 70 kcals/mole.[73] This is reasonable since rhodium bears the same relationship to iridium in the periodic classification as palladium, Q = 67 kcals/mole, does to platinum. In this connection it

is interesting to note that a single measurement of the work function of platinum exposed to 4×10^{-3} mm Hg of oxygen gave a value of $\chi'(T)$ of 145 kcals and $\log_{10} k'T^n = 4.71$ ($x = 0.5$). Clean surface measurements upon the same filament were not possible but experience with this material in measuring electron affinities has shown the work function of the clean surface to be close to 110 kcals at these temperatures. From this data the heat of adsorption of oxygen upon platinum would appear to be 70 kcals/mole, in good agreement with the value given in reference 73.

The adsorption of NO_2 upon tungsten is likely to be dissociative because of the low NO-O bond energy and high heats of adsorption of NO and O. There is insufficient data to determine the pressure dependence of the electron current, but the assumption of dissociation into NO and O leads to reasonable agreement between the measured and calculated heats of adsorption. Assuming $Q(NO_2) = Q(NO) + Q(O) - D(NO-O)$, utilising the data from this study gives $Q(NO_2) = 132 + 157 - 72 = 217$ kcals/mole, which compares favourably with the present

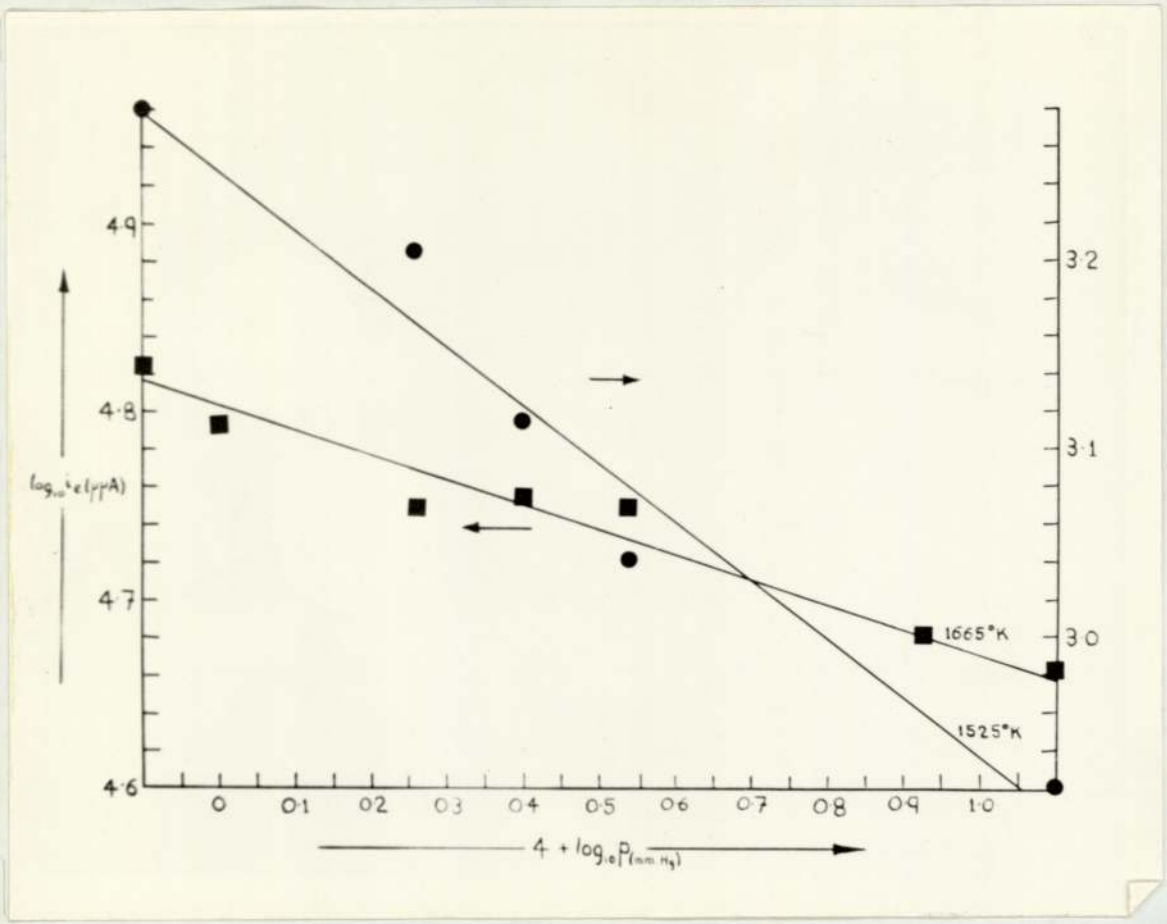

Pressure dependence of the electron current, N_2O/Ir.

FIGURE 21.

estimate of 222 kcals/mole. The value of $k'T^n$ suggests that the transition state for desorption is much more mobile than that for adsorption but, as in the O_2/W results, this may be a reflection of the importance of WO_3 in the desorption reaction.

The electron currents for the system N_2O/Ir are somewhat erratic but suggest a dependence upon $p^{-0.3}$ at low temperatures and $p^{-0.15}$ at high temperatures. These are illustrated in figure 21. If these figures are correct, the interaction of N_2O with the filament must be more complex than the other systems studied. The apparent thermionic work functions also seem to show a slight pressure dependence, in contradiction of equation 5.13.

The NO_2/Re results are also more complex than the simple theory allows. The abnormally large ion currents suggest that ion formation may perturb the simple adsorption desorption equilibrium. Both this system and the N_2O/Ir require a more extensive investigation before any detailed interpretations can be offered.

In general, the present treatment would appear to

give a satisfactory account of the order and magnitude of changes in the apparent thermionic work functions and electron currents of metal surfaces exposed to low pressures of gases which raise the local work function of the surface when adsorbed.

5.2.2. The determination of electron affinities under conditions of high surface coverage

The presence of a strongly adsorbed gas upon the surface of the filament of the magnetron will have two effects. The first of these is the alteration of the energy necessary to remove an electron from the metal and the second is the reduction in the surface area upon which other molecules may be adsorbed. The consequences of these effects with regard to the determination of electron affinities will depend upon the details of the ion forming process.

Equations 2.9 and 5.7 may be combined to give,

$$\frac{i_e}{i_i} = \frac{\bar{d}_m B T^{(2-m)}}{C.\Theta_A} . \exp\left[-(E-Q_A)/RT\right] \qquad ----- 5.16$$

Θ_A represents the fraction of the total surface area

which is covered by the ion precursor and Q_A is the associated heat of desorption. This latter term may be removed by substitution of an equation of the form of 5.11.

In the simplest type of reaction, the ion precursor will be the same as the strongly adsorbed species. If this is adsorbed without dissociation q(T) in equation 5.11 is equivalent to Q_A in equation 5.16, whence

$$\frac{i_e}{i_i} = \frac{\bar{d}_m Bk'T^{(2+n-m)}}{C.(1-\Theta).p} .\exp\left[-E/RT.\right] \quad ----- 5.17$$

The apparent electron affinity is defined by $E'(T) = -R.\left[d.\log(i_e/i_i)\right]/d(1/T)$ and if, as before, Θ remains effectively constant over the temperature range of the measurements, then $E'(T) = E + (2 + n - m)RT$. This is the process which would be expected to occur at low temperatures with NO and tungsten filaments. The magnitude of the result however is considerably in excess of the electron affinity of NO as measured upon Pt filaments and suggests the ions to be NO_2^-. The very large electron affinity of NO_2 would lead to very efficient ion formation by this material, which is

certain to be present in the apparatus due to the dissociative adsorption and recombination reactions occurring upon the hot tungsten surface. The curvature of the high temperature region of figure 17 would be in accord with the formation of more ions in this temperature range, where the adsorption is dissociative. At lower temperatures the predominant adsorption desorption process is molecular and the electron affinity measured approximates closely to that of NO_2, which must be present as a minor impurity in the gas. This effect would not be troublesome with Pt filaments since NO is not dissociatively adsorbed upon this material.

The apparent electron affinity of NO_2 when measured upon W filaments is close to the value measured upon Pt. This suggests the ion to be NO_2^-. Dr. J.T. Herron has investigated this system with a mass spectrometer and shown the predominant ion to be WO_3^- (private communication and Ref 82). The agreement would therefore seem to be fortuitous.

Finally it is pertinent to consider the effect of strongly adsorbed impurities which do not contribute to

the ion current. These will again lead to equation 5.16 and equation 5.11 may be used to substitute for Q_A. In this case the $(1-\theta)$ term in equation 5.11 must be replaced by $1-(\theta_i + \theta_A)$, where θ_i is the fraction of the total surface area which is covered by the strongly adsorbed impurity. If θ_i remains effectively constant then the poison will have no effect upon the determination of the electron affinity of A. Alternatively, if the adsorption of A is non-activated and the total surface coverage is small, the rate of adsorption will be independent of θ and so the impurity will again have no effect. Since the majority of adsorption processes are non-activated and the magnetron is normally operated under conditions of low surface coverage, the presence of small amounts of strongly adsorbed materials upon the surface of the filament, whether deriving from the gas or the interior of the metal, will not affect the determination of electron affinities. The most common impurity encountered in adsorption measurements is oxygen and this has been shown to give very small ion currents. The presence of small amounts of this gas should not therefore influence the determination of

electron affinities, even though it may raise the work function of the surface above that characteristic of the clean metal. This is an important conclusion since it demonstrates that the electron affinities determined by this method are not dependent upon the metal having a work function which is not influenced by the gases present in the system.

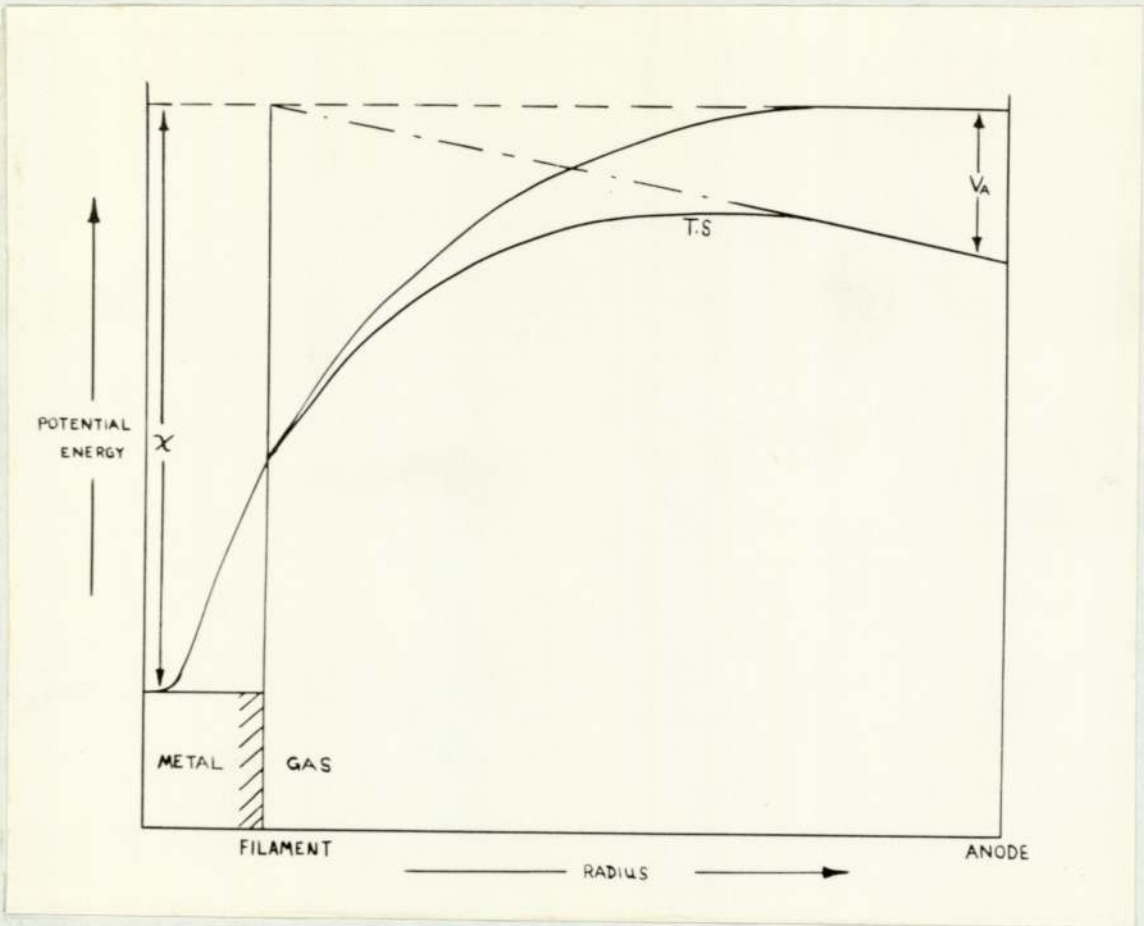

Potential energy barrier to electron emission.

FIGURE 22.

6. APPLICATION OF TRANSITION STATE THEORY TO ELECTRON EMISSION

6.1. Emission from clean surfaces

The main weakness of the kinetic approach to the determination of electron affinities by the magnetron method lies in the uncertainty of the procedure used to correct the measured values to $0^{o}K$. In an attempt to obtain more information about the rate of emission of electrons and ions from heated surfaces, the theory of rate processes of Glasstone, Laidler and Eyring[69] has been applied to the calculation of the emission currents.

The Schottky barrier for electron emission defines the maximum potential energy of an electron (relative to those in the metal) as it is transferred from the interior of the filament of the magnetron to the anode. This is illustrated in figure 22. If the methods of transition state theory can be applied to the process of electron emission, this maximum should define the energy and position of the transition state for the emission reaction.

If the transition state (T.S) is designated by an asterisk and the electrons in this state are assumed to be in equilibrium with those in the metal (designated by the subscript m), then the equilibrium constant for the formation of the T.S may be written as;

$$K^* = \frac{c^*}{c_m} = \frac{Q'^*}{Q_m}.\exp(\beta-\alpha)/kT \quad ----- \quad 6.1$$

where c represents concentration, Q the partition function for electrons per unit volume, Q' the partition function for electrons per unit area, β the zero point energy of the electrons in the metal and α the corresponding figure for electrons in the T.S. The contribution to Q'* due to motion perpendicular to the surface, which is assumed to be rate determining, may be resolved to give $Q'^* = (kT/h\nu).Q^*$, where ν is the frequency of the rate determining vibration and the other symbols have their usual meanings. $Q_m/c_m = \exp -\delta/kT$, where $\delta = (3F/5) - (\pi^2k^2T^2/12F)$ and F is the Fermi energy $F = (h^2/8m_e)(3N/\pi V)^{2/3}$, m_e being the mass of the electron and N the number of free electrons per volume V .

In the magnetron the field due to the anode is

small and of the order of $40V\ cm^{-1}$. Equating this to the image force ($\epsilon^2/4x$, where ϵ is the electronic charge and x the distance of the electron from the filament), shows the T.S to be located approximately 10^{4}Å from the surface and the potential energy of the electron (relative to an electron at infinity in the gas phase) to be about 10^{-2}eV. The zero point energy of an electron in the T.S may therefore be equated to that of an electron at infinity. Hence $N(\beta+\delta-\alpha) = \chi$, where N is Avogadro's number and χ is the electron work function of the metal.

The electron in the transition state will have three degrees of translational freedom. One of these has already been allowed for as being the rate determining motion and the other two may be treated by classical Maxwell-Boltzman statistics, whence $Q^* = 2(2\pi m_e kT)/h^2$, the factor 2 being introduced to allow for the spin degeneracy of the electron. If ν is the frequency with which the complexes pass over the barrier, the electron current per unit area of surface will be given by $i_e = c^*\nu\epsilon$. Making these assumptions and introducing the transmission coefficient $\bar{d}$ and the gas constant $R = Nk$ gives,

$$i_e = \frac{\bar{d}.4\bar{\pi}m_e(kT)^2\epsilon}{h^3}. \exp - \chi/RT \quad ----- 6.2$$

This is clearly Richardson's equation (2.8) for the electron current per unit area of surface and it would seem that transition state theory is capable of adequately describing the emission of electrons from heated metal surfaces.

6.2 The effect of strong adsorption

When a gas is adsorbed upon a metal surface the difference in the electronegativities of the metal and the adsorbate leads to a charge separation and the formation of an electrical double layer at the surface. The charge separation per individual adatom may be expressed in terms of a dipole moment and if this dipole is independent of the surface coverage, the system may be regarded as a capacitor or dipole sheet whose potential is proportional to the number of dipoles per unit area. Classical electrostatics gives the change in potential due to the double layer as $\Delta\chi = 4\bar{\pi} n_s \theta \mu$, where n_s is the number of adsorption sites per cm^2, θ the fraction of the

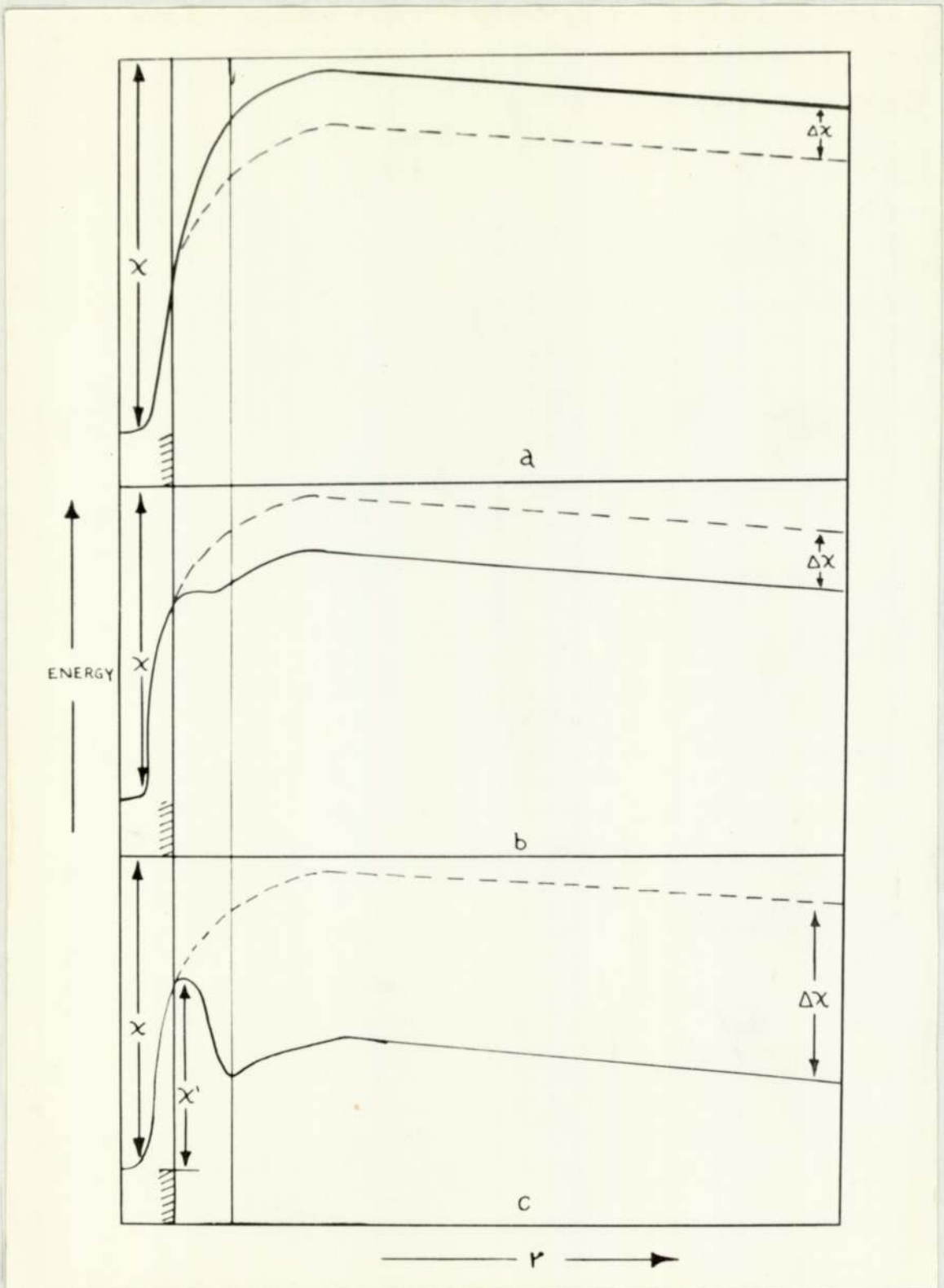

The effect of adsorbed layers upon the emission barrier.

FIGURE 23.

surface covered by adsorbed material and μ the dipole moment per adatom. Since there is no external field with a perfect double layer, the potential changes sharply at the surface and equation 6.2 may be written,

$$i_e = \frac{\bar{d}.4\pi m_e (kT)^2 \epsilon}{h^3} \cdot \exp -(\chi_o \pm 4\pi n_s \theta \mu)/RT \quad - 6.3$$

where χ_o is the work function when $\theta = 0$.

The three types of barrier resulting from the adsorption of such a layer are illustrated in figure 23. In 23a and 23b the emission current is adequately described by equation 6.3 but in the case of 23c, the height of the barrier χ' is greater than $\chi_o - \Delta\chi$. Under these circumstances χ' will define the energy of the T.S relative to the energy levels of the metal and equation 6.3 will no longer be valid. The barrier in this case will be thinner than the separation of the double layer and so an allowance must be made for the increase in $\bar{d}$ due to quantum mechanical tunnelling by the electrons. At low θ 23c will reduce to 23b.

If the reduction in the heat of adsorption with increasing surface coverage may be entirely attributed

to the reduction in the energy of the highest occupied level of the adsorbate, then $\Delta\chi = -\Delta q$. The rate of adsorption of the gas is given by transition state theory as,

$$u_a = c_s c_g \frac{kT_g}{h} \cdot \frac{Q^*_a}{Q_g Q_s} \cdot \exp\left[-E_a/RT_g\right] \quad ------ 6.4$$

where c_g is the gas phase concentration of the adsorbate, c_s is the concentration of adsorption sites, Q_g is the gas phase partition function per unit volume, Q_s the partition function per unit area for adsorption sites, Q^*_a is the partition function per unit area for the T.S for adsorption, E_a is the activation energy for adsorption and T_g is the gas temperature.

If the desorption is non-associative the rate will be given by,

$$u_d = c_A \frac{kT}{h} \cdot \frac{Q^*_d}{Q_A} \cdot \exp\left[-E_d/RT\right] \quad ------ 6.5$$

and if the desorption is associative,

$$u'_d = c_A c_B \cdot \frac{kT}{h} \cdot \frac{Q^*_d}{Q_A Q_B} \cdot \exp\left[-E'_d/RT\right] \quad ------ 6.6$$

Here Q_A and Q_B are the partition functions per unit area for the adsorbed species which recombine,

Q_d^* the partition function per unit area for the T.S for desorption, E_d is the activation energy for desorption and T the filament temperature. The adsorbed species are assumed to have attained the surface temperature. Provided that there are no side reactions, at equilibrium $u_a = u_d$.

Since $\Delta\chi$ represents the change in the energy of the highest occupied level of each adsorbed particle, it will be reflected as a corresponding change in E_d and $E_d'/2$. Combining equations 6.3, 6.4 and 6.5 with the substitutions $c_A = n_s f(\Theta)$, $c_g = p/kT_g$, $E_d = q_o - \Delta\chi$ and $c_s/Q_s = f(1-\theta)$, gives in the case of raised work functions,

$$i_e = \frac{\bar{d}_m \cdot 4\bar{\Pi} m_e (kT)^3 \epsilon\, n_s f(\Theta)}{h^3 p\, f(1-\Theta)} \cdot \frac{Q_g Q_d^*}{Q_A Q_a^*} \cdot \exp(E_a/RT_g) \cdot \exp\left[-(\chi_o + q_o)/RT\right] \quad - - - 6.7$$

For dissociative adsorption and associative desorption, combining equations 6.3, 6.4 and 6.6, and making the substitutions $c_A = c_B = n_s f(\Theta)$, $c_s/Q_s = f(1-\Theta)^2$, $E_d' = 2q_o - 2\Delta\chi - D$ and $c_g = p/kT_g$ gives,

$$i_e = \frac{\bar{d}_m \cdot 4\bar{\Pi} m_e (kT)^{5/2} \epsilon\, n_s f(\Theta)}{h^3 f(1-\Theta) p^{1/2}} \cdot \left[\frac{Q_g Q_d^*}{Q_A Q_B Q_a^*}\right]^{1/2} \cdot \exp(E_a/2RT_g) \cdot \exp\left[-(\chi_o + q_o - D/2)/RT\right] \quad - - - 6.8$$

Adsorption with a lowering of the work function only involves a change of the sign of the q_o and D terms in the exponential. These are essentially the equations which were used in the discussion of the results of section 5.

7. APPLICATION OF TRANSITION STATE THEORY TO THE EMISSION OF NEGATIVE IONS

7.1 The ion current

In extending the transition state model to the formation of negative ions, it is convenient to consider the problem in two parts, analogous to the arguments of sections 6.1 and 6.2. These are, firstly the calculation of the rate of emission of ions from a surface fully covered by ion precursors and secondly the influence of temperature and pressure upon the number of these precursors present upon the surface.

It is important to stress at the outset that the following derivation is only intended to apply to ion formation in sparse surface layers, where the interaction effects, both amongst the ions and molecules, and between the surface layers and the energy levels of the metal, may be ignored. Ions are presumed to be formed by the interaction of electrons in the metal with adsorbed ion precursors (atoms or molecules), resulting in the formation of a transition state which may be irreversibly desorbed as an ion. As with electron emission the

equilibrium constant associated with the formation of the transition state may be written as,

$$K^* = \frac{c^*}{c_A c_m} = \frac{kT}{h}\cdot\frac{Q^*}{Q_A Q_m}\cdot\exp\left[-(\alpha-\beta-\sigma)/kT\right] \quad ---- \quad 7.1$$

where σ is the zero point energy of the adsorbed ion precursor and the remaining terms have meanings analogous to those in the previous section. Making the same substitutions as before and noting that $-(\alpha-\beta-\sigma-\delta)/k = (E - \chi - E_d)/R$, gives,

$$i_i = \bar{d}\cdot\frac{kT}{h}\cdot\epsilon\cdot c_A\cdot\frac{Q^*}{Q_A}\cdot\exp\left[(E - \chi - E_d)/RT\right] \quad ---- \quad 7.2$$

where E is the electron affinity of the precursor and E_d its heat of desorption. This is the expression for the ion current which is equivalent to Richardson's equation for the electron current.

If the ion formation represents only a minor perturbation of the adsorption - desorption equilibrium, the rates of adsorption (6.4) and desorption (6.5) may be equated and substituted into equation 7.2 to give,

$$i_i = \bar{d}\cdot f(1-\Theta)\cdot\frac{p\epsilon}{h}\cdot\frac{Q^*Q^*_a}{Q_g Q^*_d}\cdot\exp(-E_a/RT_g)\cdot\exp\left[(E - \chi)/RT\right] \quad - \quad 7.3$$

For most adsorption processes at very low surface coverage the activation energy for adsorption will be zero and $f(1-\theta)$ will approximate to unity. Hence substituting

$$Q_a^*/Q_g = h/(2\bar{\pi}MkT_g)^{1/2} \quad \text{and} \quad Q^* = Q_d^* Q/Q_i$$

$$i_i = \frac{\bar{d}.p.\epsilon.Q_i}{Q(2\bar{\pi}MkT_g)^{1/2}} .\exp[(E - \chi)/RT.] \quad ----- 7.4$$

where Q_i and Q are the internal partition functions for the transition state ion and the gas phase molecule respectively, the latter being assumed identical to those for the T.S for adsorption and the T.S for desorption.

7.2 Application to magnetron measurements

In the magnetron measurements the work function term in equation 7.4 is eliminated by substitution from equation 6.2. Therefore, assuming the $\bar{d}$ terms to be identical,

$$\frac{i_e}{i_i} = \frac{4\sqrt{2}.\bar{\pi}^{3/2}.k^{5/2}.T.T_g^{2}.T_g^{1/2}.M^{1/2}.m_e.Q}{h^3.p.Q_i} .\exp[-E/RT.] \quad -- 7.5$$

Equation 7.5 represents the basic equation governing ion

formation in the magnetron. Since

$E'(T) = -R\left[d \log(i_e/i_i)\right]/d(1/T)$ differentiation of 7.5 gives,

$$E'(T) = E + 2RT. \qquad \text{- - - - - 7.6}$$

The kinetic arguments advanced in section 2.2 give,

$$E'(T) = E + (3/2)RT. \qquad \text{- - - - - 7.7}$$

since the only change in the degrees of freedom of the system is the loss of the three translational motions of the electron. Equation 7.5 is identical to the expression used by Mayer (equation 2.7) to evaluate the electron affinities of the halogens. (The difference of the factor 2 arises because of the dissociation of the substrate) As the original arguments of Page suggested, the kinetic method is seen to lead to exactly the same results as the statistical arguments of Mayer in the simplest cases.

7.3 The entropy of the reaction

Combining equations 6.2 and 7.3 and equating the $\bar{d}$ terms, noting $f(1-\theta) \simeq 1$ and substituting $Q_e^* = 2(2\pi m_e kT)/h^2$,

$$\frac{i_e}{i_i} = \frac{kT}{p}.\frac{Q_g}{Q_a^*}.\frac{Q_d^* Q_e^*}{Q^*}.\exp(E_a/RT_g).\exp(-E/RT). \quad ----- 7.8$$

This may be written in the form,

$$\frac{i_e}{i_i} = \frac{kT}{p}.K_1.K_2. = \frac{kT}{p}.\exp(-\Delta G_1/RT_g).\exp(-\Delta G_2/RT) \quad ----- 7.9$$

where K_1 and K_2 are the concentration equilibrium constants for the reactions,

$$A^*(a) = A(g) \quad ----- 7.10a$$

$$A^{-}* = A^*(d) + e^{-}* \quad ----- 7.10b$$

and ΔG_1 and ΔG_2 are the associated Gibbs' Free Energy changes. $\Delta G = \Delta H - T\Delta S = \Delta U + nRT - T\Delta S$, where n is the increase in the number of molecules in the course of the reaction.

If the adsorption process is non-activated $\Delta H_1 = 0$ and equation 7.9 may be written,

$$\frac{i_e}{i_i} = \frac{kT}{p}.\exp(-\Delta H_2/RT).\exp(\Delta S_1 + \Delta S_2)/R. \quad ---- 7.11$$

Defining $\Delta S = \Delta S_1 + \Delta S_2$ and noting

$$\frac{d}{dT}.\log\frac{i_e}{i_i} = \frac{E'(T)}{RT^2} = \frac{1}{T} + \frac{d.\log K_2}{dT} = \frac{1}{T} + \frac{\Delta U_2}{RT^2}$$

whence $\Delta H_2 = \Delta U_2 + RT = E'(T) = \Delta H$. (Since K_1 is independent of T). Therefore substituting into equation 7.11,

$$\Delta S = R.\log \frac{i_e}{i_i} + R.\log p + E'(T)/T - R.\log(kT) \quad \text{- - - - - 7.12}$$

Here ΔS is the sum of the entropy changes for the reactions of equations 7.10 with all transition states in the standard state of one mole per cm^2 and the gas molecules in the standard state of one mole per cm^3.

Comparing equations 7.8 and 7.11,

$$\Delta S = R.\log \left[\frac{Q_g Q^* Q^*_e}{Q^* Q^*_a} . \exp(E_a/RT_g) \right] - (x + 1)R. \quad \text{- - - - - 7.13}$$

where x is defined from $E'(T) = E + (x + 1)RT$.

For the purposes of calculation, it is convenient to define the function

$$\Delta G(T) = \Delta H_2 - T(\Delta S_1 + \Delta S_2) = \Delta H(T) - T\Delta S(T). \quad \text{- - - - - 7.14}$$

The equations derived in this section are applied to the discussion of the experimental data in section 8.3.

7.4 The correction of data derived from log-log plots to $0^{\circ}K$

In order to avoid the necessity of measuring the filament temperatures, it was shown in section 3.4 that the electron current could be used as an internal standard provided that the emission constants B and χ of Richardson's equation (2.8) are known.

Differentiating Richardson's equation (6.2),

$$-\left[\text{R.d.log } i_e\right] /d(1/T) = \chi_o + 2RT = \chi'(T). \quad - 7.15$$

Similarly from equations 2.9 and 2.10 (or 7.3),

$$-\left[\text{R.d.log } i_i\right] /d(1/T) = \phi + nRT = \phi(T). \quad - 7.16$$

where $\phi = \chi_o - E'_o$ and E'_o is the apparent electron affinity at $0^{\circ}K$. Hence,

$$\frac{\text{d.log } i_i}{\text{d.log } i_e} = \frac{\phi(T)}{\chi'(T)} = \frac{\chi'(T) - E'(T).}{\chi'(T)} \quad - - 7.17$$

and $E'(T) = E'_o + (2-n)RT$, which is identical to equation 2.13.

The results from log-log plots are therefore corrected to $0^{\circ}K$ in exactly the same manner as those from Arrhenius plots, providing the apparent thermionic work function is

used in equation 7.17. This is in agreement with the observation noted in the course of the NO_2/W measurements.

8. ELECTRON CAPTURE BY CYANOCARBON DERIVATIVES AND SUBSTITUTED BENZOQUINONES

In order to obtain data to test the equations derived in the previous section several compounds, for which charge-transfer measurements [75,76] had suggested large electron affinities, were studied. The cyanocarbon series proved more amenable to study by the magnetron method than the quinones because of the lower thermal stability of the latter.

8.1 Experimental - Quinones

The chloranil was supplied by messrs. B.D.H. Ltd and was recrystallised from toluene before use. The remaining materials were all prepared by Dr. P.R. Hammond[75] and were used without further purification.

8.1.1. Benzoquinone

The initial measurements were made upon iridium, but since the results were influenced by the deposition of carbon at high temperatures they were subsequently checked by the use of tungsten carbide filaments. Because of this deposition of carbon it was found to be more convenient to plot the logarithm of the ion current

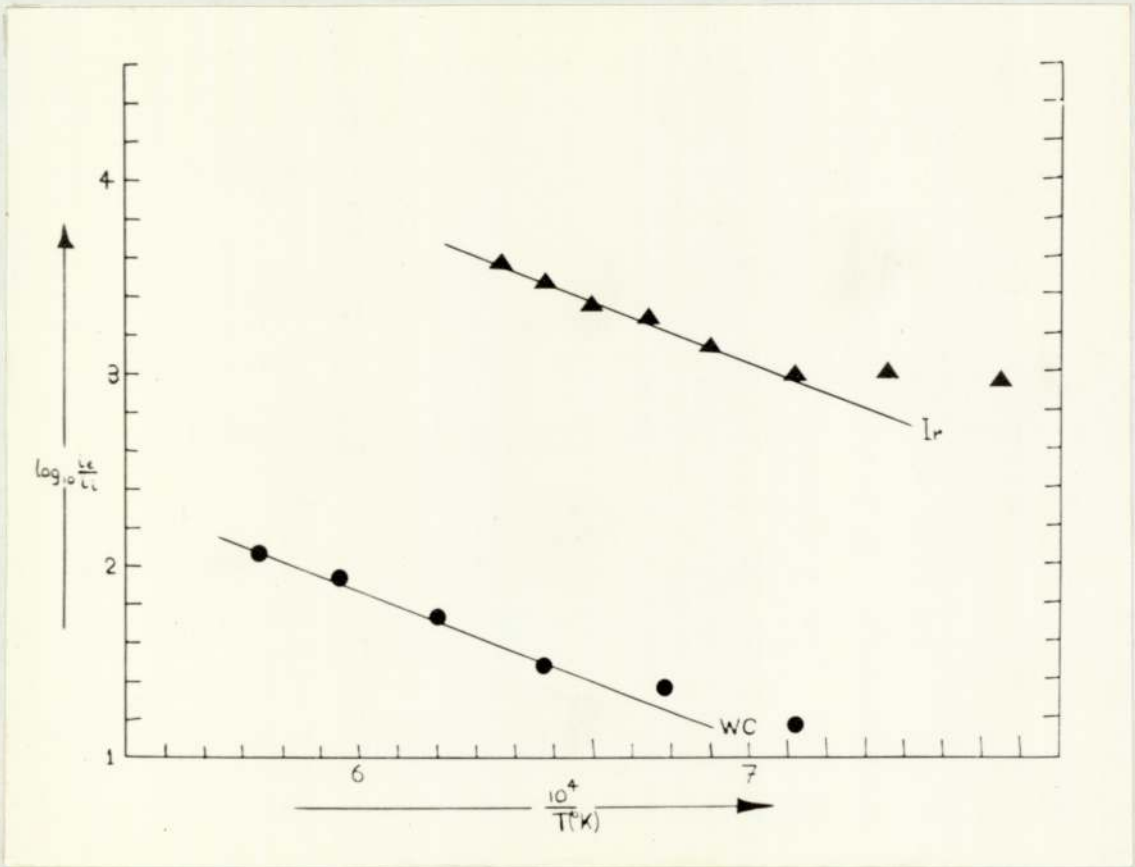

Electron capture by p-benzoquinone.

FIGURE 24.

against the logarithm of the electron current, the slope of this graph being equal to $\chi'(T) - E'(T) / \chi'(T)$, equation 7.17. $\chi'(T)$ was measured as 108 kcals and hence the following values of $E'(1450^{o}K)$ were obtained; 36.7, 36.7, 36.7, 37.2, 30.2 kcals/mole. The first two of these results were also obtained when the temperatures measured in the course of the run were used in a conventional Arrhenius plot. Omitting the value of 30.2, $E'(1450^{o}K) = 36.7 \pm 0.2$ kcals/mole. There was some evidence for a change of process at low temperatures but no reliable estimate of the slope of the graphs could be made.

When using tungsten filaments, the gas was allowed to fully carbide the surface and then care was taken to ensure that the temperature was not subsequently raised to a level where carbon deposition occurred. The following results were obtained from Arrhenius plots; 36.2, 37.0, 39.5, 36.0, 37.0, 37.1 kcals/mole. Hence, $E'(1630^{o}K) = 37.1 \pm 1.1$ kcals/mole. As before there was a change of process at low temperatures, the most reliable lines having slopes of 25.6, 24.2 and 24.8 kcals/mole at a mean temperature of $1470^{o}K$. Typical

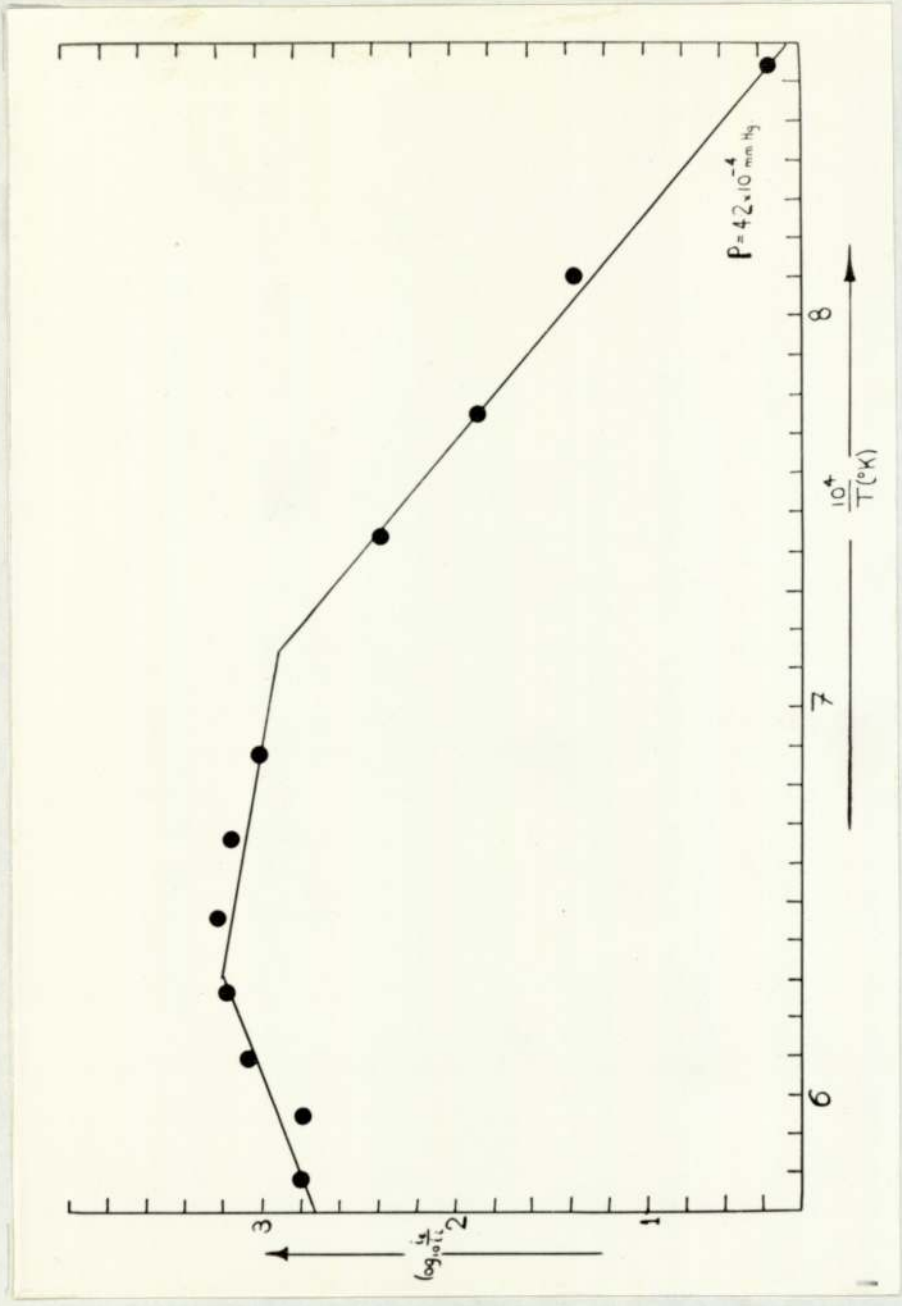

Electron capture by chloranil.

FIGURE 25.

results on iridium and tungsten carbide filaments are shown in figure 24.

8.1.2. Chloranil

Using iridium filaments and gas pressures in the region of 10^{-4} mm Hg, the following results were obtained; E'(T) = 83.2, 79.0, 79.2, 80.5, 80.5, 82.3, hence E'(1250°K) = 80.9 ± 1.5 kcals/mole. A typical measurement is illustrated in figure 25. In order to obtain sufficient pressure of chloranil and prevent its condensation upon the apparatus, the whole vessel was heated to approximately 70°C by means of a hot air blower.

8.1.3. Duroquinone

Attempts to measure the electron affinity of duroquinone were hampered by the ease with which the filaments abstracted a hydrogen atom from the molecule. The results obtained with tungsten filaments were; 25.6, 20.0, 20.0, 24.1, 19.5, 19.5, 19.5, hence E'(1600°K) = 21.5 ± 2.7 kcals/mole. (Figure 26).

The results obtained from measurements upon iridium filaments were; 14.2, 14.5, 17.4, 14.6, 14.6, 15.1,

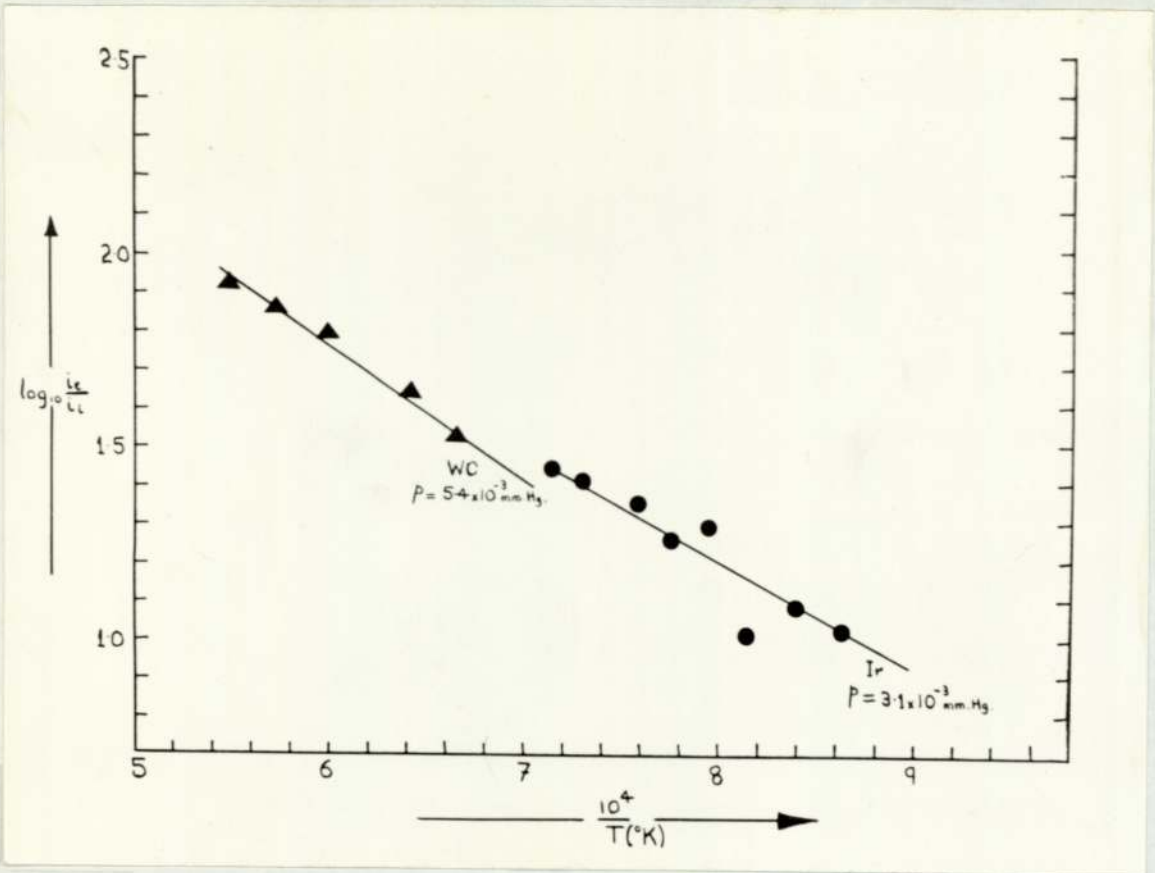

Electron capture by duroquinone.

FIGURE 26

whence $E'(1320^{\circ}K) = 15.1 \pm 1.1$ kcals/mole. There was some evidence for a change of process at low temperatures but the ion currents were too small for any reliable estimate of the slope to be made.

8.1.4. Monofluorobenzoquinone/Ir

The measurements made with this compound indicated three distinct processes and are illustrated in figure 27. The limited temperature range available for the measurements at the lowest temperatures prevented any accurate estimate of the apparent electron affinity in this region. A single measurement at a higher pressure than the remainder of the measurements indicated an apparent electron affinity of 54.8 kcals/mole at a mean temperature of $1260^{\circ}K$. It was not possible to recheck this result due to there being insufficient of the sample material. The other results obtained were,

$E'(1590^{\circ}K) = 23.8, 29.9, 30.6, 29.9, = 28.6 \pm 2.8$ kcals/mole.

$-E'(1390^{\circ}K) = 27.7, 26.0, 25.6, 26.1, = 26.4 \pm 0.8$ kcals/mole.

8.1.5. 2,3 dicyanobenzoquinone

The measurements with this compound at pressures of approximately 10^{-3} mm Hg and using iridium filaments

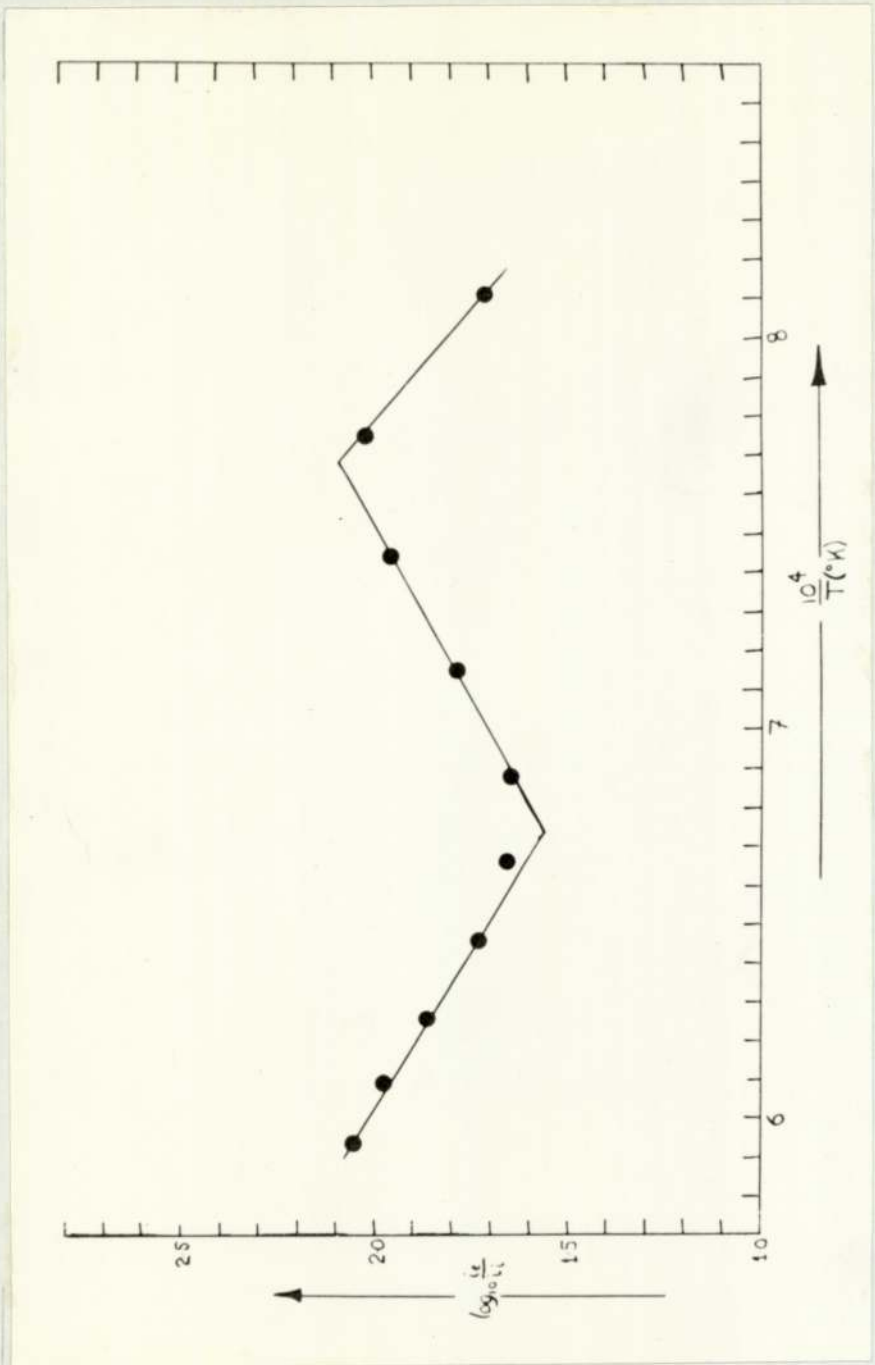

Electron capture by monofluorobenzoquinone.

FIGURE 27.

indicated a single process with E'(1490°K) = 16.5, 17.4, 13.3, 13.0, 13.9 = 14.8 ± 1.8 kcals/mole. A typical measurement is illustrated in figure 28.

8.2 Experimental - Cyanocarbon derivatives

The tetracyanoethylene and hexacyanobutadiene were supplied by Dr. O.W. Webster of E.I. duPont Inc, the 7,7,8,8 tetracyanoquinodimethan(e) and fumaronitrile were supplied by Dr. R.H. Boyd of the same company, the tetracyanobenzene by Mr. J.C. Thurman of The National Chemical Laboratory, and the tetracyanopyridine and hexacyanobenzene by Prof K. Wallenfels of the University of Freiburg.

8.2.1. Tetracynaoethylene

Measurements upon platinum filaments at gas pressures between 10^{-3} and 10^{-4} mm Hg gave the following results, E'(1360°K) = 72.3, 72.3, 72.0, 72.3, 75.0, 71.3, 71.3 = 72.3 ± 1.2 kcals/mole. Iridium filaments and gas pressures of 10^{-4} mm Hg again showed only one process with an apparent electron affinity of, E'(1350°K) = 69.0, 69.3, 72.7, 68.6, 67.2, 70.0, 70.0, 68.6 = 69.4 ± 1.5

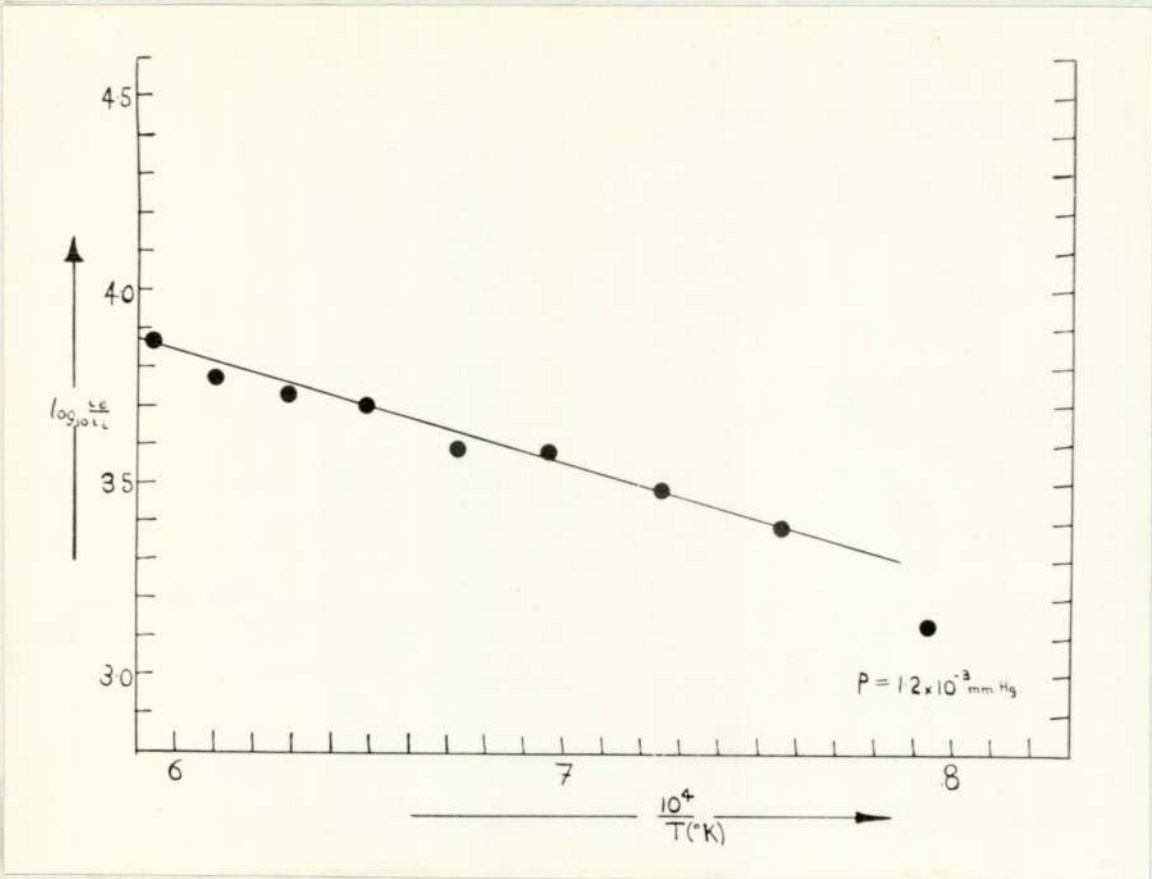

Electron capture by 2,3 dicyanobenzoquinone.

FIGURE 28.

kcals/mole. Measurements with rhodium filaments were hampered by the rate of evaporation of the metal, the following results being obtained, E'(1730°K) = 71.8, 71.6, 68.8, = 70.7 ± 1.9 kcals/mole. Typical measurements are illustrated in figure 29.

8.2.2. sym-Tetracyanobenzene

Measurements using iridium filaments and gas pressures of approximately 10^{-4} mm Hg yielded two apparent electron affinities in different temperature ranges. Approximately half the measurements were made with the sample unheated and half with it heated to approximately 50°C. Apart from a general rise in the magnitude of the ion currents upon heating, there was no significant difference between the two sets of results. The apparent electron affinities obtained were, E'(1280°K) = 65.2, 65.2, 65.2, 63.1, 62.1, 65.9, 64.0, 64.5 = 64.4 ± 1.3 kcals/mole. E'(1490°K) = 28.3, 27.6, 28.3, 30.2, 27.7 = 28.4 ± 1.0 kcals/mole. A typical measurement is shown in figure 30.

8.2.3. 7,7,8,8 tetracyanoquinodimethan(e)

The sample was heated by means of a hot water bath and sublimed across the filament. Two regions of

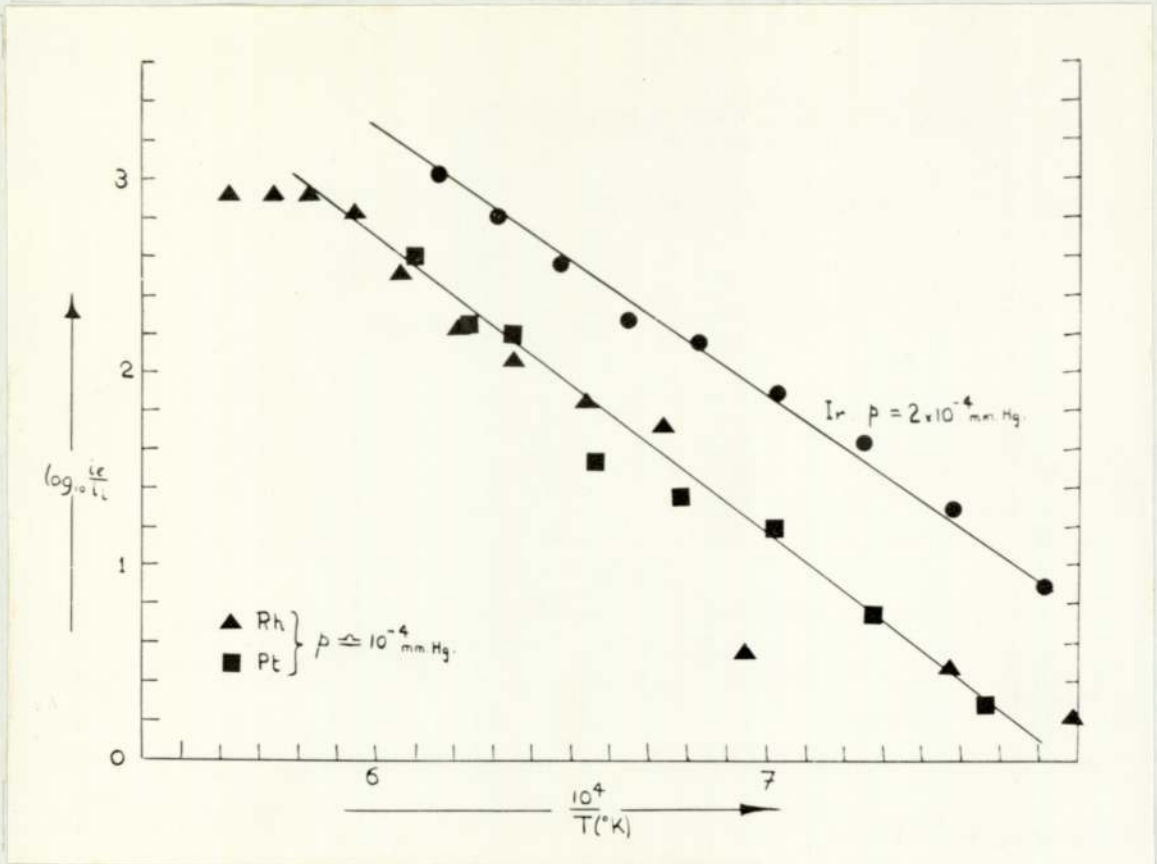

Electron capture by tetracyanoethylene.

FIGURE 29.

differing apparent electron affinity were discernable (fig 31) with the following values, E'(1270°K) = 83.6, 89.3, 87.0, 89.1, 91.0, 88.7, 89.1 = 88.3 ± 2.2 kcals/mole., and E'(1490°K) = 54.4, 55.4, 56.7, 59.4, 54.4, 56.3, = 56.1 ± 1.7 kcals/mole.

8.2.4. Hexacyanobutadiene

The sample was prepared by the oxidation of an ice cold solution of sodium 1,1,2,3,4,4 hexacyanobutenediide with 10ml of concentrated nitric acid. The product was filtered, washed with water, dried and purified by vacuum sublimation. The measurements upon iridium filaments at pressures of approximately 10^{-4} mm Hg indicated three processes (fig 32) with the following apparent electron affinities; E'(1270°K) = 95.5, 93.7, 96.6, 95.9, 97.2, 100.8, 102, = 97.4 ± 2.8 kcals/mole., E'(1390°K) = 82.7, 83.7, 80.0, 78.2, 86.9, = 82.3 ± 3.0 kcals/mole., -E'(1590°K) = 29.7, 22.4, 15.9, 21.0 = 22.0 ± 4.9 kcals/mole.

8.2.5. sym-Tetracyanopyridine

Measurements at gas pressures of approximately 10^{-4} mm Hg upon iridium filaments gave the following

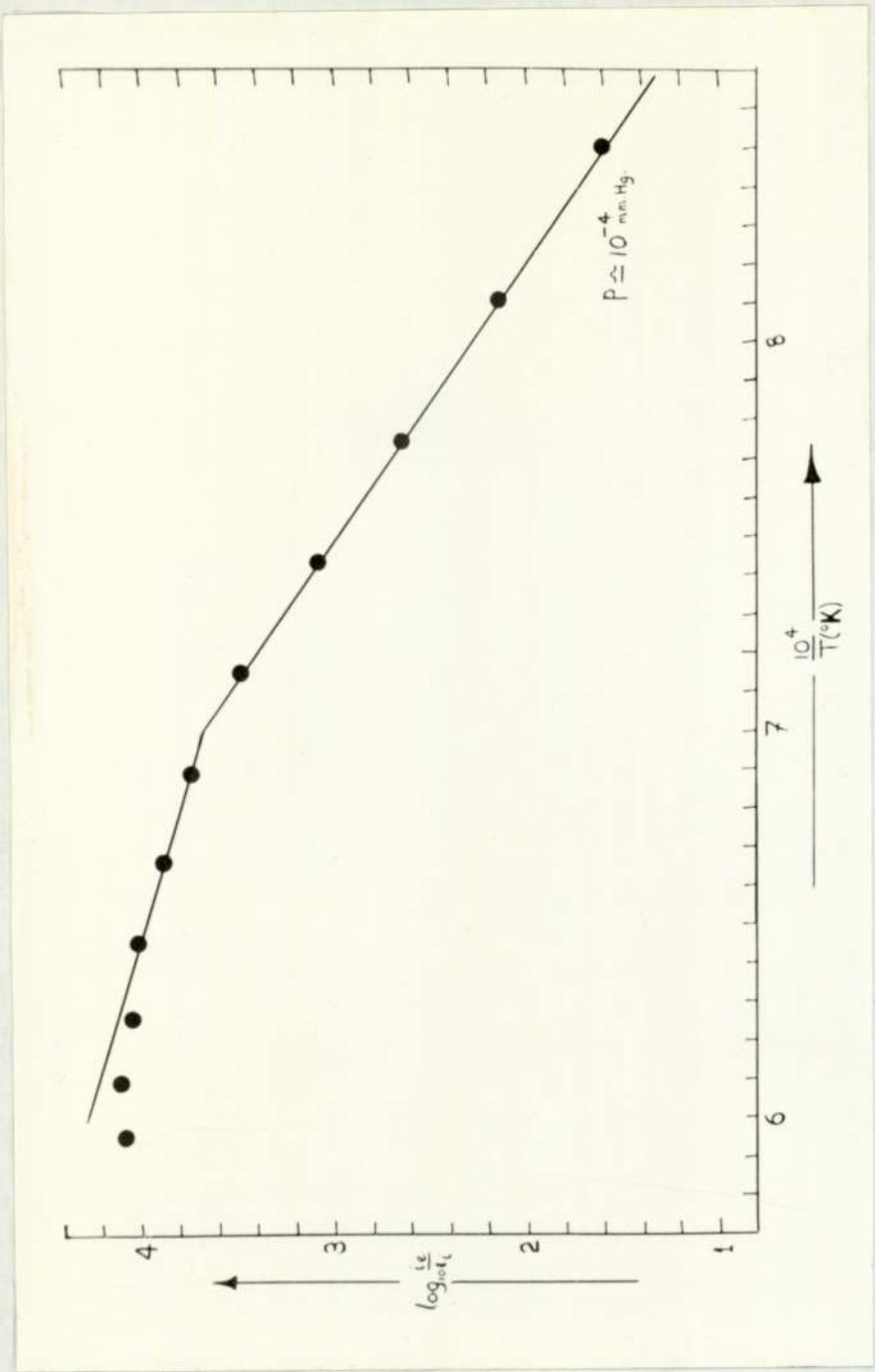

Electron capture by sym-tetracyanobenzene.

FIGURE 30.

apparent electron affinities; E'(1230°K) = 56.0, 52.2, 54.9, 54.9, 52.2, = 54.0 ± 1.9 kcals/mole. At higher temperatures there was evidence for another process occurring. This was not fully investigated since it did not appear to correspond to a direct capture process. The following electron affinities are however not greatly in error. E'(1540°K) = -17.4, -17.8, kcals/mole. A typical measurement which includes the high temperature process is shown in figure 33.

8.2.6. Hexacyanobenzene

This compound proved extremely difficult to study because of its low vapour pressure. The sample was contained in the heated sample holder (fig 6d) and sublimed directly on to the iridium filament. The background ion currents were measured before and after the measurement of E' and only those measurements were used for which the ion current in the presence of the gas was greater than 10 times the corresponding figure in its absence. The following results were obtained; E'(1390°K) = 58.4, 60.2, 62.9, 59.0, 65.7, 67.7, 63.4, 65.0, = 62.8 ± 3.1 kcals/mole.

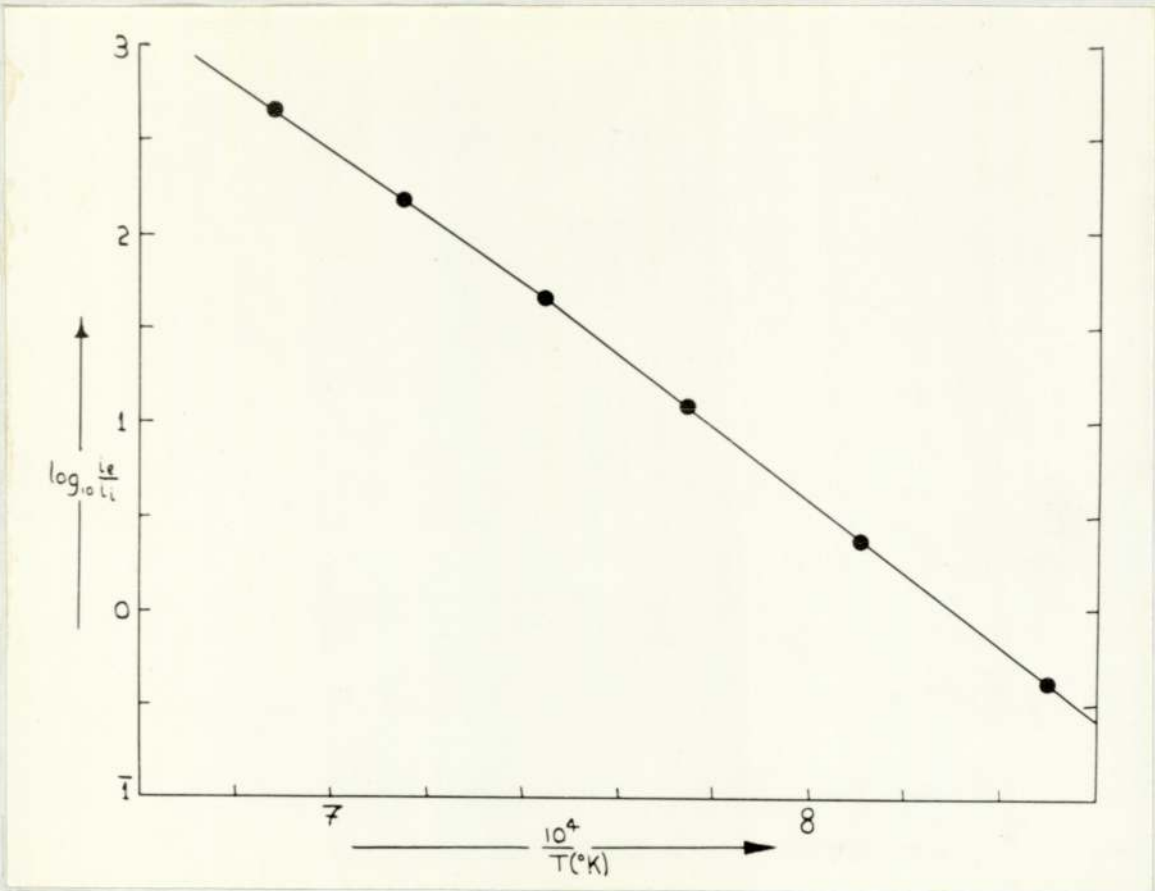

Electron capture by 7,7,8,8 tetracyanoquinodimethan(e).

FIGURE 31.

8.2.7. Phthalonitrile

Measurements at gas pressures of approximately 10^{-3}mm Hg upon iridium filaments indicated an apparent electron affinity of 30 kcals/mole. The results obtained were; E'(1540°K) = 31.3, 24.3, 31.4, 32.2, 26.4, 34.8, 30.2, = 30.1 ± 3.1 kcals/mole. A typical run is illustrated in fig 35.

Measurements at similar pressures upon WC filaments which were fully covered by an adsorbed layer of the gas (evidenced by a reversible change in work function of 26.4 kcals upon exposure to the gas) yielded the following results; E'(1520°K) = 28.9, 32.7, 30.6, 30.8, 33.0, 26.6, = 30.4 ± 2.2 kcals/mole.

8.2.8. Fumaronitrile

Measurements at 2 x 10^{-3}mm Hg upon iridium filaments gave the following apparent electron affinities; E'(1410°K) = 22.8, 22.0, 21.8, 20.9, 22.0, 24.1, 24.2, 15.1, 18.7, = 21.3 ± 2.7 kcals/mole. A previous series of measurements upon iridium filaments from another source yielded apparent electron affinities of; 18.3, 19.2, 23.2, 25.1, 24.7, whence E'(1230°K)) = 22.1 ± 2.8

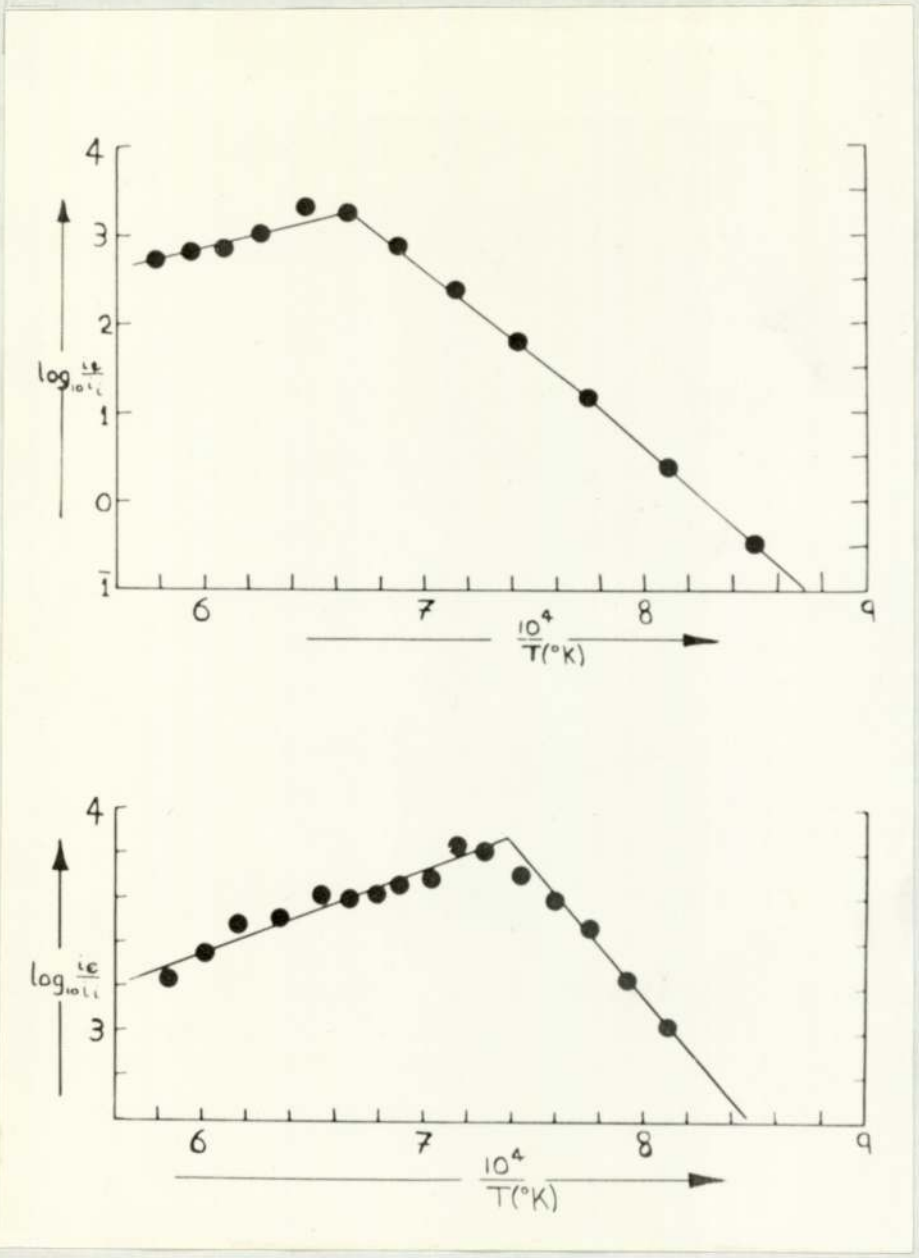

Electron capture by hexacyanobutadiene (32) and sym-tetracyanopyridine (33).

FIGURES 32 & 33.

kcals/mole. At higher temperatures the apparent electron affinity dropped markedly to $E'(1430^{\circ}K)$ = 4.6, 5.5, 9.8, 6.4, = 6.6 $\pm$ 2.0 kcals/mole. The failure of the former sample of iridium to show the high temperature process may be associated with differences in the purity of the two samples. This explanation would be in accord with the observed difference in thermionic work functions of the two samples, the former having $\chi'(1500^{\circ}K)$ = 88 kcals and the latter $\chi'(1500^{\circ}K)$ = 102 kcals. These figures were measured many times and in the presence of many different gases. The deviation from the values given was never greater than 5 kcals.

Measurements upon tungsten were hampered by the ease with which the gas reacted with the filament to form a carbide. Careful measurements in which the temperature was kept below that at which the reaction commenced gave the following apparent electron affinities; $E'(1620^{\circ}K)$ = 13.1, 13.7, 17.2, 16.5, 16.5, = 15.4 $\pm$ 1.9 kcals/mole. In the course of these measurements there was no evidence for carbiding of the filament. After the carburisation reaction was allowed to proceed to

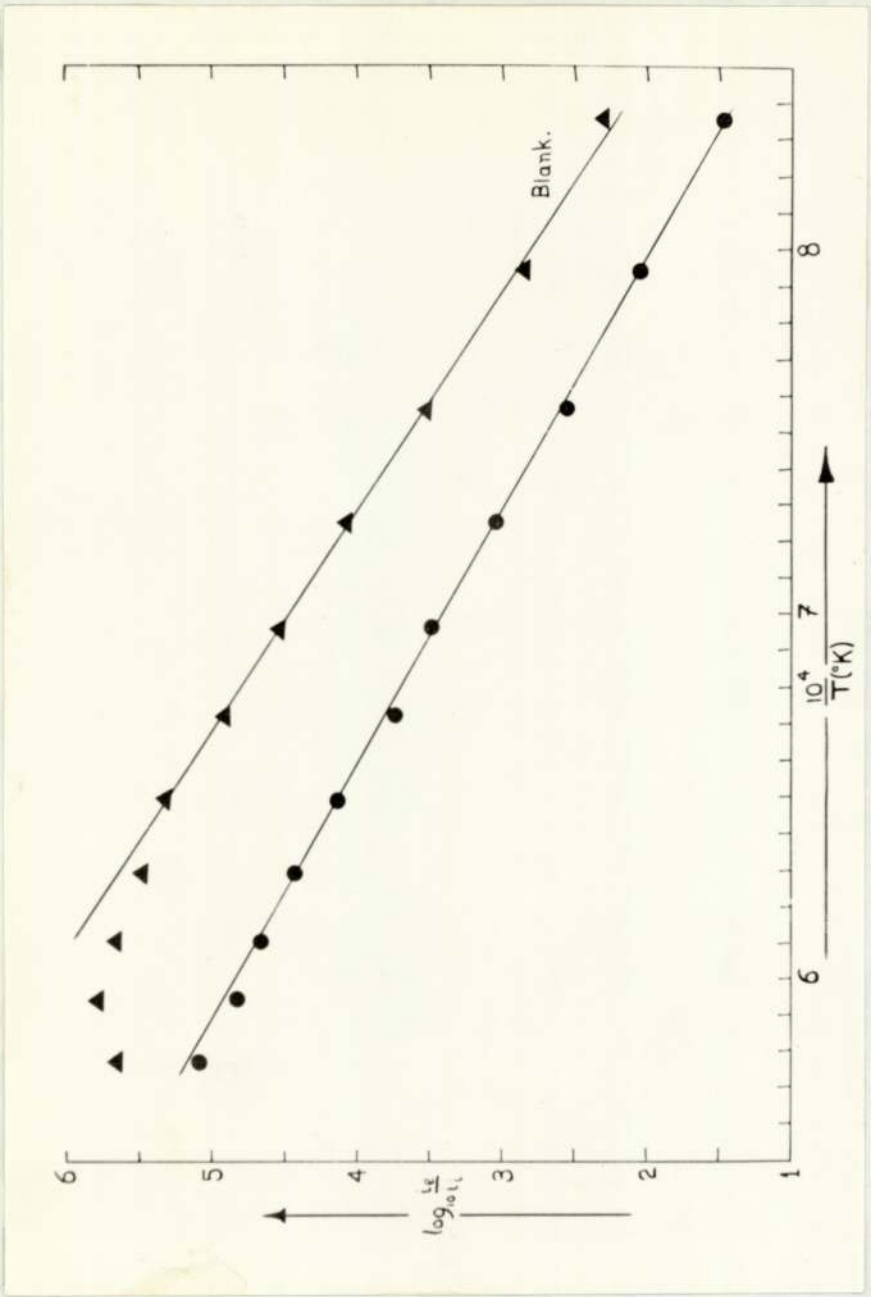

Electron capture by hexacyanobenzene.

FIGURE 34.

completion, the following results were obtained;

$E'(1430^{\circ}K)$ = 18.3, 18.3, 18.8, 19.2, 17.4, 20.9, 18.2, 19.6, 17.4, = 18.7 $\pm$ 1.0 kcals/mole.

8.3 Discussion of results

Table 8.1 lists the entropy, enthalpy and 'free energy' changes defined by equation 7.14, for those reactions in sections 8.1 and 8.2 which are thought to correspond to the direct capture of an electron and such other data as is at present available. In the calculation $\Delta H(\bar{T})$ has been assumed to be numerically equal to $\Delta H(T)$.

Substrate	No	$T^{\circ}K$	P	$\log i_e/i_i$	$-\Delta G(T)$	$\Delta H(\bar{T})$	$\Delta S(T)$	ΔS_K	E
C_6F_6	1.	1300	5.0	2.01	92.6	32.4	96.2	98.8*	27.2
SF_6	2.	1233	8.0	1.53	86.3	38.0	100.9	98.5*	33.1
NO	3.	1542	3.2	3.02	114.9	25.6	91.2	97.3*	19.1
B.Q.	4.	1732	4.2	2.09	120.6	37.1	91.1	99.8*	30.6
F.N.	5.	1475	2.7	2.78	108.0	21.3	87.7	98.2*	15.7
P.N.	6.	1530	1.7	3.56	116.0	30.1	95.5	98.8*	24.0
CCl_4	7.	1250	6.8	2.20	90.9	52.6	114.8	112.8	47.7
$CHCl_3$	8.	1250	6.5	1.97	88.5	44.2	106.2	110.5	39.2
TCNB	9.	1344	.1	3.18	92	64.4	117	112.8	59.3
TCNPy	10.	1290	0.4	2.86	90.6	54.0	113.1	112.7	49.1
TCNE/Ir	11.	1414	.1	1.83	88	69.4	112	111.8	64.0
TCNE/Pt	12.	1475	.1	2.33	95	72.3	114	111.9	66.9

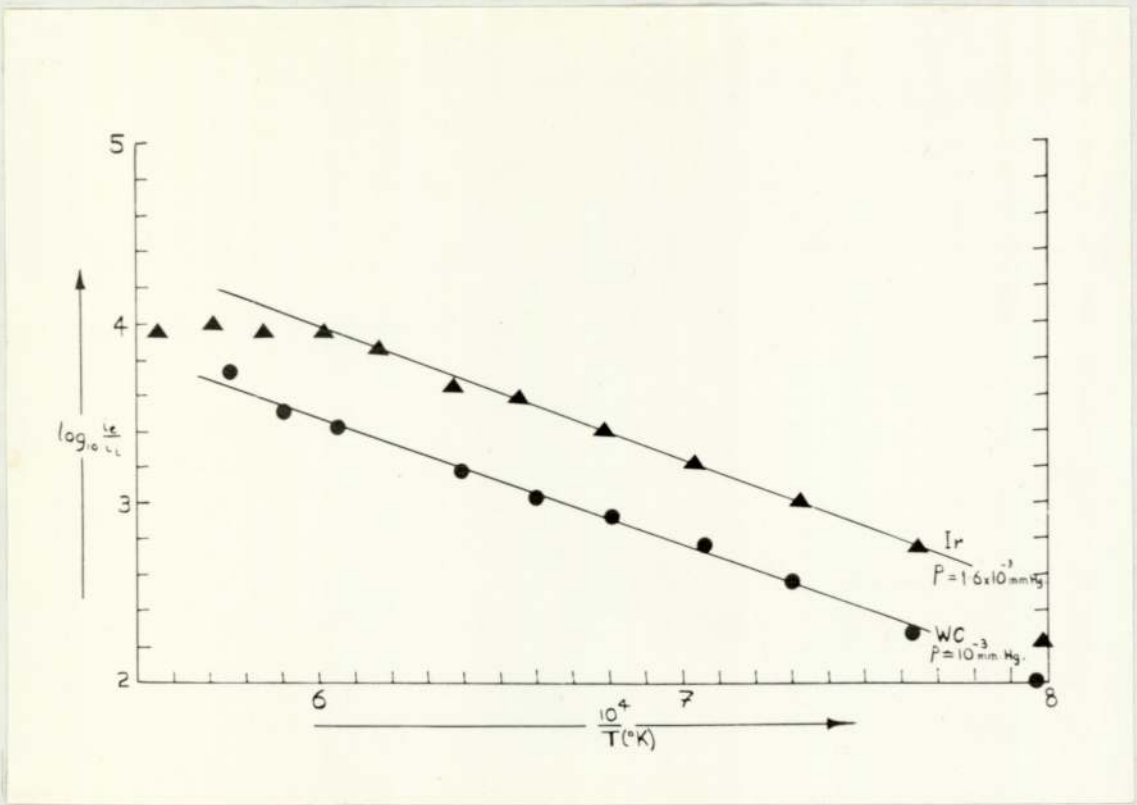

Electron capture by phthalonitrile.

FIGURE 35.

Substrate	No	$T^{o}K$	P	$\log i_e/i_i$	$-\Delta G(T)$	$\Delta H(\bar{T})$	$\Delta S(T)$	ΔS_K	E
FBQ	13.	1234	8.5	1.87	88.5	54.8	116.2	110.5	49.8
Chloranil	14.	1345	0.4	2.35	91.1	80.9	127.9		75.9
TCNQ	15.	1290	.1	1.07	76	88.3	128		83.3
HCNBd	16.	1290	.1	1.16	77	97.4	135		92.4
NO_2	17.	1537	3.0	2.43	110.3	96.2	134.4		90.1
TCNQ*	18.	1500	.1	4.11	109	56.1	110		50.2
HCNBd*	19.	1450	.1	2.92	96	82.3	123		76.8
NO_2*	20.	1670	9.0	2.19	121.3	5.0	75.6		-1.6

TABLE 8.1

1 = hexafluorobenzene, 2 = sulphur hexafluoride, 3 = nitric oxide, 4 = p-benzoquinone, 5 = fumaronitrile, 6 = phthalonitrile, 7 = carbon tetrachloride, 8 = chloroform, 9 = sym-tetracyanobenzene, 10 = sym-tetracyanopyridine, 11 = tetracyanoethylene, 13 = monofluorobenzoquinone, 15 = 7,7,8,8 tetracyanoquinodimethan(e), 16 = hexacyanobutadiene, 17 = nitrogen dioxide. The recorded pressures are in units of 10^{-3}mm Hg. The 'free energy' changes for all these reactions approximate to 96 kcals/mole. This is a consequence of the apparatus design since the working pressure range is limited to 10^{-2} - 10^{-5}mm Hg, the current ratios to 1 - 10^{5} and

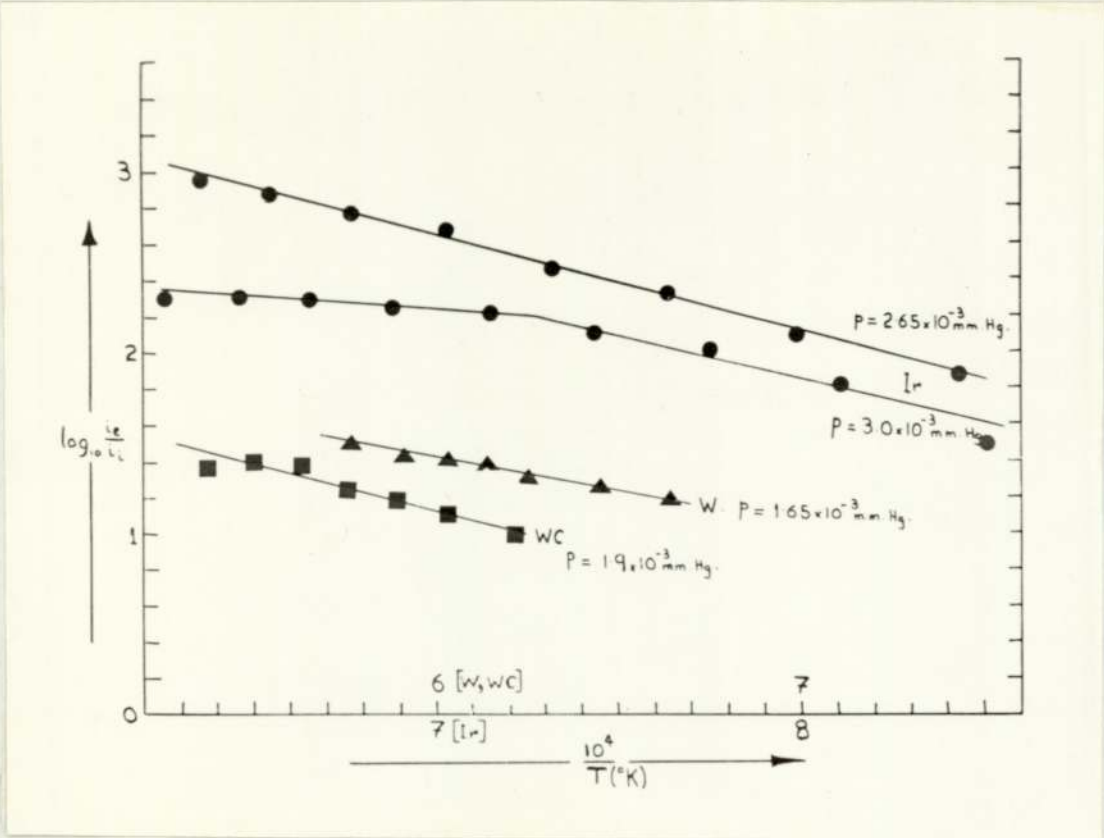

Electron capture by fumaronitrile.

FIGURE 36.

the temperature to 1000 - 2000°K. This results in $\Delta G(T)$ being limited to the range 55 - 171 kcals/mole, with most systems giving values in the 100 kcals/mole region.

Since $\Delta H(T)$ varies considerably in the reactions studied, the constancy of $\Delta G(T)$ implies a compensation effect between $\Delta H(T)$ and $T.\Delta S(T)$. This is illustrated in fig 37. The magnitude of $\Delta S(T)$ is, in principle, calculable from equation 7.13. The assumptions used in the derivation of equation 7.5, with $Q_i = 2Q$ gives

$$\Delta S_K = 4.57 \left[18.25 + \log_{10} T + \frac{1}{2} \log_{10} M \right] - 3.96 \text{ e.u.} \quad \text{- - - - - 8.1}$$

where M is the mass of the molecule in a.m.u and T is the filament temperature in °K. The entropy changes calculated from equation 8.1 are marked with an asterisk in table 8.1. For all the compounds studied this predicts entropy changes of approximately 98 e.u and is in satisfactory agreement with the observed change for reactions involving molecules with electron affinities below 35 kcals/mole. These values of ΔS_K give the contribution to $\Delta S(T)$ of simple kinetic terms. The

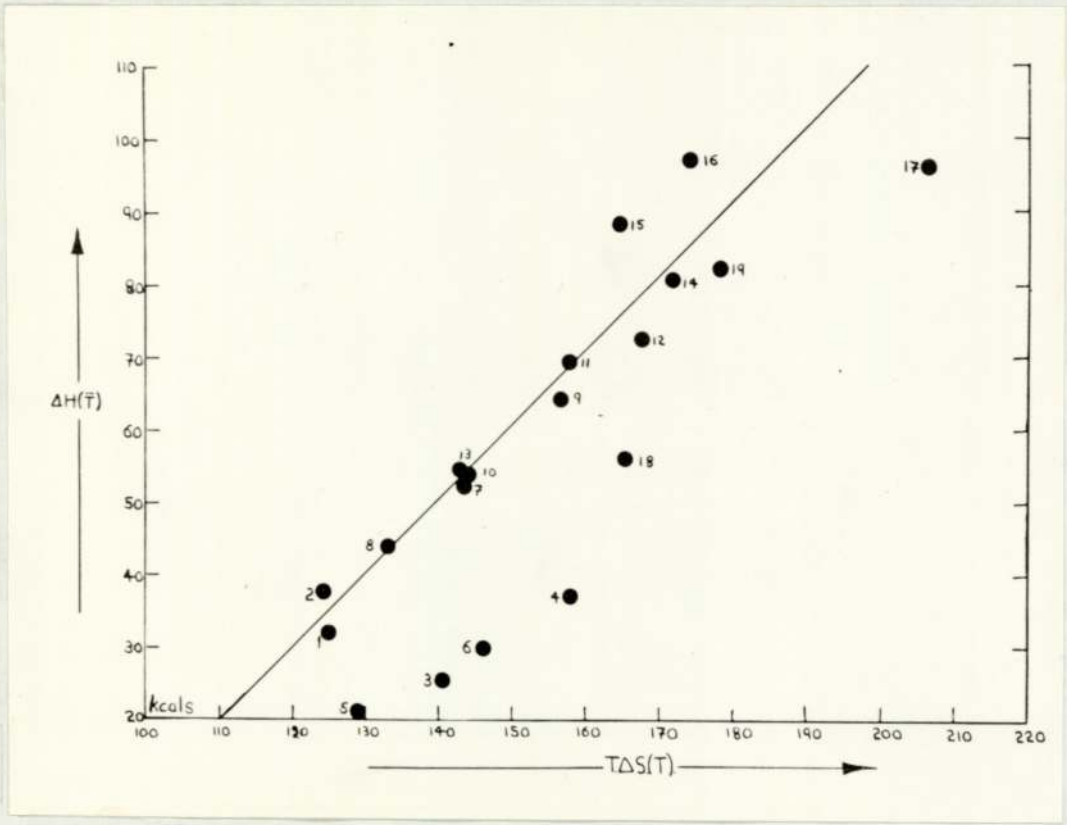

ΔH - TΔS compensation effect.

FIGURE 37.

discrepancy $T\left[\Delta S(T) - \Delta S_K\right]$ should therefore give the contribution to $\Delta G(T)$ of vibrational and electronic terms. This function is plotted against $\Delta H(T)$ in fig 38. The lower line corresponds to the kinetic entropies (ΔS_K) calculated from equation 8.1 and it is readily apparent that a much closer relationship exists between $\Delta H(T)$ and the entropy deficit term $T\left[\Delta S(T) - \Delta S_K\right]$ than between the former and $T\Delta S(T)$. From the lower line of fig 38, $\Delta H(T) = T\left[\Delta S(T) - \Delta S_K\right] + K$, whence, if $K = \Delta H^{\circ}$,

$$\Delta G(T) = \Delta H^{\circ} - T.\Delta S_K. \qquad \text{- - - - - 8.2}$$

Similar relationships are frequently observed with reactions in solution[77] and are generally ascribed to solvent - solute interactions. This would be in accord with the postulate that the entropy deficits in the present systems are due to electronic contributions to the partition functions. For materials of low electron affinity $\Delta H^{\circ} = 35.0$ kcals/mole. This will represent the value of $\Delta H(T)$ for which the net interaction term is zero. For molecules having an apparent electron affinity greater than this, there appears to be an abrupt increase in

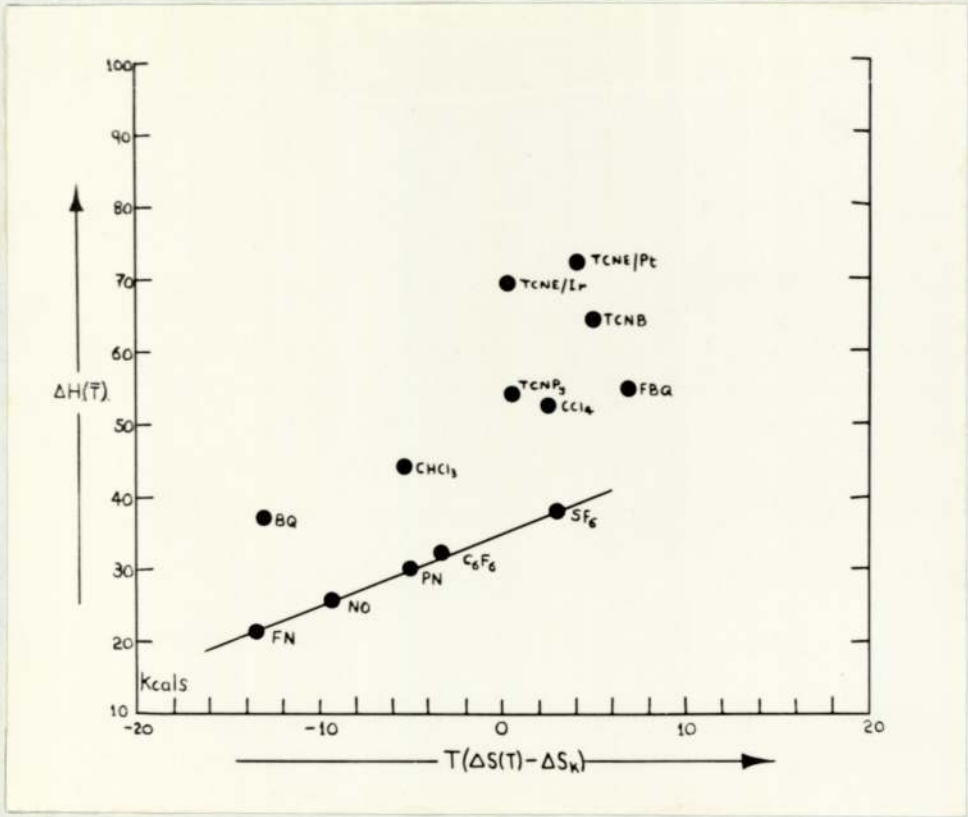

Entropy deficit.

FIGURE 38.

$\Delta S(T)$. Inspection of equation 7.13 suggests that this is most probably associated with a decrease in the magnitude of Q^* or Q_a^*.

If the transition state ion is located at the Schottky barrier it is improbable that it would loose any degrees of freedom which would not also be lost by the transition state for desorption, which will be located nearer the surface. The possible inferences are therefore that, either the transition state corresponding to the rate determining step for ion emission is not located at the Schottky barrier, but much closer to the surface, or the degrees of freedom are lost by the transition state for adsorption. The former of these assumptions would appear to require electron capture to be rate determining. If this were so the activation energy for ion emission would have to be greater than $-(E - \chi - E_d)$, (equation 7.2) and therefore $\Delta H(T) < E$. This would seem to be unreasonable in view of the broad measure of agreement between the 'magnetron' and other estimates of E (eg NO_2, TCNQ etc). This would seem to require the abrupt change in entropy to be associated with a reduction in the degrees of freedom of the transition state for adsorption.

If this corresponds to the loss of two degrees of rotational freedom equation 8.1 becomes modified to,

$$\Delta S_K = 4.57 \left[18.85 + \frac{1}{2} \log_{10}(I_x I_y M) - \log_{10} \frac{\sigma(g)}{\sigma(s)} + \log_{10} T \right] - 3.96 \quad - - 8.3$$

The rotational degree of freedom retained is presumed to be about an axis normal to the surface and having an associated moment of inertia I_z. $\sigma(g)$ represents the Ehrenfest symmetry number of the gas phase rotational partition function and $\sigma(s)$ is the corresponding figure for rotation on the surface. The agreement between $\Delta S(T)$ and ΔS_K is again quite good for electron affinities below 80 kcals/mole, but the data is insufficiently accurate for any relationship between $\Delta H(T)$ and $T\left[\Delta S(T) - \Delta S_K\right]$ to be discerned. The main source of the error in the calculated values lies in the estimated value of $p = 0.1 \times 10^{-3}$ mm Hg used for reactions where the pressure was too low to be recorded on the 'Pirani' gauge. The values of $\Delta S(T)$ appear to increase further with molecules having very large electron affinities, but this effect may be entirely due to the inaccuracies in the estimated gas pressures.

These observations suggest the model used in the analysis of direct capture reactions to be adequate and that E may be calculated from the apparent electron affinity by means of equation 7.6 for all these measurements. Using the present notation this becomes,

$$\Delta H(\bar{T}) = E + 2R\bar{T}. \qquad \text{- - - - - 8.4}$$

The values of E defined by equation 8.4 are recorded in table 8.1.

The appearance of two processes for HCNBd and TCNQ, both of which appear to correspond to simple electron capture is unexpected. The high electron affinity value for the latter compound is in good agreement with an estimate of 86 kcals/mole from thermochemical data.[78] Charge-transfer measurements suggest the electron affinity of HCNBd to be greater than that of TCNQ and this would seem to indicate that the high values for both these compounds are the normal electron affinities. These latter are both associated with larger entropy changes than the low values, which would be consistent with the formation of ground state and excited ions respectively. In both cases the difference in the entropies of the two processes is approximately the same

as the difference between the predictions of equations 8.1 and 8.3. The closeness of approach of the molecule to the surface during the process of electron capture will influence the efficacy of the latter as a third body. Under these circumstances it would seem reasonable that the formation of the excited ions should be associated with weak interactions with the surface, as predicted by equation 8.1, and that the formation of ground state ions should require the stronger interactions implied by equation 8.3. Similar considerations would appear to apply to the ions from NO_2, one of which has been postulated as being in an excited state (section 4.2). With this particular system however it is difficult to assess how far dissociation of the substrate has influenced the value of $\Delta G(T)$. Changes in the structure of the ion relative to the molecule can also influence the entropy change for the reaction. Such an influence is possible with chloranil, where the ion is known to be more distorted than the parent molecule.[79]

The hexacyanobenzene result of section 8.2.6 is also believed to correspond to a simple direct capture reaction, but the necessity of subliming the sample on

to the heated filament made it impossible to estimate the pressure and hence $\Delta G(T)$ with any accuracy. The result obtained becomes 57.3 ± 3.1 kcals/mole at $0^{\circ}K$. This is lower than the electron affinity of tetracyanobenzene. Possible reasons for this are discussed in Part 3 of this dissertation together with a comparison of the present data and charge-transfer measurements.

Table 8.2 lists the $\Delta G(T)$, $\Delta H(\bar{T})$ and $\Delta S(T)$ values for reactions which are presumed to correspond to dissociative capture of the electron without adsorption of the residue.

Substrate	$T^{\circ}K$	$p(mm.10^{3})$	$\log^{i} e/i_{i}$	$-\Delta G(T)$	$\Delta H(\bar{T})$	$\Delta S(T)$	ΔS_{k}	$-E'$
FBQ	1420	0.92	1.86	95.1	26.4	48.4	57.5	31.9
TCNPy	1344	0.15	3.95	98.1	17.4	60.0	58.6	23.5
NO_2	1420	0.92	1.90	95.3	32.1	44.5	56.5	39.4
HCNBd	1680	0.2	3.64	120.5	22.0	58.0	57.3	28.3

TABLE 8.2

For reactions of the type

$$AB(g) + e^{-}(m) \longrightarrow A^{-}(g) + B(g) \quad -- \; 8.5$$

the probable contributory steps are,

(1) $AB(g) = AB(s)\ T_g \begin{cases} \nearrow AB(s)\ T \\ \searrow A(s) + B(s)\ T \end{cases}$ $\qquad u_1 = k_1 \cdot c_g$

(2) $AB(s) \longrightarrow AB(g)\ T$ $\qquad u_2 = k_2 \cdot c_{AB}$

(3) $A(s) + B(s) \longrightarrow AB(g).$ $\qquad u_3 = k_3 \cdot c_A \cdot c_B$

(4) $2A(s) \longrightarrow A_2(g)$ $\qquad u_4 = k_4 \cdot c_A^2$

(5) $2B(s) \longrightarrow B_2(g)$ $\qquad u_5 = k_5 \cdot c_B^2$

(6) $A(s) \longrightarrow A(g)$ $\qquad u_6 = k_6 \cdot c_A$

(7) $B(s) \longrightarrow B(g)$ $\qquad u_7 = k_7 \cdot c_B$

(8) $A(s) + e_m^- \longrightarrow A^-(g)$ $\qquad u_8 = k_8 \cdot c_A \cdot c_m$

(9) $AB(s) + e_m^- \longrightarrow A^-(g) + B(g)$ $\qquad u_9 = k_9 \cdot c_{AB} \cdot c_m$

Hence,

$$k_1 \cdot c_g = k_2 \cdot c_{AB} + k_3 c_A c_B + k_4 c_A^2 + k_5 c_B^2 + k_6 c_A + k_7 c_B + k_8 c_A c_m + k_9 c_{AB} c_m. \qquad \text{- - - - - 8.6}$$

If reactions (8) and (9) represent only minor perturbations of the adsorption-desorption equilibrium,

$$i_i = c_m \epsilon \left\{ k_8 \frac{\left[k_1 c_g - k_2 c_{AB} - c_B(k_5 c_B + k_7)\right]}{k_3 c_B + k_4 c_A + k_6} + k_9 \frac{\left[k_1 c_g - c_A(k_3 c_B + k_4 c_A + k_6) - c_B(k_5 c_B + k_7)\right]}{k_2} \right\} \qquad \text{- - - - - 8.7}$$

Unless many of these reactions may be neglected, the temperature dependence of the ion current will not be capable of any expansion in terms of electron affinities and bond energies.

The simplest reaction scheme possible is that resulting from a neglect of reactions 3, 4, 5, 6, 7, and 8, giving,

$$i_i = c_m \epsilon c_g \cdot \frac{k_1 k_9}{k_2} \cdot \qquad \text{- - - - - 8.8}$$

If the transition state for reaction (9) is AB^-*, equation 8.8 is formally identical to equation 7.3. The electron affinity E must, however, be replaced by the apparent electron affinity E', where E' = E - D, E being the electron affinity of the acceptor A, and D the A-B bond energy.

An equally simple scheme results from the neglect of reactions 2, 4, 5, 6, 7 and 9, and gives,

$$i_i = \frac{c_m c_g \epsilon k_1 k_8}{c_B k_3} \cdot \qquad \text{- - - - - 8.9}$$

Because of the c_B term this is not a useful expression

unless A = B, when

$$i_i = c_m \epsilon c_g^{1/2} . k_8 \sqrt{\frac{k_1}{k_3}} . \qquad \text{- - - - - 8.10}$$

Substituting the absolute reaction rate theory values for k_1, k_3 and k_8,

$$i_i = \bar{d} . (kTp)^{1/2} . \frac{\epsilon}{h} . \sqrt{\frac{Q^{*2} Q_a^*}{Q_g Q_d^*}} . \exp(-E_a/2RT_g) . \exp[(E' - \chi)/RT.] \qquad \text{- - - - - 8.11}$$

Equations 8.8 and 8.11 correspond to the expressions proposed by Page for these reactions. Neglect of reactions 2, 3, 4, 5, 7 and 9 gives the expression proposed for electron capture by molecules of low bond energy and is very similar to the arguments used by Mayer in the original work on the halogens.

All of the reactions considered in table 8.2 are presumed to be of the type governed by equation 8.8. The entropy of the reaction may be estimated by use of equation 7.13 with the assumptions, $Q_a^* = Q_g . h/(2\bar{\pi} M k T_g)^{1/2}$, $E_a = 0$, $Q_d^* = Q^* Q_i q_i^3 / Q\, q_A^3$, $Q_i = 2Q$ and $q_i^3/q_A^3 = (kT/hc\bar{\nu})^3$ with $\bar{\nu} \simeq 100\ cm^{-1}$ (80). Here q represents the vibrational contribution to the partition function from the vibrations which are excited to a frequency

corresponding to 100 cm^{-1} in the transition state ion. Only those vibrations associated with the bond which eventually breaks are assumed to be excited in the ion, all others are presumed to be the same in the transition state ion and the adsorbed molecule. If all the vibrations in the adsorbed molecule are excited to the filament temperature (T), each term in q_A will contribute approximately RT to $\Delta H(T)$ and x in equation 7.13 will be 1. This gives the expressions,

$$\Delta S_K = 4.57 \left[18.72 + \frac{1}{2} \log_{10} M - 2\log_{10} T \right] - 3.96 \qquad - - - - - 8.12$$

and,

$$\Delta H(\bar{T}) = E' + 2R\bar{T}. \qquad - - - - - 8.13$$

The values of ΔS_K and E' given in table 8.2 are calculated from these relationships.

The agreement for TCNPy and HCNBd is very satisfactory but less so for NO_2 and FBQ. Addition of the apparent electron affinity of NO_2 to the NO - O bond energy of 72 kcals/mole, gives the electron affinity of the capturing species as 32.6 $\pm$ 1.7 kcals/mole. This is close to the estimates given in section 4.1.1. and the photodetachment value for O of 33.4 kcals/mole.

If the ion formed from fluorobenzoquinone is assumed to be F^-, and the electron affinity of F is assumed to be 79.4 kcals/mole, the C-F bond energy may be calculated as being 111.3 $\pm$ 1 kcals/mole. This figure is well in line with other C-F bond energies. The spectroscopic value for C-F is 106 kcals, somewhat uncertain but close to the values in methyl fluoride (107 kcals) and trichlorofluoromethane (102 kcals). This figure is lower than the first dissociation energy in carbon tetrafluoride (121 kcals) and perfluorobenzene (about 145 kcals).

If the C-H bond energy in sym-tetracyanopyridine is assumed to be 102 kcals, by analogy with benzene, the electron affinity of the 2,3,5,6 tetracyanopyridyl radicle may be estimated as being 78.5 kcals/mole. This is considerably in excess of the electron affinity of the phenyl radicle (51 kcals/mole) estimated by Gaines and Page.[22] A more probable interpretation of this result is that it corresponds to the loss of CN either as the ion or the radicle. Assuming the electron affinity of CN to be 59.1 kcals/mole[21] gives the C-CN bond energy as 82.6 kcals. The assumption of the same

reaction for hexacyanobutadiene gives D_{C-CN} = 87.4 kcals. These figures are very much lower than the value in methyl cyanide (103 kcals) but are not unreasonable in view of the repulsion between the dipoles which must exist in these molecules.

It is, in principle, possible to obtain a more accurate estimate of the electron affinity of the capturing species in reactions of this type by inserting all the vibrational terms into the partition functions Q. This is unfortunately not possible in the case of complex polyatomic molecules since the vibrational frequencies of the ion are not, in general known. The transition states in equation 7.13 will also have the vibrational frequencies of some bonds slightly affected by interaction with the surface. The extent of this alteration will not be known and so the approximations used in conjunction with equation 2.15, although representing a more refined argument than the assumption that each vibrational term in q_A contributes RT to the experimental slope, are unlikely to be any more accurate. Changes in the structure of the transition state ion will also influence the rotational partition function and hence the entropy

change of the reaction. The derivation of equation 8.12 has assumed this ion to retain the same structure as the parent molecule. If the model used to describe the reaction sequence is correct, the transition state for the emission reaction will be some distance from the surface and the ion may be able to alter its structure during the transition from the surface to the Schottky barrier. Under these circumstances the electron affinities measured in the magnetron will be adiabatic and not vertical. Such a rearrangement in the structure of the ion could explain the discrepancy between $\Delta S(T)$ and ΔS_K for the NO_2 and FBQ reactions and the unexpectedly large electron affinities obtained during measurements upon naphthalene and anthracene.[81]

Table 8.3 lists the $\Delta G(T)$, $\Delta H(\bar{T})$ and $\Delta S(T)$ values calculated for reactions which are presumed to proceed by a process of dissociative electron capture with adsorption of the residue. The entropy changes for these reactions fall between the limits given by the direct, and simple dissociative capture reactions. The dissociation with adsorption reaction may be described by exactly the same sequence of reactions as

was given for equation 8.5, with the sole exception of the replacement of B(s) for B(g) in reaction 9.

Substrate	p	$\log_{10} i_e/i_i$	$-\Delta G(T)$	$\Delta H(\bar{T})$	$\Delta S(T)$	$\Delta S'_K$	$\Delta S''_K$	E'	D-E
BQ/WC	4.2	1.34	99.3	24.8	84.4	71.9	84.7	16.0	56.0
TCNB/Ir	.1	3.90	108	24.8	88	73.4	89.7	15.9	50.1
$CHCl_3$/Pt	6.6	1.68	100.1	15.7	81.0	76.8	84.7	7.1	50.9
FN/Ir	1.7	2.15	104.0	6.6	73.7	70.6		-1.9	67.9
FN/W	1.6_5	1.30	104.5	15.4	74.9	71.1		5.8	66.2
DQ/WC	3.5	2.11	102.0	21.5	85.6	72.8	88.0	12.0	60.0
DQ/Ir	2.2_5	1.28	89.0	15.1	77.4	72.9		7.9	58.1
FBQ/Ir	1.0	1.89	107.3	28.6	84.9	71.6	85.3	19.1	46.9
2,3 diCN-BQ/Ir	1.2	3.73	114.6	14.8	86.9	73.0	88.2	5.9	60.1

TABLE 8.3

The pressures in table 8.3 are in units of 10^{-3} mm Hg Neglecting reactions 3,4,5,6,7 and 8 again gives equations 8.8 and 7.3 with $E' = E - D + q_r$, where q_r is the heat of adsorption of B on the filament surface. This is the expression used by Page in the interpretation of many of the reactions given in section 2.2.

The inclusion of the q_r term implies that the T.S ion possesses an interaction energy q_r with the surface.

This is clearly impossible if this T.S is located at the Schottky barrier. The model adopted for these reactions therefore assumes the T.S to consist of a linear ($S - B - A^-$) complex with three excited vibrations having the limiting vibration frequencies corresponding to 100 cm^{-1}. The rate determining motion is assumed to be stretching of the $B - A^-$ bond instead of translation of the whole complex normally to the surface. This model will result in the loss of two rotational degrees of freedom by the complex. This may also be associated with the loss of rotational freedom by the transition state for adsorption. These assumptions give the expression

$$\Delta S'_K = 4.57 \left[16.84 + \frac{1}{2}\log_{10}(I_x I_z M) - \log_{10} T - \log_{10} \{\sigma(g)/\sigma^*\} \right] - 5.95 \quad - - 8.14$$

if the transition state for adsorption retains three rotational degrees of freedom. I_y is the moment of inertia about the S-B-A^- axis and σ^* is the symmetry number of the complex. If the transition state for adsorption also looses two degrees of rotational freedom,

$$\Delta S''_K = 4.57 \left[19.91 + \frac{1}{2}\log_{10}(I_x I_z M) + \frac{1}{2}\log_{10}(I_x I_y M) - \log_{10} \{\sigma(g)^2/\sigma^* \sigma(s)\} - 2\log_{10} T \right] - 5.95.8.15$$

The transition state for adsorption being assumed to retain only the rotational freedom about an axis normal to the plane of the molecule with a moment of inertia I_z and associated symmetry number $\bar{\sigma}(s)$.

The choice of the retention of I_z in the partition function for the transition state for adsorption was made by analogy with direct capture reactions. The experimental data are not sufficiently accurate to enable a distinction between I_y and I_z to be made since the calculated values of ΔS_K are very little influenced by the choice of the rotation retained. The values of $\Delta S'_K$ and $\Delta S''_K$ calculated from equations 8.14 and 8.15 are given in table 8.3 and are clearly in very satisfactory agreement with the observed values of $\Delta S(T)$. The apparent electron affinities are calculated from the relation

$$\Delta H(\bar{T}) = E' + 3R\bar{T}. \qquad ----- \quad 8.16$$

This again assumes that each of the three vibrations excited to 100 cm^{-1} in the T.S contributes $R\bar{T}$ to the experimental slope. The values of D-E are calculated on the assumption that each reaction corresponds to the loss of a hydrogen atom with $q_H(Ir)$ = 66 kcals/mole,

q_H(W=WC) = 72 kcals/mole and q_H(Pt) = 68 kcals/mole.

Taking D_{C-H} = 90 kcals/mole in chloroform gives $E(CCl_3)$ = 29.1 kcals/mole, which is 4 kcals ~~greater~~ less than the value calculated by Kay and Page from the same data. If the C-H bond energy in duroquinone is taken to be similar to that in toluene (78 kcals/mole), the WC result gives E = 18.0 and the iridium figure E = 19.9 kcals/mole. These are close to the electron affinity of benzyl (20.8 $\pm$ 1.9) given in table 2.1. This latter is a direct capture measurement by benzyl radicles and therefore is not subject to the possible sources of error inherent in the interpretation of the present reaction. The result of Gaines and Page[22] when corrected to $0^{o}K$ on the basis of equation 7.6 instead of 7.7 gives E = 19.3 $\pm$ 1.9 kcals/mole, in better agreement with the present figures. The inverse calculation with E = 19.3, when applied to their toluene results gives D_{C-H} = 78.4 or D - E = 59.1 kcals/mole, in excellent agreement with the present estimates for duroquinone.

All of the remaining figures in table 8.3 refer to hydrogen loss from an sp^2 hybridised carbon atom and so,

to a first approximation, it would be reasonable to expect D - E to be constant. This is clearly not the case. Referring again to the work of Gaines and Page,[22] the direct capture electron affinity of phenyl radicles derived from benzil was found to be 50.9 ± 1.1 kcals/mole. On the basis of equation 7.6 this becomes 49.4 ± 1.1 kcals/mole. Their benzene result of 34.5 kcals/mole at 1563°K gives E-D = 46.8 kcals/mole at 0°K. The work of Herron and Rosenstock has shown that this latter reaction is probably more complex than was expected and so the best estimate of D-E is probably 102 - 49.4 = 52.6 kcals/mole. This is very close to the p-benzoquinone and tetracyanobenzene figures. Assuming D = 102 kcals in these cases gives E = 46.0 and 51.9 kcals/mole respectively. Fluorobenzoquinone is rather higher at 55.1 kcals/mole. The enhancement is possibly due to the effect of the dipole moment of the molecule. A dipole moment of 1.2Debye located 4.0Å from the capturing orbital would be expected to increase the electron affinity by approximately 5 kcals/mole. This is in satisfactory agreement with the order of magnitude of the effect observed here. Unfortunately the same argument when applied to 2,3 dicyanobenzoquinone predicts an increase

in the electron affinity of the radicle and not a decrease as is observed here.

The fumaronitrile results also do not fit into this simple picture. If D remains at 102 kcals the electron affinity becomes 34.1 kcals/mole from the results on Ir filaments and 35.8 kcals/mole from the WC figures. These values are much closer to the electron affinity of methyl than phenyl and suggest a considerable modification of the hybridisation of the carbon atom by the attached CN groups. There is the possibility that the reaction observed is the loss of two hydrogen atoms with the formation of the dicyanoacetylene anion, but this would appear to be ruled out by the agreement between the Ir and WC values which should differ by approximately 12 kcals if two hydrogen atoms were adsorbed.

The measurements upon WC filaments have not been included in table 8.3 since the modification of the work function by the adsorbed molecules renders Richardson's equation in its simplest form untenable. These measurements give D-E = 61.8 kcals/mole or E = 40.2 kcals/mole. These are 6 kcals in excess of the Ir result and do suggest the loss of two hydrogen atoms. Assuming this

to be so $D_1 + D_2 - E = 133.8$ kcals from the WC result and 133.9 from the iridium data. (ignoring any changes in the correction of the apparent electron affinities to $0^{\circ}K$) Making the assumption that the electron affinity of dicyanoacetylene may be calculated on the basis of the arguments of section 10.1 as 2x16.8 kcals/mole, the sum of the C-H bond energies in fumaronitrile becomes 100.2 kcals. If the bond energy in the hydrogen molecule is taken as 103.2 kcals, the difference in the heats of formation of fumaronitrile and dicyanoacetylene becomes -3.0 kcals/mole. The measured heats of formation of TCNE and ethylene of 168.5 and 14.5 kcals/mole respectively give the heat of formation of fumaronitrile as approximately 91.5 kcals/mole. Since the experimental heat of formation of dicyanoacetylene is 128 kcals/mole, these figures are not in very good agreement with the estimate of -3.0 kcals/mole for their difference.

The evidence would therefore suggest the agreement between the Ir and WC results for this reaction to be fortuitous. The source of error is almost certainly the strong adsorption of the gas which changes the work

function of the surface. The complexity of such a system is well illustrated by the data of section 9.

The general nature of these results again suggests the model used for the interpretation of these reactions is reasonable. It is very difficult however to assess the reliability of any particular values since discrepancies between the measured and comparison values may be real or only apparent. The work of Herron and Rosenstock[82] has shown that the interpretation of some of the early work in this field was incorrect in that a simple interpretation of a complex reaction was advanced due to lack of information about the ions formed. This source of error is particularly likely with substrates such as duroquinone where $D_{C-H} \backsimeq q_{H}$. With such systems the high heat of adsorption will facilitate dissociation before electron capture and it will be possible to obtain ions by alternative routes to the one assumed in equation 8.8. Errors of this type can be to some extent avoided by measuring the electron affinity on more than one filament material, but as the fumaronitrile figures show, the results are not necessarily unequivocal.

Even when the nature of the ion is known with

certainty the neglect of side reactions may make the estimation of electron affinities meaningless. Such a case would appear to be electron capture by HCl upon iridium filaments where preliminary measurements have shown that the enthalpy change $\Delta H(\bar{T})$ for the reaction $HCl + e^- \longrightarrow Cl^- + H(s)$ differs in the presence and absence of excess hydrogen and in neither case appears to bear any simple relation to the known electron affinity, bond energy and heat of adsorption.

The results of the measurements discussed in this section are generally in adequate agreement with the theory advanced and apart from minor differences in the correction of the apparent electron affinities to $0^{o}K$ substantiate the kinetic approach advanced in section 2.2.

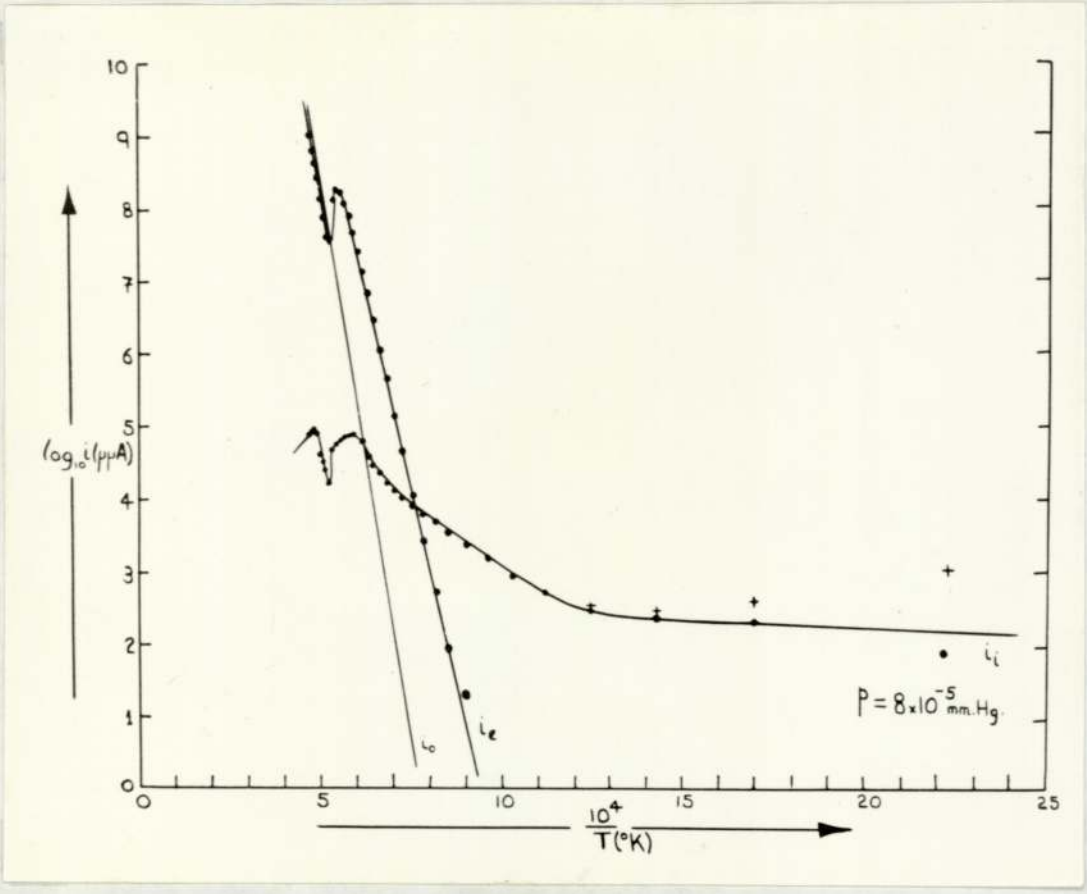

Emission currents, TCNE/WC.

FIGURE 39.

9. ELECTRON CAPTURE BY TETRACYANOETHYLENE UPON TUNGSTEN, TANTALUM AND MOLYBDENUM FILAMENTS

9.1 Preliminary observations

The data of section 8.2.1, when corrected to $0^{\circ}K$, gives the electron affinity of TCNE, when measured upon platinum, rhodium and iridium filaments as 65.2 $\pm$ 1.5 kcals/mole. This is considerably less than the initial estimate of 150 kcals/mole[23] which was derived from measurements upon tungsten filaments. The reason for this discrepancy is to be found in the complex nature of the interaction of TCNE with tungsten, tantalum and similar metals.

The most notable effects of this interaction are shown in figure 39. In the presence of TCNE at a pressure of 8×10^{-5} mm Hg the electron current from a tungsten carbide filament is increased, relative to the emission current from the same surface in the absence of the gas, at temperatures below $1890^{\circ}K$ and decreased at temperatures above this. The difference between the apparent thermionic work functions of the 'clean' surface and that exposed to the gas is about 1 volt at

temperatures below 1840°K. The increase in the magnitude of the electron current is, however, less than would be predicted by a change in the work function of the whole surface of this amount. Both the level of the electron current and the thermionic work function are sensibly independent of the gas pressure but very dependent upon the previous history of the filament.

At temperatures below 1300°K the negative ion current is greater than the electron current. At very low temperatures (approximately 500°K) increasing the filament temperature causes an initial large increase in the ion current (marked with crosses in fig 39) and then a rapid fall to the equilibrium value. Upon decreasing the temperature only these latter currents are obtained. Below 1840°K the logarithm of the electron to ion current ratio has a temperature dependence characteristic of an enthalpy change, $\Delta H(\bar{T})$, of 76 kcals/mole.

9.2 The electron current

Tungsten and tantalum in the absence of any substrate vapour behave quite normally having thermionic work functions of 4.56 and 4.21 eV respectively. These

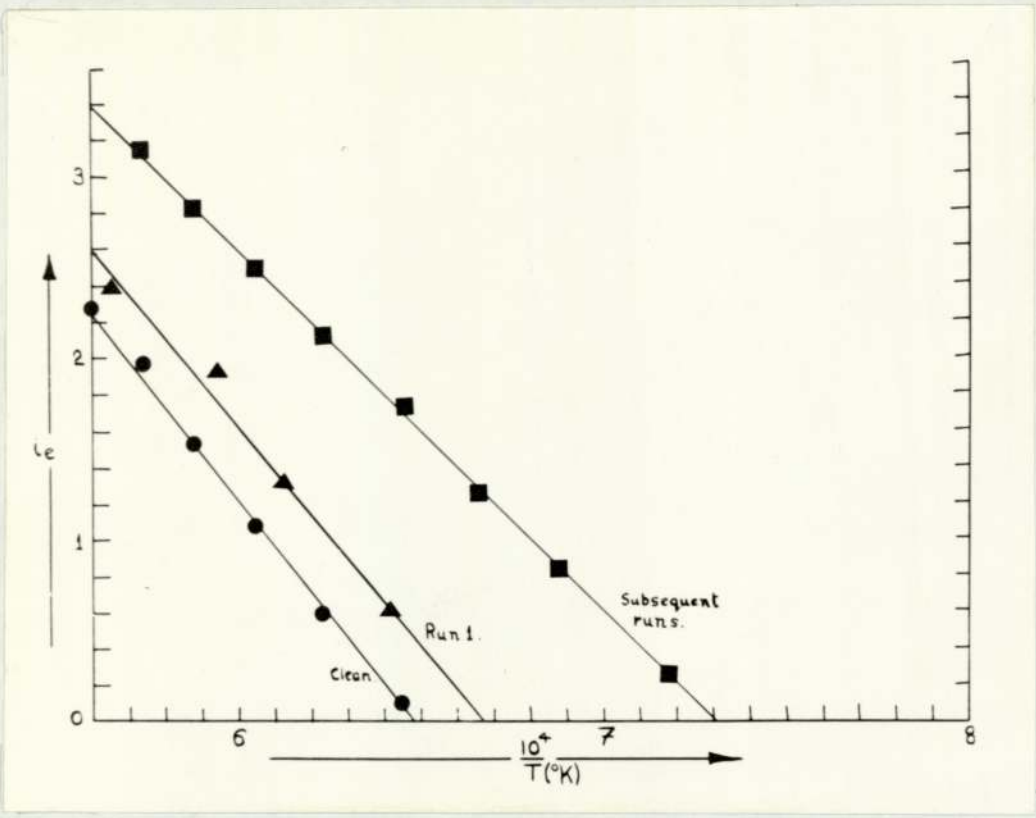

Electron work functions, Ta & TCNE/Ta.

FIGURE 40.

compare favourably with preferred thermionic values of 4.54 and 4.25 eV.[34] The behaviour of these two metals upon exposure to the vapour, however, is significantly different.

The initial measurements when a fresh tantalum filament was exposed to TCNE were somewhat erratic until the surface had become conditioned by the vapour. The electron currents showed a slight increase in magnitude but for the first runs the work function remained that characteristic of the clean surface. Determinations of the electron affinity from the ion/electron current ratios on fresh tantalum filaments gave, for the first runs, values of 146, 158, 162 and 161 kcals/mole. Subsequent runs gave apparent electron affinities which tended to become progressively smaller with the number of determinations. Typical values were 161, 123, 135, 133, 111 and 118 kcals/mole for one series and 162, 138, 122, 129 and 131 kcals/mole for another. The second and subsequent runs upon all of these filaments had work functions of 3.74 ± 0.23 eV (14 determinations). The effect of changing electron current level is shown in figure 40. Removing the source of vapour and pumping the apparatus

showed the work function of the underlying surface to have changed to 4.69 eV. It is well known that tantalum is very prone to surface recrystallisation and that the surface crystal habit is readily modified by the presence of vapours and so this behaviour is understandable. The first electron affinity determinations on new filaments have a mean value of 156 $\pm$ 6.8 kcals/mole and the mean of the second and subsequent runs is 128 $\pm$ 8.5 kcals/mole (13 determinations). The difference between these figures, 28 kcals, is close to the difference in the clean and covered surface work functions (19 kcals). Heating the filament for 15 mins at 2000^{o}K caused the work function to revert to the value characteristic of annealed tantalum (4.21 eV). Re-exposure to the gas again gave random measurements until the work function had fallen to 3.74 eV. Exposure of a surface of work function 4.69 eV to the vapour caused an almost immediate increase in the electron current and change to χ_o = 3.74 eV.

If the temperature of the filament was raised above 1800^{o}K in the presence of TCNE, the measured work functions again became erratic for some time before finally

stabilising at a value of 4.63 eV, becoming 5.24 eV upon removal of the vapour. This change in work function appeared to be accompanied by a change in the resistivity of the filament material and necessitated a recalibration of the filament temperatures. A filament which had been subjected to this treatment appeared to loose the facility for surface recrystallisation and it was impossible to reproduce the behaviour described in the previous paragraph. An X-ray examination of one of these filaments revealed the presence of considerable amounts of tantalum carbide.

This type of behaviour was also found to a lesser extent with tungsten filaments. Immediately upon exposure to the gas the work function measurements became erratic before finally stabilising at a value of 4.55 eV, which became 4.85 eV upon removal of the gas. The initial measurements of the electron affinity were again in the region of 150 - 160 kcals/mole and these were the values reported by Kay and Page.[23] As with tantalum the magnitude of the result fell with continued measurements, finally reaching a value of about 76 kcals/mole. X-ray examination again showed the presence of carbide.

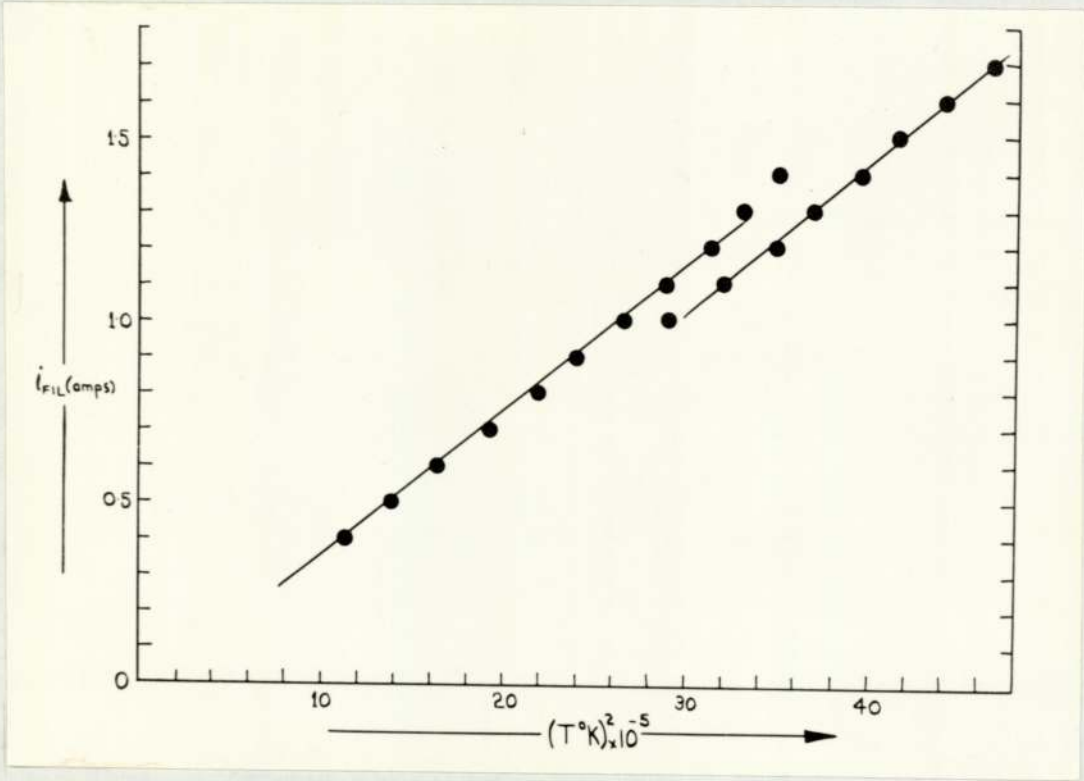

Filament temperature calibration, MoC.

FIGURE 41.

In a subsequent series of measurements it was noted that tungsten carbide filaments prepared by exposure of tungsten to fumaronitrile at temperatures of about 2000°K showed a considerably enhanced facility for the adsorption of TCNE. The work function of such a surface in vacuo was 5.05 ± 0.07 eV, becoming reduced by 0.94 eV upon exposure to TCNE. Similar behaviour was observed with fumaronitrile (χ_o reduced by 1.02 eV) and phthalonitrile (χ_o reduced by 1.07 eV).

Studies using molybdenum filaments were hampered by the ease with which the gas reacted with the metal to form a carbide. This latter appeared to show a phase change at 1825 - 1850°K which was evidenced by a discontinuity in the filament heating current - temperature calibration. The calibration temperatures exhibited hysteresis about this point, the effect being illustrated in figure 41. In the absence of the vapour both phases appeared to have a work function of 4.80 eV. In the presence of TCNE the low temperature phase showed a slight increase in electron current and a reduction in work function of 0.27 eV. At the temperature of the phase change the electron current increased rapidly by

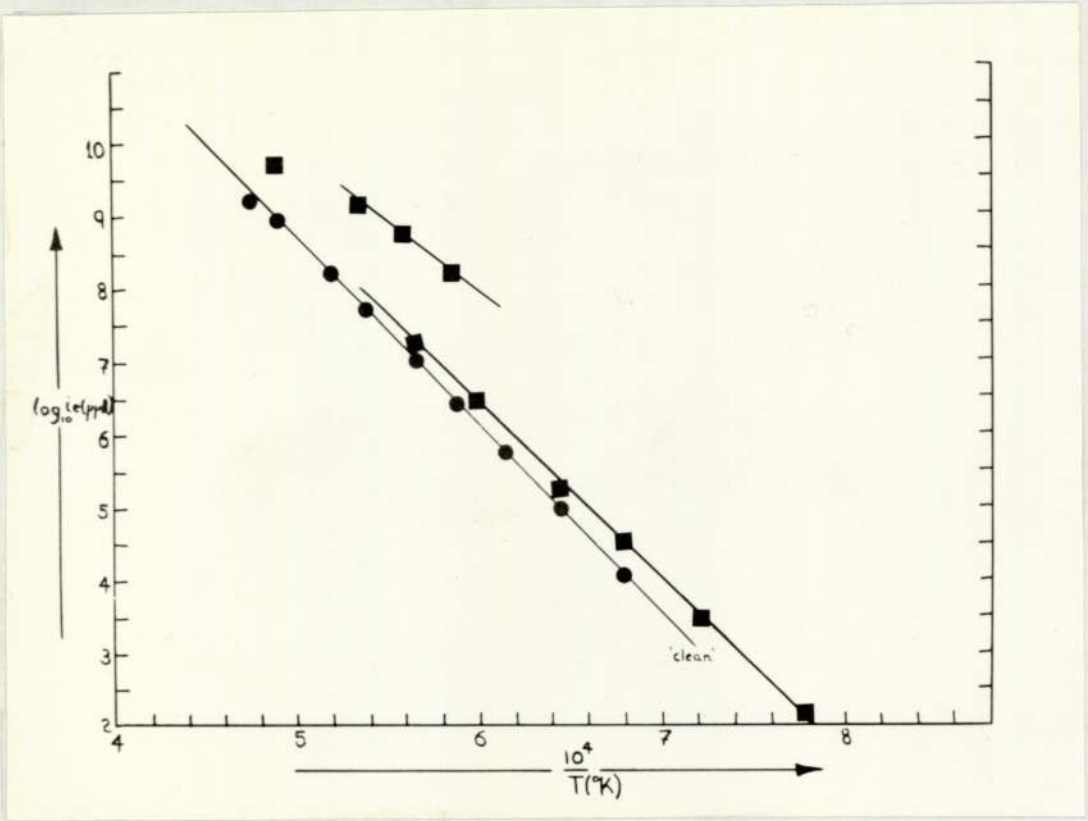

Thermionic currents, MoC & TCNE/MoC.

FIGURE 42.

a factor of about 20 and the work function dropped by about 1 volt. It was difficult to make any more precise estimate of the change in work function because desorption appeared to set in as the temperature was raised further. These facts are illustrated in figure 42.

From the data so far presented the interaction of TCNE with W, Ta and Mo filaments would seem to involve adsorption of the material with a high specificity in the nature of the adsorption sites. This is particularly well illustrated by the necessity for the occurrence of surface recrystallisation with tantalum and a phase change with molybdenum carbide, before adsorption can take place. The dependence upon the material used to carbide tungsten filaments also argues in favour of this interpretation. The similarity of the change in work function consequent upon the adsorption of TCNE, fumaronitrile and phthalonitrile suggests that the same or a similar species is responsible for this in each case. If these molecules were adsorbed with their planes parallel to the surface of the filament they would create dipole fields at the surface which would lower the work function in the manner experienced. The adsorption energy however can hardly

be electrostatic in origin since TCNE possesses a dipole field, located on the axis of the molecule, which would be expected to be twice as great as those in fumaronitrile and phthalonitrile. This would presumably lead to a greater lowering of the work function and electrostatic heat of adsorption for this compound. The former of these predictions is certainly not true and the latter is also unlikely since all three materials appear to be equally strongly adsorbed and must possess a considerable heat of adsorption to remain on the surface at 1800°K. Measurements of the pressure dependence of the ion current described in section 9.3 suggest the heat of adsorption of TCNE upon TaC to be 118 kcals/mole. This is close to the heat of chemisorption of ethylene upon Ta (138 kcals /mole) and W (102 kcals/mole). The evidence would therefore seem to suggest the opening of the double bond carrying the CN groups upon the adsorption of each of these molecules. This should lead, in each case, to a similar configuration of the CN dipoles relative to the surface and hence similar changes in the work function. This method of adsorption will also be very specific with regard to adsorption sites. The heats of ethylene chemisorption are known to fall rapidly in the series

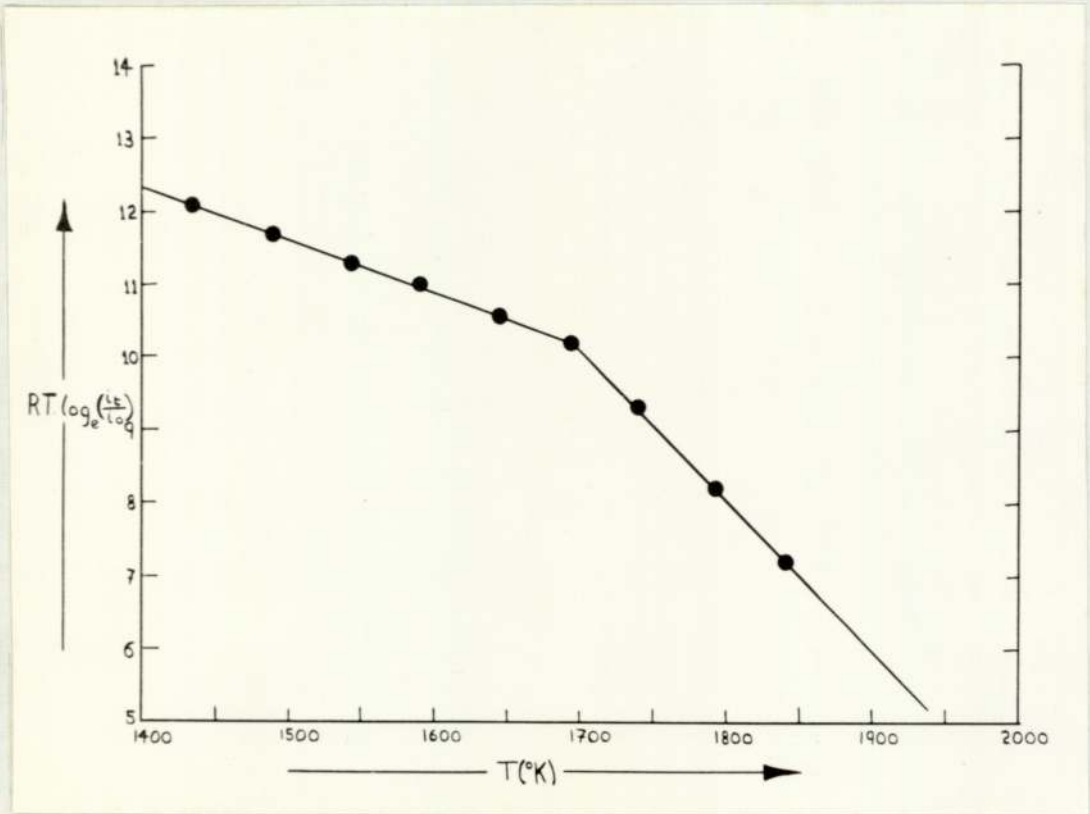

Relative thermionic electron currents, TCNE/TaC - TaC.

FIGURE 43.

Ta $>$ Nb $>$ W,Cr $>$ Mo $>$ Fe $>$ Mn $>$ Ni,Co $>$ Rh $>$ Pt,Pd $>$ Cu,Au

and so the fact that TCNE was not adsorbed by Rh ($q_{ethylene}$ = 50 kcals/mole) and Pt is understandable.

Comparing the electron currents from the clean (i_o) and covered (i_t) surfaces by means of equation 5.10, gives in the present case

$$RT.\log(i_t/i_o) = RT.\log\alpha + \Delta\chi_m(T). \quad - - - \quad 9.1$$

where α is the ratio of the transmission coefficients. This is plotted in figure 43 for a tantalum filament exposed to 1.8×10^{-4} mm Hg of TCNE. The other data is summarised in table 9.1. The magnitude of α in all these systems shows that the adsorption is accompanied by a considerable decrease in the transmission coefficient for electrons leaving the metal. This suggests a potential energy barrier of the type shown in figure 23c. The transmission coefficient through such a barrier, assuming a perfect double layer and no image force effects, has been calculated by Fowler.[74] A barrier of this type is illustrated in figure 44.

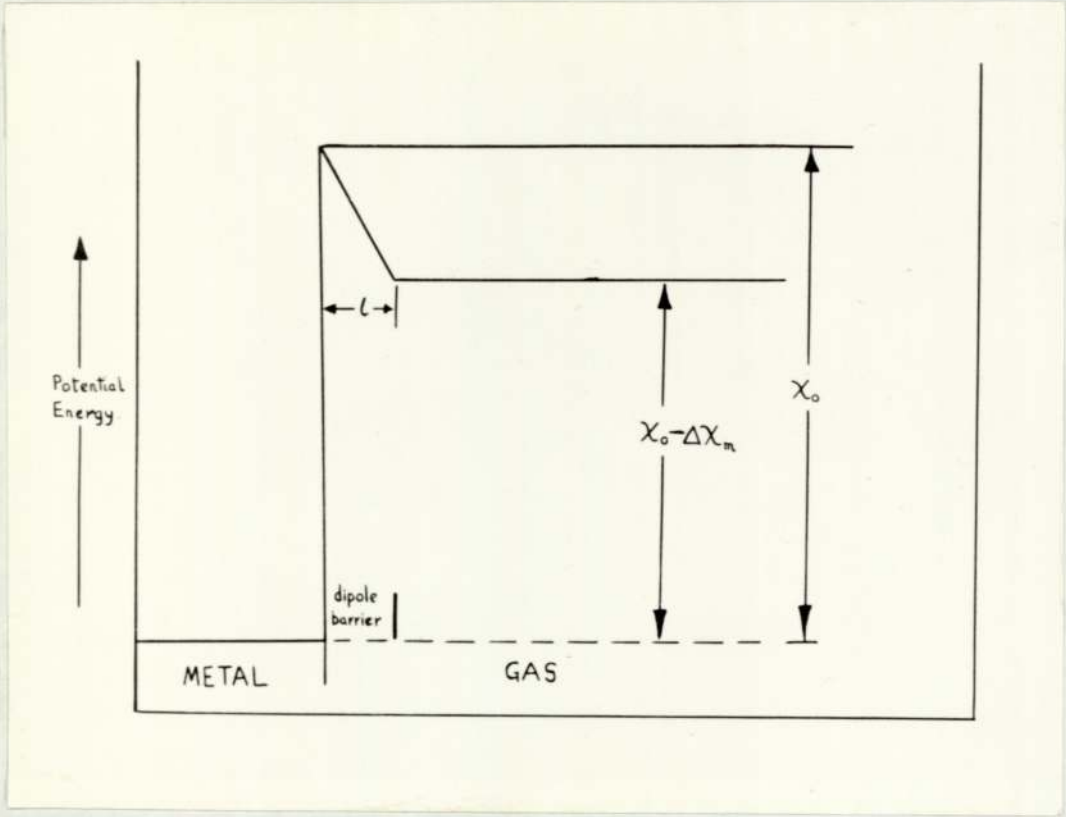

Ideal dipole barrier.

FIGURE 44.

Filament	p (mm Hg)	$\Delta\chi_m(T)$	α	1(Å)	θ
Ta	1.0×10^{-5}	11.7	9.31×10^{-2}	7.6	0.32
Ta	2.0×10^{-5}	19.6	3.86×10^{-2}	7.3	0.28
Ta	1.8×10^{-4}	22.0	3.34×10^{-2}	7.0	0.32
Ta	5.0×10^{-4}	22.0	3.30×10^{-2}	7.0	0.32
Ta	1.0×10^{-3}	21.7	3.34×10^{-2}	7.0	0.32
WC*	1.0×10^{-4}	22.7	1.08×10^{-1}	5.2	1.0
WC*	8.0×10^{-5}	22.5	1.01×10^{-1}	5.3	1.0
WC*	2.0×10^{-5}	22.9	1.08×10^{-1}	5.2	1.0
WC	1.5×10^{-4}	6.8	3.46×10^{-1}	6.5	0.64
MoC	1.1×10^{-4}	6.3	3.29×10^{-1}	6.9	0.56
MoC	1.1×10^{-4}	30	7.84×10^{-3}	7.8	0.14
TaC	2.0×10^{-4}	14.0	6.58×10^{-2}	7.6	0.29

TABLE 9.1

An asterisk denotes a carbide prepared by exposure to fumaronitrile, all others were prepared by exposure to TCNE. The values of $\Delta\chi_m(T)$ are in kcals/mole.

For the square barrier corresponding to χ_o in figure 44 the transmission coefficient will be given by

$$\bar{d}_o = 2\left[\overline{11}\,kT/\chi_o\right]^{1/2} \qquad \text{- - - - - 9.2}$$

and for the barrier corresponding to $\chi_o - \Delta\chi_m(T)$ the

transmission coefficient through the potential energy hill will be,

$$\bar{d}_t = 8\frac{\left[\bar{\pi}\, kT(\chi_o - \Delta\chi_m(T)\right]^{1/2}}{\chi_o} \exp - \frac{4}{3}\, z.l.\left[\Delta\chi_m(T)\right]^{1/2} \quad \text{----- 9.3}$$

where $z^2 = 8\bar{\pi}^2 m_e/h^2$ and l is the thickness of the potential energy hill. Combining equations 9.2 and 9.3,

$$\alpha' = 4\left[\left\{\chi_o - \Delta\chi_m(T)\right\}/\chi_o\right]^{1/2} \exp - \frac{4}{3} zl\left[\Delta\chi_m(T)\right]^{1/2} \quad \text{----- 9.4}$$

The values of l calculated from the experimental values of χ_o, $\Delta\chi_m(T)$ and α, via equation 9.4, are given in table 9.1. These figures represent lower limits for l, since the effect of image forces will be to reduce the effective height of the barrier and therefore increase the transmission coefficient.

The effective thickness of the barrier can also be estimated by assuming that the double layer is defined by the thickness of the adsorbed layer and the first layer of atoms of the metal. Summing the covalent radii of carbon and the metal and approximating to the separation of the layers by adding the separation of the components

in a charge-transfer complex (3.2 Å), 1 = 5.3Å. This is in excellent agreement with the estimate made from the transmission coefficient for tungsten carbide prepared by exposure of W to fumaronitrile. Estimates from the other materials are, however, much too large.

If the adsorbed species is the same upon all of these materials, then the WC* and Ta figures would suggest that the local work function in the presence of an adsorbed molecule is reduced by approximately 1 volt. Smaller changes in work function must therefore be ascribed to a reduction in the fraction of surface covered by adsorbate. If these adsorbed molecules are perfectly randomly arranged upon the surface equations 5.7 and 9.1 will adequately define the emission current. If however adsorption occurs preferentially upon one type of site, the arrangement will not be quite random and so a summation over all surface sites similar to equation 5.1 must be used. Approximating this, in the present case, to emission from two types of patch, covered or uncovered, gives the thermionic electron current as,

$$i_t = \bar{d}_o(1-\Theta)BAT^2\exp(-\chi_o/RT). + \bar{d}_\theta\Theta BAT^2\exp\left[-(\chi_o - \Delta\chi)/RT.\right]$$

- - - - - 9.5

where Θ is the fraction of the total surface with the reduced work function, and χ_o is assumed to be uniform over the whole surface. If the second term is much larger than the first,

$$RT.\log(i_t/i_o) = RT.\log \alpha' \Theta + \Delta\chi \quad . \quad - - \quad 9.6$$

Since $\Theta < 1$, the values of α defined by equation 9.1 will be smaller than the true values α'. Comparing equations 9.1 and 9.6, $\Delta\chi = \Delta\chi_m(T)$. Combining equation 9.4 with the estimate of 5.3Å for the barrier thickness allows Θ to be calculated from the experimental value of α. These figures are recorded in table 9.1.

The small values of $\Delta\chi_m(T)$ from WC and MoC makes the neglect of the first term in equation 9.5 unreasonable and the approximate value of the large work function change for the latter material again makes the accuracy of the estimate of Θ uncertain. All of the tantalum figures suggest a value of Θ of 0.32, which is a reasonable estimate of the maximum statistically probable coverage by a rigid layer of molecules of such size. Roberts[83] has shown that the adsorption of a diatomic molecule occupying two sites into an immobile layer

results in some 8% of the sites remaining unoccupied. In the present case the molecule will cover some 5 x 6 = 30 sites. To a first approximation, it may be assumed that only if the space between two molecules is greater than the molecular dimensions may a third be placed between them. If the molecules are therefore adsorbed into an immobile layer by random adsorption from the gas phase, each one will be surrounded by a clear band half the molecular size in width. This leads to a maximum probable surface coverage slightly greater than 0.25, in excellent agreement with the observed value. This is the type of surface structure which would be expected on tantalum filaments where the total surface coverage would be expected to be governed by the random adsorption of the molecules. The fact that $\Delta\chi_m(T)$ changes very little from Θ = 0.32 on Ta to Θ = 1 on WC*, suggests that the emission occurs predominantly from the region of the adsorbed molecule.

The WC* figures suggest that the carbiding of the surface with fumaronitrile leads to a regular surface structure which is capable of adsorbing a much larger number of molecules. This interpretation is in agree-

ment with the observation that removal of the vapour by pumping and flashing led to reproducible 'clean' surface work functions but readsorption of the gas, although giving reproducible work functions, only gave reproducible electron currents after the temperature of the filament had been raised to 1840°K. This corresponds to a temperature at which the rate of desorption of the gas is significant and therefore rearrangement of the randomly adsorbed molecules to accommodate new arrivals is possible, leading to a much greater surface coverage.

In the temperature range 1700 - 1800°K, the electron current passes through a maximum which may be used to estimate the heat of adsorption of the gas upon the surface. The rate of adsorption will be given by equation 6.4 which, with the assumptions $p = 10^{-4}$ mm Hg, $E_a = 0$, $c_s/Q_s = (1-\Theta)$, $\Theta = 0.3$ and $Q_a^*/Q_g = h/(2\pi MkT_g)^{1/2}$ gives $u_a = 1.2 \times 10^{16}$ mols.cm^{-2}.sec^{-1}. If the adsorbed molecules and the transition state for desorption are equally mobile, equation 6.5 gives the rate of desorption as $1.2 \times 10^{28} \exp -q/RT$ molecules.cm^{-2}.sec^{-1} at 1840°K and $\Theta = 0.3$. If the adsorbed molecules are immobile and the transition state for desorption is mobile, the

pre-exponential term becomes approximately 10^{34}. In the present system the adsorbed layer is probably immobile, therefore estimating the rate of desorption as $10^{32} \exp - q/RT$ mols.cm^{-2}.sec^{-1}, and equating the rates of adsorption and desorption at 1840°K gives q(WC) = 137 kcals/mole. The break in the line of figure 43 corresponds to the onset of desorption and the same calculation applied to this point gives q(Ta) = 126 kcals/mole.

9.3 The ion current

The emission of ions from the surface will be governed by an expression of the form,

$$i_i = \Theta CA \exp - \phi/RT. \qquad ------ 9.7$$

where C is approximately constant, A is the surface area, Θ the fraction of the total surface covered by ion precursors and ϕ is the heat of desorption of the ion. The fraction of surface covered by adsorbed TCNE is known from the results of the previous section to be effectively constant, provided the temperature is not raised above 1800°K, and sensibly independent of the gas pressure. If this were the same adsorbed species as that giving rise

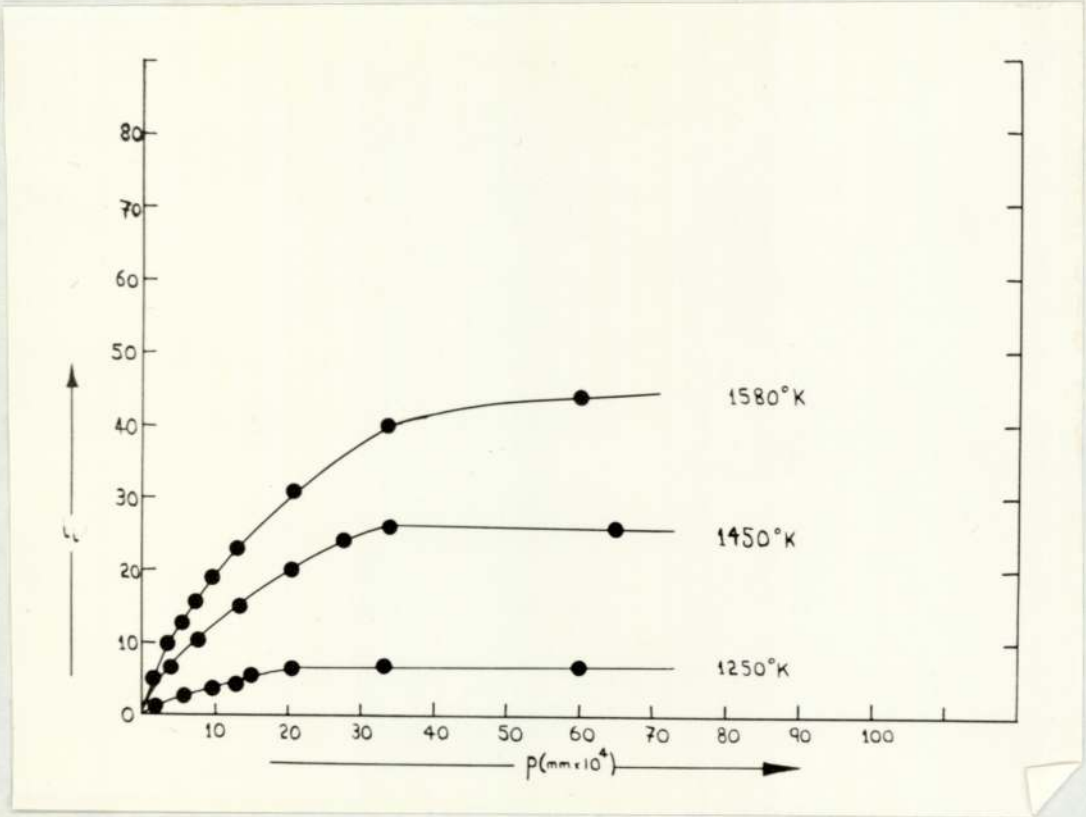

Pressure dependence of the ion current, TCNE/TaC.

FIGURE 45.

to ions, i_i should be correspondingly independent of pressure. That this is not so is shown by figure 45 where the ion current deriving from TaC filaments can be seen to increase with pressure up to $p = 5 \times 10^{-3}$ mm Hg. Similar behaviour was observed with all filament materials. Figure 39 shows the ion current to exhibit a maximum at the same temperature as the electron current. This suggests that even though the negative ions are not formed by the strongly adsorbed layer, their formation is in some way associated with its presence. In the region of this maximum the variation of Θ in equation 9.7 can probably be neglected compared to the variation in A, if this latter can be equated to the area of surface covered by strongly adsorbed TCNE ($\Theta_s A_o$).

At the maximum $di_i/dT = 0$, which becomes for Langmuir type adsorption, $\phi = (1-\Theta_s)q_s$ where q_s is the heat of adsorption of the strongly adsorbed layer. Now,

$$(1-\Theta_s)/\Theta_s = k_2/k_1 p \qquad ------ 9.8$$

where $k_1 p$ is the rate of adsorption and k_2 the rate of desorption, whence,

$$k_2/k_1 p = \phi/(q_s - \phi). \qquad ------ 9.9$$

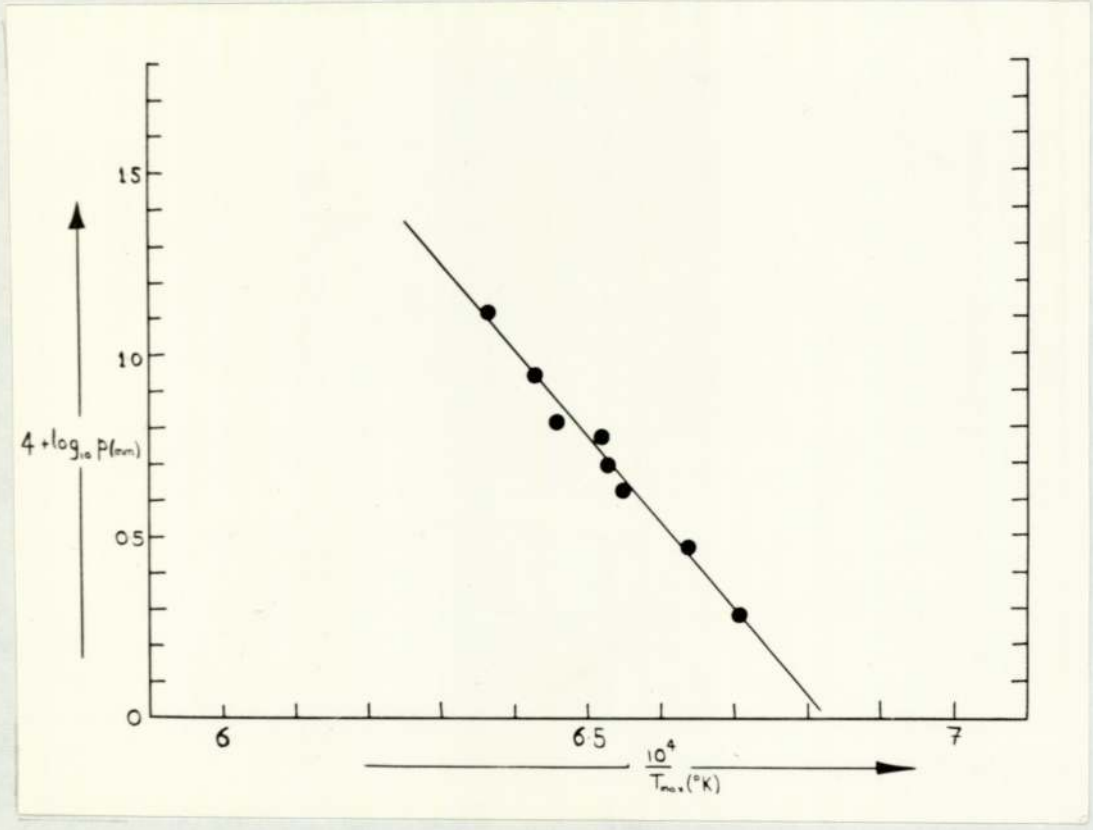

The activation energy for desorption, TCNE/TaC.

FIGURE 46.

Therefore substituting $k_2 = k_o \exp[-q_s/RT,]$

$$\log p = \log(k_o/k_1) + \log (q_s - \phi)/\phi - q_s/RT \qquad \text{- - - - - 9.10}$$

Plotting log.p against 1/T, where T is the temperature at which the maximum in the ion current occurs when the pressure is p, should yield a straight line of slope q_s/R. This is shown for measurements upon TaC in figure 46. The average value of q_s from several such measurements was 118 $\pm$ 4 kcals/mole, in good agreement with previous estimates.

The intercept of figure 46 has a value of 16.34. Figure 47 shows that the slope on the high temperature side of the maximum in the ion current is constant and independent of the gas pressure, and since, by differentiation of equation 9.7 this is equal to $(1-\theta_s)q_s - \phi$, this constancy implies that θ does not vary greatly. Assuming it to be vanishingly small, $q_s - \phi =$ 28 kcals/mole and hence $\phi \simeq$ 90 kcals/mole. (The data are taken from figure 47). Since the pressures of figure 46 are in units of 10^{-4} mm Hg, log k_1 becomes 16.22 (assuming $(1-\theta_s) = 1$) and hence $\log_{10} k_o = 33.07$. This is close to the value estimated

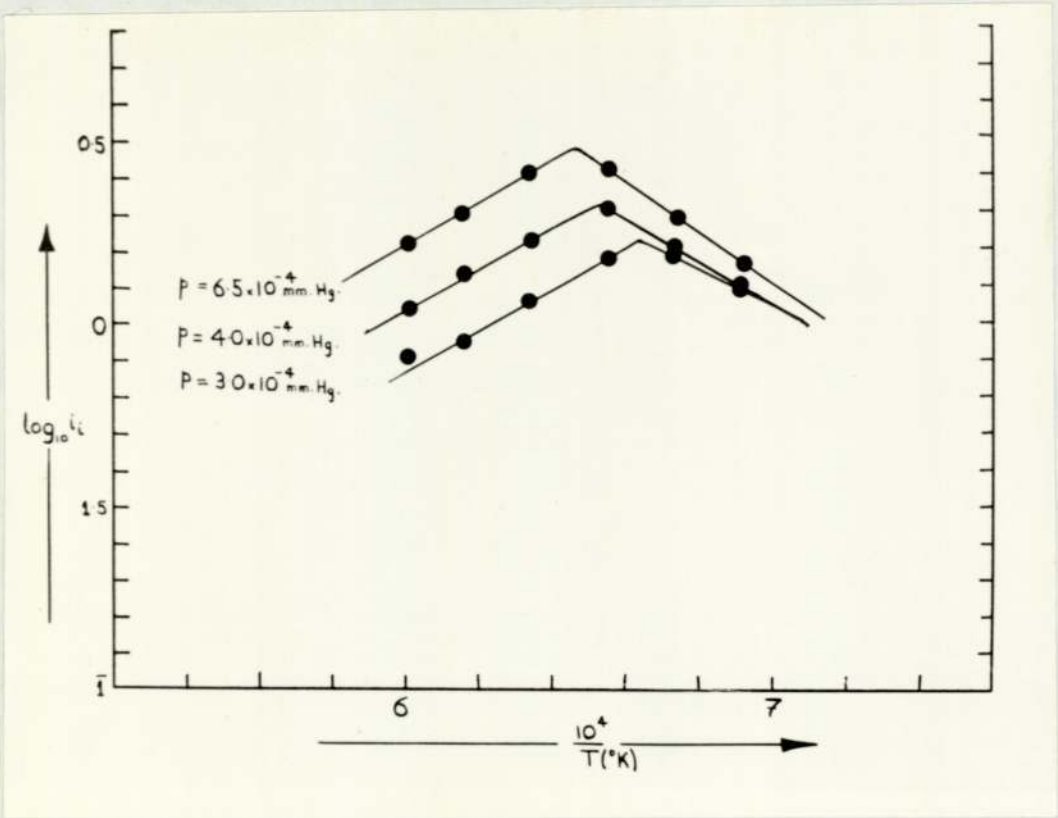

The thermionic ion currents, TCNE/TaC.

FIGURE 47.

for desorption from an immobile adsorbed layer and in agreement with the predictions of adsorbate immobility made from the measurements of the previous section.

In the early measurements of Kay and Page it was assumed that the ions were formed in the primary adsorbed layer. If this were so, $-\phi = E' - \chi - q_s$ and therefore $q_s - \phi = E' - \chi$. Under the present conditions χ is constant and equal to 128 kcals/mole over this temperature range so that apparently $E' = 156$ kcals/mole. This is also the apparent electron affinity which was measured in the first runs upon fresh tantalum filaments (156 ± 6.8 kcals/mole.) As noted in the previous section subsequent measurements gave $E' = 128 \pm 8.5$ kcals/mole, the difference being due to the change in work function accompanying the increased surface coverage of the filament.

If these results are to be interpreted on the basis of the superimposition of a changing effective surface area for electron capture upon the normal temperature dependence of the ion current, then $128 = E' + q_s$ and $E' = 10$ kcals/mole. This is clearly very far removed from the value of 72 kcals/mole derived from measurements

upon Pt, Ir and Rh. The reasons for this apparent discrepancy are almost certainly to be found in the assumption that the high temperature slope of figure 47 is equal to $q_s - \phi$. This will only be true if equations 9.7 and the Langmuir equation apply. At low surface coverage $\Delta\chi_m(T)$ will vary with θ and therefore a better expression for the slope of figure 47 in this region would be $(1-\theta_s)q_s - \phi - T.d\Delta\chi_m(T)/dT$. For the apparent electron affinity of 128 to yield a true electron affinity of 72 kcals/mole, with $\theta \triangleq 0$, the $T.d\Delta\chi_m(T)/dT$ term must contribute 62 kcals/mole to the experimental slope. This would correspond to a change of 5.3 kcals/mole in $\Delta\chi_m(T)$ between the maximum and minimum in figure 47. A variation of this order of magnitude is quite feasible.

Measurements of the apparent electron affinity of TCNE, when confined to the low temperature side of the maximum in the ion current, gave much more reproducible figures. These are summarised below.

(i) Measurements near maximum, film desorbing slowly.

<u>TaC</u> $\Delta H(\bar{T})$ = 75.9, 73.6, 67.6, 72.8, 72.3, 70.7, 68.2, 70.5, 66.4, 65.0, 68.6, 73.6, 76.4, 73.2,

75.4, 78.6, 76.1. Hence

$E'(1550^{\circ}K) = 72.5 \pm 3.8$ and

$E = 66.1 \pm 3.8$ kcals/mole.

WC $\Delta H(\bar{T}) =$ 79.6, 76.4, 76.0, 78.8, 75.5. Hence

$E'(1590^{\circ}K) = 77.3 \pm 1.6$ or

$E = 71.0 \pm 1.6$ kcals/mole.

(ii) Measurements with constant surface coverage.

Ta $\Delta H(\bar{T}) =$ 73.4, 73.8, 73.4, 71.8, 73.1, 73.6, 74.1, 74.6, 74.6, 72.3. Hence

$E'(1430^{\circ}K) = 73.5 \pm 1.0$ or

$E = 67.8 \pm 1.0$ kcals/mole.

WC $\Delta H(\bar{T}) =$ 72.2, 76.5, 77.7, 76.4, 76.3, 76.4, 77.0, 76.4. Hence $E'(1300^{\circ}K) = 76.1 \pm 1.5$ or

$E = 71.0 \pm 1.5$ kcals/mole.

The determinations of the electron affinity of TCNE are summarised in the following table.

Filament	Pt	Ir	Rh	Ta	TaC	WC
E	66.9	64.0	63.8	67.8	66.1	71.0
$\sqrt{\ }$	1.2	1.5	1.9	1.0	3.8	1.6
no of detmns	7	8	3	10	17	13

TABLE 9.2

The weighted mean of these results is 67.2 $\pm$ 2.5 kcals/mole. (∇)

It is instructive to calculate the thermodynamic functions, defined by equation 7.14, associated with the formation of ions by TCNE upon covered surfaces. Equations 7.14 and 7.9 may be combined in the slightly modified form,

$$i_e/i_i = (\alpha kT/p).\exp\left[-\Delta G/RT.\right] \quad ----- \quad 9.11$$

This gives the following figures,

Filament	Pt	Ir	Ta	TaC	WC*
$T^{\circ}K$	1475	1414	1450	1620	1222
$p(mm \times 10^{3})$	.1	.1	0.30	0.14	0.08
α	1	1	3.34×10^{-2}	6.58×10^{-2}	1.08×10^{-1}
$\log_{10} i_e/i_i$	2.33	1.83	$\bar{1}.26$	$\bar{1}.10$	$\bar{1}.17$
$-\Delta G(T)$	95	88	106.4	90.3	66.6
$\Delta H(\bar{T})$	72.3	69.4	73.5	72.5	76.1
$\Delta S(T)$	114	117	110.3	100.5	116.8

TABLE 9.3

The entropy changes are close to those obtained for

electron capture by TCNE upon metals where there is no strong adsorption and so the mechanism of ion formation upon the covered surface is presumably identical to that upon the clean surface.

At very low temperatures the ion current deriving from WC* filaments suggests an apparent electron affinity of 84.0 $\pm$ 0.6 kcals/mole (10 determinations) in the temperature range 800 - 1170^{o}K if the work function of the filament is assumed to remain unchanged. However since the temperatures used in deriving this data were extrapolated values from the temperature calibration graph, no great reliance can be placed on the absolute magnitude of this result. If this increase is real it must be associated with either a change in work function or else a change in the mechanism of ion formation. Of these two the former would appear more likely since the electron current at low temperatures has already been noted as suggesting multilayer adsorption. This process has also been observed in adsorption studies upon iron powders.[84] The change in apparent electron affinity would require a lowering of the clean surface work function by 35.5 kcals consequent upon multilayer adsorption.

PART III

APPLICATIONS AND CONCLUSIONS

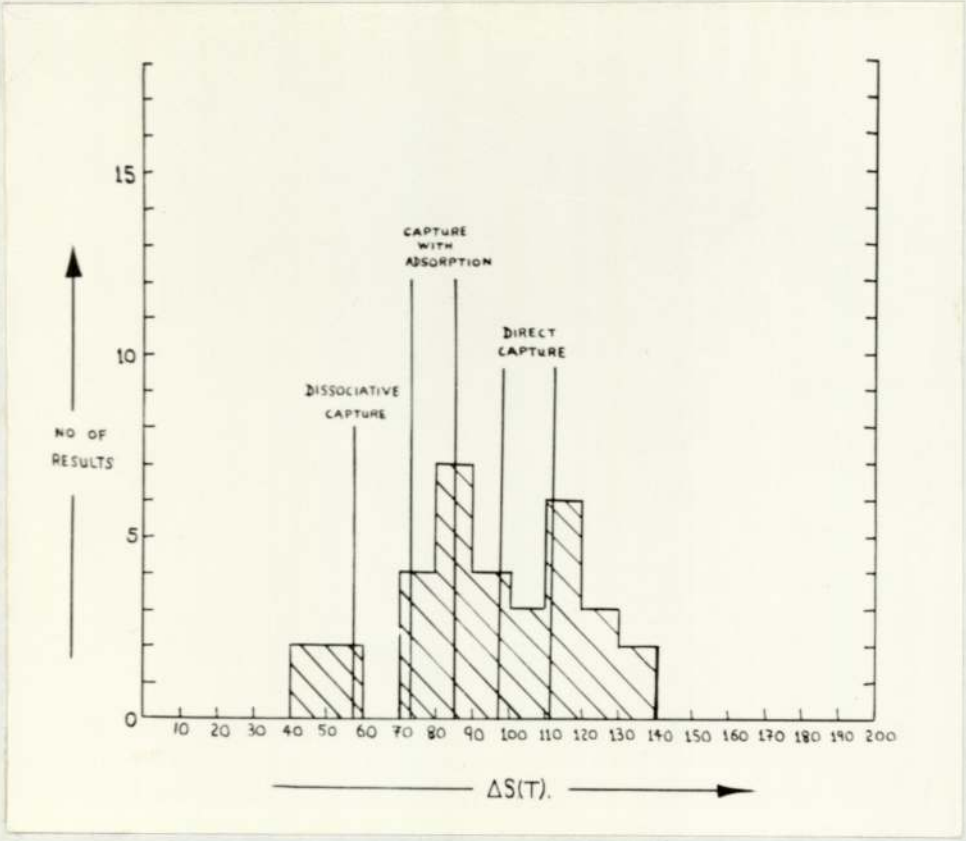

Entropy of reaction histogram.

FIGURE 48.

10. DISCUSSION OF RESULTS

10.1 The Measured values

From the data given in tables 8.1, 8.2 and 8.3 the entropy changes associated with the direct capture (C), dissociative (D) and dissociative capture with adsorption (A) reactions may be calculated as; (Figure 48)

$$\Delta S(C) = 110 \pm 17 \text{ eu } (98, 112).$$
$$\Delta S(A) = 82 \pm 5 \text{ eu } (73, 85). \quad \text{- - - - - 10.1}$$
$$\Delta S(D) = 53 \pm 7 \text{ eu } (57).$$

The values given in brackets are calculated on the basis of equation 7.13. These figures appear to be characteristic of the reactions occurring and the value of $\Delta S(T)$ may therefore be used as a diagnostic test for the reaction type. This information should supplement an interpretation of the process on the grounds of the feasibility of the enthalpy change $\Delta H(\bar{T})$. It is unfortunate that the compensation effect between $\Delta H(\bar{T})$ and $T.\Delta S(T)$ prevents the electron affinities being calculated from the absolute magnitude of the ion/electron current ratio, by the methods of statistical mechanics.

The application of transition state theory to the emission of ions and electrons from heated metal surfaces has shown that the measured apparent electron affinities may be identified with the enthalpy change $\Delta H(\bar{T})$ for the reaction

$$A^{-}* = A* + e^{-}*. \qquad \text{- - - - - 10.2}$$

where the asterisk signifies that all species are in their respective transition states for emission from the surface. The values of ΔH at the temperature of the reaction $(\bar{T})$ are related to the values at $0^{o}K$ by the approximate relationships,

$$\Delta H(\bar{T}) = H_{o} + 2R\bar{T}. \qquad \text{- - - - - 10.3}$$

for direct capture and simple dissociative reactions, and

$$\Delta H(\bar{T}) = H_{o} + 3R\bar{T}. \qquad \text{- - - - - 10.4}$$

for dissociative reactions involving adsorption of the residue. The exact relationship between $\Delta H(\bar{T})$ and ΔH_{o} requires a more complete knowledge of structure and vibration frequencies of the transition state ion than is generally available. The errors introduced by these approximations however would appear to be small in view of the agreement between the data derived from

direct capture measurements upon radicles and that derived from measurements involving dissociation with adsorption.

The electron affinities which have been measured in this work are summarised in table 10.1. The data for the dissociative reactions has been discussed in section 8.3. The direct capture electron affinities of the cyanocarbon derivatives and quinones given in the table show evidence of an additive relationship between the number of substituents and the electron affinity. This is illustrated in table 10.2.

TABLE 10.1

Substrate	$\Delta H(\bar{T})$	ΔH_o	E	D	q_H
NO_2/Pt	96.2 ± 3.7	90.1			
	-32.1 ± 1	-39.4	32.6	(72)	
	5.0 ± 2.2	-1.6			
NO/Pt	25.6 ± 2.5	19.1			
BQ/Ir	36.7 ± 0.2	30.9			
BQ/WC	37.1 ± 1.1	30.6			
	24.8	16.0	46	(102)	(72)
chloranil	80.9 ± 1.5	75.9			
DQ/WC	21.5 ± 2.7	12.0	18.0	(78)	(72)
DQ/Ir	15.1 ± 1.1	7.2	19.2	(78)	(66)
diCNBQ/Ir	14.8 ± 1.8	6.0	42.0	(102)	(66)
FBQ/Ir	54.8	49.8			
	-26.4 ± 0.8	-31.9	(79.4)	111.3 (C-F)	
	28.6 ± 2.8	19.1	55.1	(102)	(66)
TCNE/Pt	72.3 ± 1.2	66.9			
TCNE/Ir	69.4 ± 1.5	64.0			
TCNE/Rh	70.7 ± 1.9	63.8			
TCNE/Ta	73.5 ± 1.0	67.8			
TCNE/TaC	72.5 ± 3.8	66.1			
TCNE/WC	76.1 ± 1.5	71.0			
TCNB/Ir	64.4 ± 1.3	59.3			
	28.4 ± 1	15.9	51.9	(102)	(66)
TCNQ/Ir	88.3 ± 2.2	83.3			
	56.1 ± 1.7	50.2			
HCNBd/Ir	97.4 ± 2.8	92.4			
	82.3 ± 3.0	76.8			
	-22.0 ± 4.9	-28.3			
TCNPy/Ir	54.0 ± 1.9	49.1			
	-17.4	-23.5	(59.1)	82.6 (C-CN)	
HCNB/Ir	62.8 ± 3.1	57.3			
PN/Ir	30.1 ± 3.1	24.0			
PN/WC	30.4 ± 2.2	24.4			
FN/Ir	21.3 ± 2.7	15.7			
	6.6 ± 2.0	-1.9	34.1	(102)	(66)
FN/W	15.4 ± 1.9	5.8	35.8	(102)	(72)

Values given in brackets are assumed in the calculation of E or D.

Molecule	E (kcals/mole).
PN	2 x 15.8 - 4 x 1.9
TCNB	4 x 15.8 - 2 x 1.9
HCNBd	6 x 15.3
TCNE	4 x 16.8
BQ	2 x 19.2 - 4 x 1.9
FBQ	2 x 19.2 - 3 x 1.9 + 17.1
Chloranil	2 x 19.2 + 4 x 9.4
HCNB	6 x 9.6
FN	2 x 16.8 - 2 x 9.0

TABLE 10.2

Each CN group appears to contribute 16 kcals/mole to the total electron affinity whereas each hydrogen atom appears to decrease the measured value by 2 kcals/mole. For most of these molecules the first unoccupied orbital will be low lying and, if this is so, the major contribution to the electron affinity will be the work done in bringing the electron up to the molecule from infinity against the field due to the dipoles of the substituents. It may be simply shown that this is equal to $\frac{2}{3}\sum \frac{\mu \epsilon}{x^2}$, where

μ is the resolved part of the dipole acting along a line joining its centre to the centre of the molecule, the separation between these latter two being x. This equation may be used, in conjunction with the experimental dipole contributions to the electron affinity, to compute the dipole moments of the substituents. The data is summarised in table 10.3

Bond	ΔE(kcals)	x(Å)	$\mu(D)_{calc}$	$\mu(D)$[85]	ΔE_{calc}
C-H	-1.9	2.17	-0.20	-0.4	-3.9
C-CN	15.8	3.42	4.04	3.99	15.6
C-F	17.1	2.17	1.75	1.19	11.6
C=O	19.2	2.08	1.81	2.3	24.4
C-Cl	9.4	2.17	0.96	1.30	12.7
C-Br		2.17		1.33	13.0
C-I		2.17		1.30	12.7
C-Me		3.65		-0.77	-2.7
$C-NO_2$		3.53		3.81	14.1
C-CN(TCNE)	16.8	2.36	2.04		
C-H(FN)	-9.0	1.28	-0.32		

TABLE 10.3

The agreement between the observed and calculated values is impressive for C-H, C-N and C=O. The reduced C-Cl dipoles in chloranil and TCNE are possibly due to mutual polarisation effects. This would be in accord with the observation[85] that the dipole moments of the substituents in fully substituted compounds are reduced by approximately

20%. This calculation may be inverted and the measured bond dipole moments used to calculate the bond contributions and hence the electron affinities of a range of dipolar substituted benzenes. The values obtained from such a calculation are given in tables 10.3 and 10.4.

No	Compound	E_{expt}(eV).	E_{calc}(eV).	$h\nu^{95}_{expt}$(eV).	$h\nu_{calc}$(eV).
1	BQ	1.34	1.44	2.77	2.80
2	NO_2 "		2.22	1.88	2.30
3	CN "		2.29	2.24	2.12
4	F "	2.16	2.11	2.63	2.25
5	Cl "		2.16	2.53	2.21
6	Br "		2.17	2.50	2.20
7	I "		2.16	2.55	2.21
8	Me "		1.49	2.84	2.60
9	diCN "		3.14	1.73	1.70
10	tetra CNBQ		3.87*	1.10	1.27
11	tetra CIBQ	3.29	3.44	2.03	1.15
12	TCNB	2.57	2.39	2.51	2.63
13	HCNB	2.49	3.27*	1.95	2.02
14	TCNXy		1.99*	2.83	2.80
15	PCNT		2.63*	2.32	2.43
16	TCNE	2.92		1.71	1.71
17	TNB		1.31	2.79	3.35
18	TCNQ	3.61		1.62	
19	HCNBd	4.01		1.43	

TABLE 10.4

9 = 2,3 dicyanobenzoquinone, 14 = tetracyanoxylene, 15 = pentacyanotoluene, 17 = sym-trinitrobenzene. All values marked with an asterisk have been reduced by 20% to allow for the effects of full substitution.

10.2 The relationship between charge-transfer measurements and electron affinity

The characteristic absorption bands of many molecular complexes, which can be attributed to neither partner alone, are believed to be associated with the transfer of an electron from one molecule, termed the donor, to the other, termed the acceptor. Mulliken[86] considered the complex to be due to the interaction of a no bond ground state $\Psi_o(D,A)$ and a polar excited state $\Psi_1(D^+,A^-)$ to produce a stabilised ground state having a wave function

$$\Psi_o' = \Psi_o(D,A) + \alpha\Psi_1(D^+,A^-)$$

and an excited state, the charge-transfer state,

$$\Psi_1' = \Psi_1(D^+,A^-) + \beta\Psi_o(D,A)$$

The charge-transfer band is then associated with the transition $\Psi_o' \longrightarrow \Psi_1'$.

The energy change associated with the charge-transfer process is given by,[87]

$$h\upsilon_{CT} = I_D(v) - E(v) + G_1 + G_o + X_1 + X_o \qquad \text{- - - - - 10.5}$$

where $I_D(v)$ and $E(v)$ are the vertical ionisation potential and electron affinity of the donor and acceptor respectively. X represents the resonance energy of the interaction between the 'no bond' and 'dative' states, and the G's contain the remaining interaction energy terms.

When α and β are very small the X terms may be neglected to give the linear relationship,[88]

$$h\nu = I - E - C. \qquad \text{- - - - - 10.6}$$

where C represents the interaction energy of the excited state relative to the ground state. This equation and the closely related quadratic form[89] have been extensively used in the measurement of ionisation potentials,[90] and several attempts have been made to relate the charge-transfer energy to the electron affinities of a series of acceptors.[91]

In all of these measurements the assumption is made that the interaction energy is approximately constant

throughout a series of complexes of similar bond type. In the case of ionisation potential measurements this assumption has the backing of experimental evidence, since the ionisation potentials so measured can be compared with the values obtained from photoionisation and electron impact studies. The paucity of electron affinity data, however, has precluded attempts to justify this assumption in relation to their measurement by charge-transfer methods. The data is currently so scarce that it has hitherto only been possible to use a single, rather dubious, electron affinity as the basis of a whole series of extrapolated values. Briegleb[92] has attempted to overcome this by comparing the results of several different methods of measuring electron affinities and has produced a table of relative electron affinities which have a more reliable background than the original extrapolation procedure of Batley and Lyons.[91]

Unfortunately the electron affinities predicted by these methods are uniformly much lower than the results of the magnetron measurements predict. In the case of charge-transfer measurements this would appear to be due to the neglect of charge-dipole interactions in the

excited state of the charge-transfer complex.

If the interaction energy of the excited state of the complex is entirely electrostatic in origin, the value of C may be calculated by summing the charge-charge, charge-dipole and reaction field contributions and adding to this the work of charging the dipole of the complex.[93] Hence,

$$C = \frac{\epsilon^2}{r} - \frac{2}{3}\sum_i \frac{\mu_i.\epsilon.x_i}{(r^2 + x_i^2)^{3/2}} - \frac{2}{3}\sum_j \frac{\mu_j.\epsilon.x_j}{(r^2 + x_j^2)^{3/2}}$$

$$- \frac{1}{2}\frac{f.\mu^2}{(1-f.\alpha)} - \frac{\mu^2}{2\alpha} \qquad \text{- - - - - 10.7}$$

where the first term represents the charge-charge interaction between the excited donor and acceptor at a separation r. The second term is the contribution due to the interaction between the charge on the acceptor with the dipoles of the donor, x and r having the same meanings as previously. The third term is the interaction energy of the acceptor dipoles with the charge on the donor. The fourth term is the contribution due to the reaction field of the dipole μ of the excited complex with the solvent. Here f represents the term,

$$f = \frac{1}{a^3} \cdot \frac{(2\Gamma - 2)}{(2\Gamma + 1)}$$

where a^3 is the volume of the cavity in the dielectric in which the complex lies, Γ being the dielectric constant and α the polarisability of the complex. The final term is an approximation to the self energy of the dipole μ and represents the work of charging the dipole in a medium of polarisability α .

In the previous section the electron affinity was shown to be given, to a good approximation, by $E = \frac{2}{3}\sum_j \mu_j \epsilon / x^2$. This may be combined with equations 10.6 and 10.7 to give,

$$h\nu = I - \frac{2}{3}\sum_j \frac{\mu_j \epsilon}{x^2}\left[1 - \frac{x_j^3}{(r^2 + x_j^2)^{3/2}}\right] - \frac{\epsilon^2}{r}$$

$$+ \frac{2}{3}\sum_i \frac{\mu_i . \epsilon . x_i}{(r^2 + x_i^2)^{3/2}} + \frac{f.\mu^2}{2(1-f.\alpha)} + \frac{\mu^2}{2\alpha}. \qquad - 10.8$$

which reduces, for a given acceptor and series of donors to;

$$h\nu = I + \frac{2}{3}\sum_i \frac{\mu_i . \epsilon . x_i}{(r^2 + x_i^2)^{3/2}} + K'. \qquad - - 10.9$$

and for a given donor and series of acceptors,

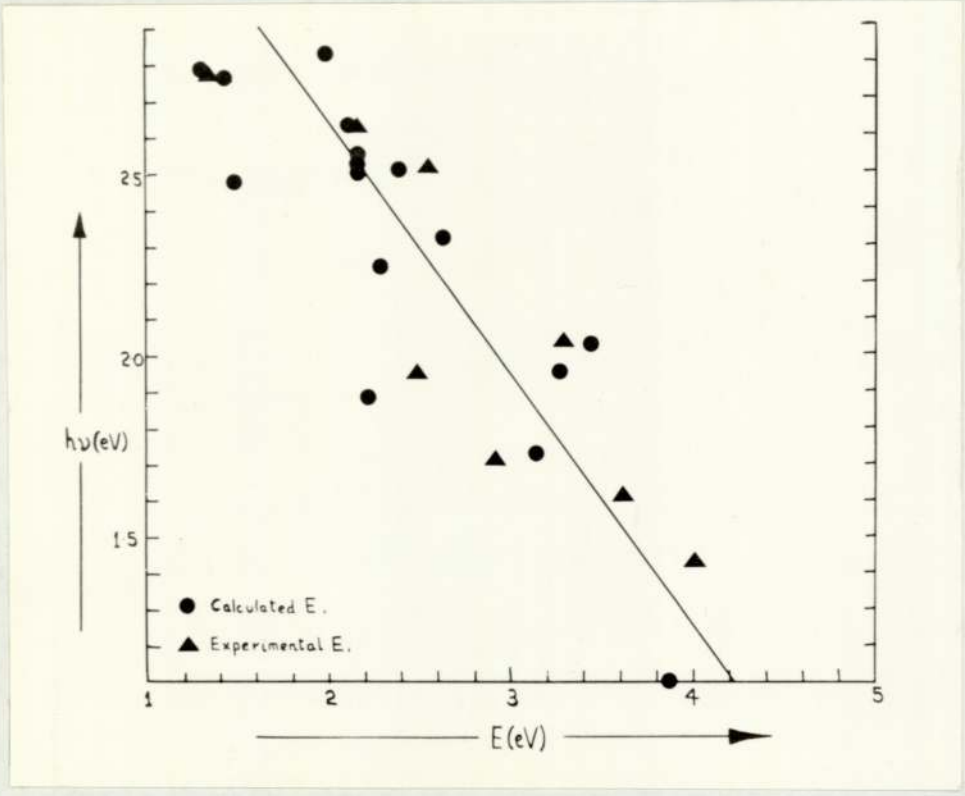

Charge transfer energy as a function of the electron affinity of the acceptor.

FIGURE 49.

$$h\nu = K - \frac{2}{3}\sum_j \frac{\mu_j \epsilon}{x_j^2}\left[1 - \frac{x_j^3}{(r^2 + x_j^2)^{3/2}}\right] \quad \text{- 10.10}$$

If x_j is approximately constant this reduces to,

$$h\nu = K - bE. \quad \text{- - - - - 10.11}$$

where $b < 1$.

The majority of donors used in charge-transfer studies are hydrocarbons in which μ_i will be small and x_i large. The interaction energy term in equation 10.9 will therefore be small and a plot of $h\nu$ against E should have an approximately unit slope. This is generally observed. The converse is true for charge-transfer from a given donor to a series of acceptors since x_j^3 will generally be comparable to $(r^2 + x_j^2)^{3/2}$. For typical values of x_j = 3.65Å and r = 3.2Å, b = 0.62. Figure 49 shows a plot of the observed values of $h\nu$ against the calculated and, where available, experimental electron affinities for the charge-transfer reactions between pyrene and a series of dipolar substituted acceptors. The slope of the line drawn is 0.69.

The value of K in equation 10.10 may be estimated, for the donor pyrene, by assuming the following data; $r = 3.2\mathring{A}$, $\mu(C-H) = -0.4D$, $a = 2r$, $\Gamma(CHCl_3) = 4.82$, $\mu = 10D$,[94] $\alpha = \alpha_A + \alpha_D = 4.8 \times 10^{-23}$cc. Combining this data with the polarographic estimate of 7.53eV for the ionisation potential of pyrene gives K = 4.01 eV. The values of b for various substituents are given in the following table.

Group	x_j	b_j
H,F,Cl,Br,I	2.17	0.853
CN	3.42	0.659
C=O	2.08	0.866
Me	3.65	0.621
CN(TCNE)	2.36	0.825
NO_2	3.53	0.624

TABLE 10.5

These figures are combined with the group contributions to the electron affinity given in table 10.3 and the estimate K = 4.01 eV to give the calculated values of the charge-transfer maxima in table 10.4. Apart from the chloranil figure the agreement is excellent. The line

of figure 48 has the equation $h\nu$ (eV) = 4.01 - 0.69E, in good agreement with the calculated values of K and b.

In view of the crudity of the model used for these calculations, the agreement between theory and experiment is impressive. The results suggest that attempts to derive electron affinities by means of linear extrapolations in a series of compounds will yield reasonable approximations only if due allowance is made for the proportionality term b associated with the electron affinity. The derivation of accurate electron affinities by means of charge-transfer measurements would appear to require more information about the dimensions of the complex and the dipole moments of the substituents than is generally available.

10.3 The relationship between the Polarographic reduction potential and electron affinity

It has been demonstrated by many workers that the cathodic reduction of organic molecules proceeds by a reversible step involving one electron.[96-101] This was shown by Matsen and Hedges[100,101] to be related to the electron affinity of the species reduced by the equation,

$$E_1 = E + \Delta E_{sol} - \chi(Hg) - E^{\circ}. \quad ---- 10.12$$

where E_1 is the reversible one electron reduction potential, ΔE_{sol} the difference between the solvation energies of the ion and the neutral molecule, $\chi(Hg)$ the work function of the mercury surface and E° is the absolute potential of the reference electrode. ΔE_{sol} is usually taken as being equivalent to the solvation energy of the ion, that of the neutral molecule being assumed to be negligible.

Maccoll[102] has demonstrated the existence of a linear relationship between the polarographic reduction potential and the calculated energy of the lowest lying unoccupied orbital of the molecule (E_i) and Pople and Brickstock[103] have shown this energy to be related to the electron affinity by the relation

$$E_i = -E = \alpha - F. \quad ---- 10.13$$

The energy of the highest occupied orbital is similarly related to the ionisation potential of the molecule by,

$$E_j = -I = \alpha + F. \quad ---- 10.14$$

F may be calculated by the semiempirical ASMOSC (Antisymmetrical Molecular Orbital Self Consistent) method.

α was normalised by Hedges and Matsen[101] to give, with the calculated value of F, I = 8.12 eV for naphthalene. The electron affinities, for a range of polycyclic aromatic hydrocarbons, calculated using this value of α were then related to E_1. The solvation energy term in equation 10.12 was found to decrease with increasing number of rings in the molecule. This was attributed to the effects of charge delocalisation in the ion, which increases with the number of rings.

Peover[104] applied equation 10.12 to the reduction of quinones and demonstrated the existence of a linear relationship between the reversible polarographic reduction potential E_1 and energy of the charge-transfer absorption band. He also attempted to calculate the electron affinities by estimating the solvation energy of the ion. The charge distribution in semiquinone ions is expected to be largely independent of the number or size of the rings[105] since molecular orbital calculations suggest that the charge will remain almost exclusively on oxygen and contiguous carbon atoms. By estimating the solvation energy of the p-benzoquinone ion as being similar to that of the benzene ion, and close to that of the other

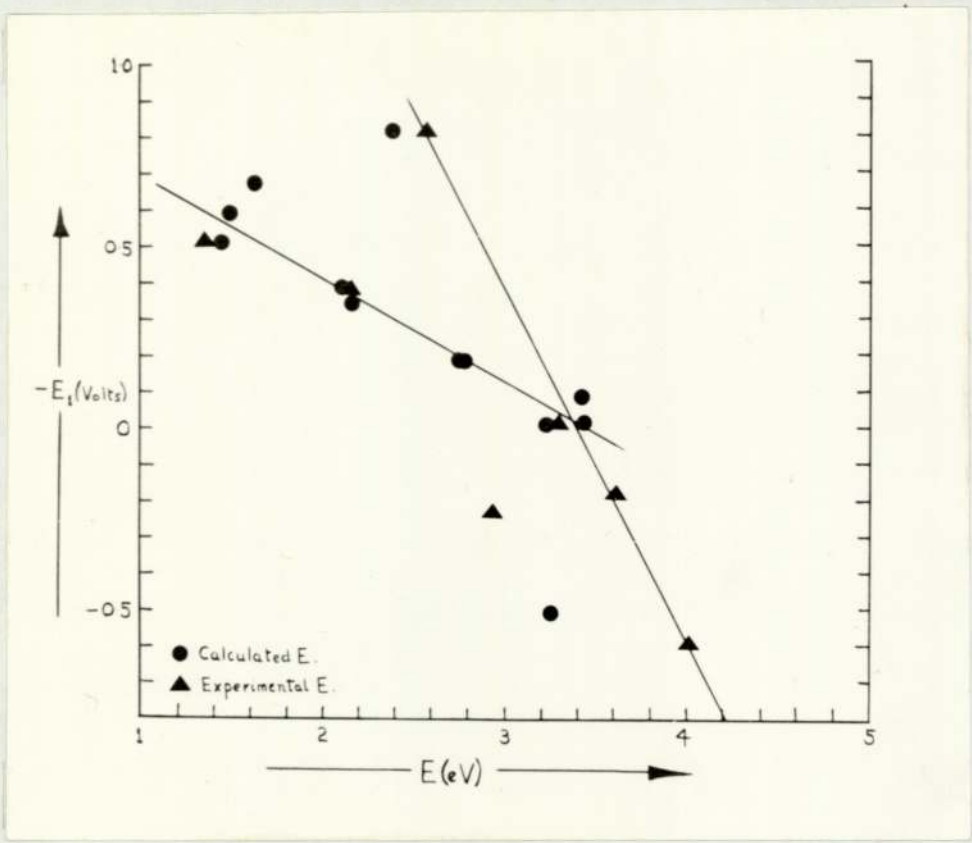

Polarographic reduction potential as a function of the electron affinity of the acceptor.

FIGURE 50.

semiquinones, Peover was able to give upper and lower limits for the electron affinities of a range of quinones. His upper limit of 1.46 eV for p-benzoquinone is close to the value measured in the magnetron, which was used by him in a later paper[75] as a reference electron affinity to establish a scale of solution electron affinity values.

Unfortunately the predicted electron affinities of the substituted benzoquinones from both these papers seem much too low. As in the case of the charge-transfer measurements this can probably be attributed to the assumption that the interaction energy term, in this case the solvation energy, remains constant throughout the series. In figure 50 the reversible polarographic reduction potentials are plotted against the experimental and calculated electron affinities. The slope of the line drawn is 0.35, which suggests that the solvation energy changes more rapidly with electron affinity than does the charge(donor)-dipole(acceptor) energy in charge-transfer from pyrene complexes. The linear relationship between charge-transfer and polarographic measurements would seem to imply a similar form of interaction in the two systems.

The estimation of ionic solvation energies is a particularly difficult problem which has not, as yet, been adequately solved. The basis of most treatments is the theory of Born[106] who regarded the ion as a rigid sphere of radius r_i and charge $z\epsilon$. He showed the difference in the free energy of the ion a vacuum and continuous medium of dielectric constant Γ to be,

$$\Delta G = -\frac{(z\epsilon)^2}{2r_i}\left[\frac{\Gamma - 1}{\Gamma}\right]. \quad - - - \ 10.15$$

from which,

$$\Delta H = -\frac{(z\epsilon)^2}{2r_i}\left\{\frac{\Gamma-1}{\Gamma} - \frac{T}{\epsilon^2}\left(\frac{\partial\Gamma}{\partial T}\right)_p\right\}. \quad - - - \ 10.16$$

The entropy term in equation 10.16 is usually small and often ignored. The direct application of this expression is difficult for two main reasons, one being that the ions are not rigid spheres and so the estimation of r_i is difficult, and the other is that the dielectric constant in the region of the ion is not that of the bulk solvent.

Extensions of equation 10.16 have usually involved an attempt to allow for the structure imposed upon the solvent in the immediate neighbourhood of the ion. The first such approach was made by Bernal and Fowler[107] who,

for the solvation of ions by water, derived essentially the expression,

$$\Delta H = \sum \frac{z.\epsilon.\mu}{(r_i^2 + r_s)^2} - \frac{(z\epsilon)^2}{2(r_i + 2r_s)} \left[\frac{\Gamma - 1}{\Gamma}\right] + U_s. \quad 10.17$$

The first term represents the ion dipole interactions in the primary solvation sheath; the second term the Born energy of the primary solvated complex, and the last term represents the electrostatic energy of one solvent molecule in the bulk solvent. This calculation was refined by Eley and Evans[108] and Verwey.[109] It is difficult to assess the reliability of these calculations since the only function which can be measured is the sum of the solvation energies of positive and negative ions and the division of this into contributions from each ion is always subject to the assumption that the model used is correct.

In the solvation of the ions encountered in polarographic reduction of organic molecules, the ion can hardly be considered as being a rigid sphere and the use of acetonitrile as a solvent causes the solvation number to be large since the solvent molecules are, in general, much smaller than the ion. With large anions which are capable of extensive charge delocalisation, the local

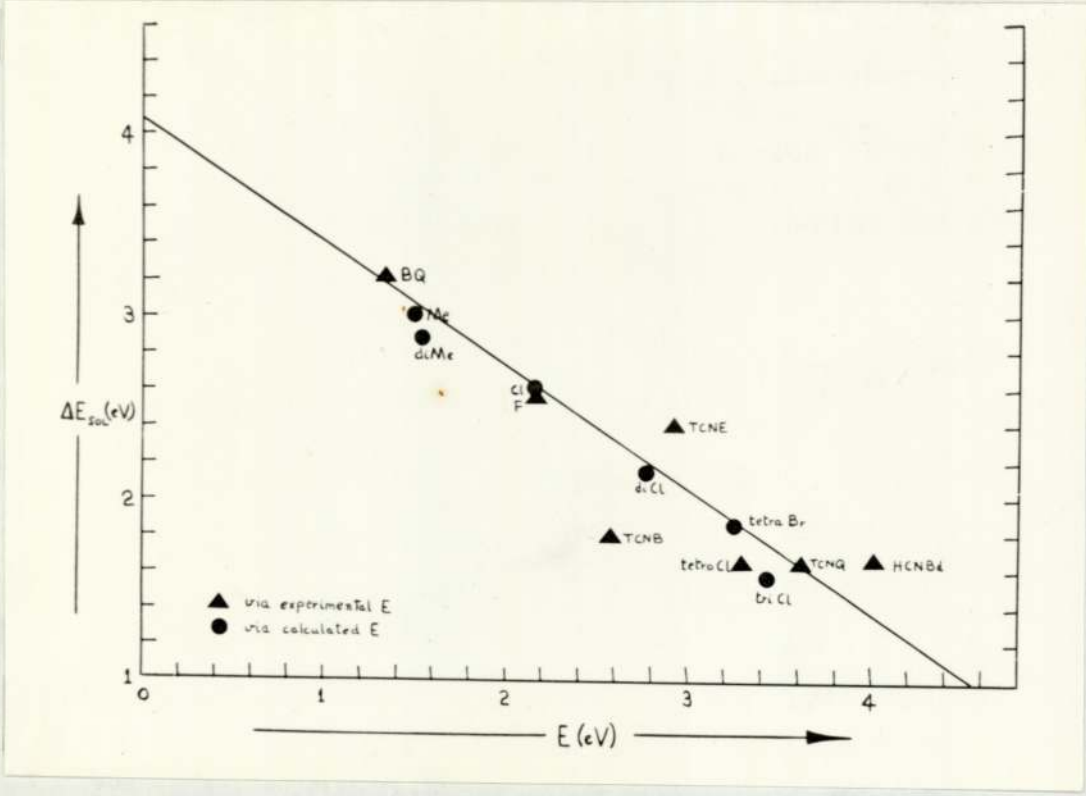

Solvation energy as a function of electron affinity.

FIGURE 51.

effects upon the solvent will be similar for both the anion and neutral molecule and so the solvation energy should approximate to the Born energy of the solvated complex. The limiting value found in table 10.6 of 1.65 eV, corresponds to an effective ionic radius of 4.5Å, which would appear to be reasonable for such molecules as TCNQ and HCNBd.

Acceptor	$-E_1^{75,104}$	E	$-\Delta E_{sol}$ (eV)
BQ	0.51	1.34	3.22
Me "	0.58	1.49	3.00
2,5 diMe "	0.67	1.53	2.87
Cl "	0.34	2.16	2.57
2,6 diCl "	0.18	2.76	2.13
2,5 diCl "	0.18	2.76	2.13
triCl "	0.08	3.43	1.56
tetraCl "	-0.01	3.29	1.64
diCl, 5,6 diCN "	-0.51	3.25	2.33
HCNBd	-0.60	4.01	1.66
FBQ	0.37	2.16	2.54
TCNB	0.71	2.57	1.79
TCNQ	-0.19	3.61	1.64
TCNE	-0.24	2.92	2.39
tetraBr BQ	0.00	3.24	1.85

TABLE 10.6

For the smaller molecules the solvation energy would appear to increase with decreasing electron affinity according to the relation,

$$-\Delta E_{sol} = 4.1 - 0.67E. \quad \text{- - - - - 10.18}$$

It would be tempting to ascribe this increase to a reduction in the solvation energy of the neutral molecule, but unpublished work by Peover[110] has shown that E_1, for TCNE and benzoquinone is only very slightly dependent upon the nature of the solvent used. This would appear to rule out any molecule-solvent interaction as being responsible for the change.

The similarity of the charge-transfer and polarographic data would appear to imply similar types of interactions in the two systems and the lack of any solvent dependence of E_1 suggests that the term is a charge-dipole (acceptor) rather than a dipole (solvent) - dipole (acceptor) interaction. If the rate determining step is, as generally supposed, electron transfer at the metal surface, the separation between this surface and the molecule will be too small for electrical images to have any meaning and the relevant interaction term would therefore

seem to involve a discrete charge located in or at the surface. The rate determining step would seem to be analogous to charge-transfer either from the metal or an adsorbed ion to the acceptor molecule.

These systems would appear to require a more extensive investigation as to the nature of the rate determining step before a more exact interpretation of the interaction terms can be evaluated.

10.4 Conclusions

The two main objectives of this work, namely the investigation of the formation of negative ions at hot metal surfaces and the application of electron affinity data to the study of the formation of negative ions in solution, have both shown indications of being susceptible to the theoretical treatments advanced.

The application of reaction rate theory to the magnetron measurements has resulted in a better understanding of the possible sources of error in electron affinity determinations by this method, but it does little to prevent the tendency to oversimplify the interpretation

of the results. The use of the entropy of the reaction as a diagnostic test for the type of process occurring is a useful aid to the interpretation of the measurements. In this respect, change of filament material is also a convenient means of identifying adsorption processes. The study of ion formation by tetracyanoethylene has proved to be a very useful test of the equations derived for both ion and electron emission and the nature of the results encourages the view that the arguments advanced are essentially correct.

The application of 'magnetron' electron affinities to charge-transfer data has shown a strong correlation between the electron affinity and the energy of the charge-transfer absorption band. The nature of this relationship suggests that the neglect of charge-dipole terms in the interaction energy of the excited state of the complex is not justified. A simple electrostatic model for the complex gives surprisingly good agreement between the observed and calculated absorption maxima for the molecules considered.

The discussion of the polarographic measurements is limited by a lack of information as to the exact nature

of the rate determining step. The existence of a functional relationship between the electron affinity and the interaction term (the 'solvation energy') is demonstrated, but the lack of any dependence of the reversible one electron reduction potentials on the solvent used suggests this interaction to be one involving the electrode rather than the solvent. Further studies upon all of the systems investigated here would clarify the mechanisms of the processes occurring and demonstrate more clearly the limitations of the naive theoretical models advanced in the course of this study.

REFERENCES

1 Moeller, 'Inorganic Chemistry', (Wiley,New York,1957)

2 Glasstone, 'Textbook of Physical Chemistry', (MacMillan,London,1948), page 50

3 Moeller, 'Inorganic Chemistry', (Wiley,New York,1957) page 152

4 Field and Franklin, 'Electron Impact Phenomena', (Academic Press,New York,1957)

5 Stiener, Seman and Branscombe, 'Atomic Collision Processes' (North Holland Publishing Co, Amsterdam,1964) page 537

6 Tsuda & Hamil, Reported at the Paris meeting of the Mass Spectrometry Discussion Group, 1964

7 Rolla and Piccardi, Atti.Acad.Linei, 1925.VI.2.29, 128,173,334

8 Padley, Page and Sugden, Trans.Farad.Soc, 1961.57.1552

9 Page, Rev.inst.francais du petrole.1958.13.692

10 Bulewicz and Padley, 9th Int.symp.Combustion, (A.P.1962) page 638, 647

11 Glockler & Calvin, J.Chem.Phys, 1936.4.492

12 Dukelskii & Ionov, J.Exptl.Theor.Phys.USSR, 1940.10.1248

13 Sutton & Mayer, J.Chem.Phys, 1934.2.145

14 Page, Trans.Farad.Soc, 1960.56.1742

15 Page, Nature, 1960.188.1021

16 Page, Trans.Farad.Soc, 1961.57.359

17 Page, ibid, 1961.57.1254

18 Page, Proc.8th symp.Combustion, (Williams & Wilkins, Baltimore, 1962)

19 Ansdell & Page, Trans.Farad.Soc, 1962.58.1084

20 Page, 'Advances in Chemistry', 1962.36.68

21 Napper & Page, Trans.Farad.Soc, 1963.59.1086

22 Gaines & Page, ibid, 1963.59.1266

23 Kay & Page, Nature, 1963.199.483

24 Kay & Page, Trans.Farad.Soc, 1964.60.1042

25 Farragher, Page & Wheeler, Disc.Farad.Soc, 1964.60.1042

26 Doty & Mayer, J.Chem.Phys, 1944.12.323

27 McCallum & Mayer, ibid, 1943.11.56

28 Vier & Mayer, ibid, 1944.12.28

29 Mitchell & Mayer, ibid, 1940.8.282

30 Massey, 'Negative Ions' (C.U.P, 1950)

31 Weisblatt, Ph.D dissertation, Johns Hopkins University, 1938.

32 Bernstein & Metlay, J.Chem.Phys, 1951.19.1612

33 Berry & Reimann, ibid, 1963.38.1540

34 Metlay & Kimball, ibid, 1948.16.774

35 Branscombe, Burch, Smith & Geltmann, Phys.Rev, 1958.111.504

36 Branscombe, Smith & Tisone, J.Chem.Phys, 1965.43.2906

37 Kingdon, Phys.Rev, 1924.24.510

38 Reimann, 'Thermionic Emission', (Chapman & Hall, London, 1934)

39 Culver & Thompkins, 'Adv.in Catalysis', 1959.XI.67

40 Hayward & Trapnell, 'Chemisorption' (Butterworths, London, 1964) page 161

41 Huang & Wylie, Disc.Farad.Soc, 1950.8.18

42 Eley, ibid, 1950.8.34

43 Fowler & Guggenheim, 'Statistical Thermodynamics', (C.U.P, 1939) page 94

44 Kay & Page, Final Technical Report, U.S. Army contract No DA/91/591/EUC/6/3206

45 Hull, Phys.Rev, 1921.18.31

46 Parker, 'Electronics', (Arnold,London 1963)

47 ibid, Appendix 9, page 1014

48 Dodd & Robinson, 'Experimental Inorganic Chemistry', (Elsevier, Amsterdam 1954)

49 Addison & Hathaway, J.Chem.Soc, 1958.3099

50 Cottrell, 'The Strengths of the Chemical Bonds', (Butterworths, London 1958)

51 Langseth & Walles, Z.Phys.Chem, B.1934.27.209

52 Yatskimirskii, Izvest.Acad.Nauk.SSSR, Odtel.Khim. Nauk, 1947.453.411

53 Kapustinsky, Acta.Physicochim, 1943.18.370

54 Pritchard, Chem.Revs. 1953.52.529

55 Smith & Seman, quoted in Branscombe, 'Proc.5th Int. Conf. Ionisation Phenomena in Gases', 1961, page 9

56 Curran, Phys.Rev, 1962.125.910

57 Branscombe, 'The Threshold of Space', (Pergamon 1957) page 101

58 Fox, J.Chem.Phys, 1960.32.285

59 Trawick & Eberhardt, ibid, 1954.22.1462

60 Johnson & Heppner, Trans.Amer.Geophys.Union, 1956.37.350

61 Webber, Proc.5th.Nat.Conf.Ionosphere. London, July 1962, page 63.

62 Harteck, 'The Threshold of Space', (Pergamon 1957) page 37

63 Reid, J.Geophys.Res, 1961.66.4071

64 Culver & Tompkins, 'Adv.in Catalysis', 1959.XI.77

65 Eisinger, J.Chem.Phys, 1957.27.1206

66 Reimann, Phil.Mag, 1935.20.594

67 George & Stier, J.Chem.Phys, 1962.37.1935

68 Mignolet, Bull.soc.chim.Belg, 1955.64.126

69 Glasstone, Laidler & Eyring, 'The Theory of Rate Processes', (McGraw - Hill, New York,1941)

70 Rigby, Canad.J.Phys, 1964.42.1256

71 Ehrlich, J.Chem.Phys, 1961.34.39

72 Redhead, Trans.Farad.Soc, 1961.57.641

73 Hayward & Trapnell, 'Chemisorption', (Butterworths, London 1964)

74 Fowler, 'Statistical Mechanics', (C.U.P, 1936) page 338 et seq.

75 Davis, Hammond & Peover, Trans.Farad.Soc, 1965.61.1516

76 Wallenfels & Friedrich, Tetrahedron Letters, 1963.19.1223

77 Laidler, 'Reaction Kinetics', vol 2, (Pergamon 1963) page 46

78 Boyd, J.Chem.Phys, 1963.38.2529

79 Harding & Wallwork, Acta.Cryst, 1955.8.787

80 Glasstone, Laidler & Eyring, 'The Theory of Rate Processes', (McGraw - Hill, New York 1941) page 219.

81 Rees, Dip.Tech.Project 1964, C.A.T. Birmingham

82 Herron, Rosenstock & Shields, Nature, 1965.206.611

83 Morrison & Roberts, Proc.Roy.Soc, 1939.A.173.1

84 Levina, Lobanova, Berlin & Sherle, Proc.Acad.Sci. USSR, (Phys.Chem).1962.145.546

85 Smythe, 'Dielectric Constant & Molecular Structure', (McGraw - Hill, New York, 1931)

86 Mulliken, J.Amer.Chem.Soc, 1950.72.600

ibid, 1952.74.811

J.Phys.Chem, 1952.56.801

87 Mulliken & Person, Ann.Revs.Phys.Chem, 1962.13.107

88 McConnell, Ham & Platt, J.Chem.Phys, 1953.21.66

89 Hastings, Franklin, Schiller & Matsen, J.Amer.Chem.Soc, 1953.75.2900

90 Briegleb & Czekalla, Z.Electrochem, 1959.63.6

91 Briegleb & Czekalla, Angew.Chem, 1960.72.401
Batley & Lyons, Nature, 1962.196.573

92 Briegleb, Angew.Chem, (internat.Ed), 1964.3.617

93 Böttcher, 'Theory of Electric Polarisation', (Elsevier, Amsterdam, 1952)

94 Chakabarti & Basu, Trans.Farad.Soc. 1964.60.465

95 Data from ref's 75, 76 and
Beukers & Szent-Gyorgi, Rec.Trav.Chim, 1962.81.255
HCNBd figure is a private communication from O.W. Webster

96 von Stackelberg & Weber, Z.Electrochem, 1952.56.806

97 Lange, ibid, 1952.56.46

98 Holleck & Exner, ibid, 1952.56.46

99 Elving, Rec.Chem.Prog. 1953.14.99

100 Matsen, J.Chem.Phys, 1956.24.602

101 Hedges & Matsen, ibid, 1958.28.950.

102 Maccoll, Nature, 1949.163.178

103 Pople, Trans.Farad.Soc, 1953.49.1375
Brickstock & Pople, ibid, 1954.50.901

104 Peover, ibid, 1962.58.1656., ibid, 1962.58.2370

105 McConnel, J.Chem.Phys, 1956.24.632
Adams, Blois & Sands, ibid, 1958.28.774

106 Born, Z.Phys, 1920.1.45

107 Bernal & Fowler, J.Chem.Phys, 1933.1.515

108 Eley & Evans, Trans.Farad.Soc, 1938.34.1093

109 Verwey, Rec.Trav.Chim, 1942.61.127

110 Private communication to F.M. Page